

Cytochromes P450:
Inhibition of CYP2A Enzymes Involved in Xenobiotic Metabolism and
Generation of CYP26 Enzymes Involved in Retinoic Acid Metabolism

By

Copyright 2012

Eva S. Stephens

Submitted to the graduate degree program in Medicinal Chemistry and the Graduate Faculty of
the University of Kansas in partial fulfillment of the requirements for the degree of Master
Science.

Chairperson: Emily Scott

Barbara Timmermann

Jennifer Laurence

Date Defended: May 18, 2012

The Thesis Committee for Eva S. Stephens
certifies that this is the approved version of the following thesis:

Cytochromes P450:

Inhibition of CYP2A Enzymes Involved in Xenobiotic Metabolism and
Generation of CYP26 Enzymes Involved in Retinoic Acid Metabolism

Chairperson: Emily Scott

Date approved: May 29, 2012

Abstract

The cytochrome P450 (P450) superfamily of mixed function oxidase enzymes catalyze the metabolism of a variety of endogenous and exogenous biochemicals, including steroids, fatty acids, vitamins, eicosanoids, drugs, pesticides, and toxins. P450-mediated oxidative metabolism often serves a beneficial role in the clearance of foreign compounds and the regulation of endogenous molecules, both of which are necessary for the maintenance of homeostasis. However, the reactions catalyzed by P450 enzymes also have the potential to promote disease and injury, whether it be in the activation of procarcinogens or by undermining the therapeutic efficacy of a drug. Altogether, these processes make P450 enzymes important subjects of interest for the prediction of chemical toxicology and the development of therapeutic agents. The focus of this thesis research is the characterization of the CYP26 and CYP2A families of P450 enzymes in an effort to contribute to an understanding of how substrates and inhibitors specifically interact with the individual enzymes within these families.

The functional enzymes of the human CYP2A family include CYP2A6 and CYP2A13. CYP2A6 is primarily a hepatic enzyme, while CYP2A13 is mainly expressed within the respiratory tract. Though these two enzymes are primarily localized to different tissues within the body, they share many substrates in common as a result of their 94% amino acid sequence identity. These substrates include: nicotine, cotinine, *para*-nitrophenol, and coumarin. However, CYP2A13 appears to preferentially activate a number of procarcinogens, including the tobacco-specific nitrosamine 4-(methylnitrosamino)-1-(3-pyridyl)-1-butanone (NNK), into reactive intermediates that can result in DNA adducts and the initiation or promotion of carcinogenesis. In order to evaluate the relative involvement of CYP2A6 activity versus that of CYP2A13 in the metabolism and/or activation of potentially harmful chemical agents *in vivo*, selective inhibitors

are needed. A number of compounds were reported to selectively inhibit CYP2A6 before CYP2A13 was determined to be a functional member of the CYP2A family, or have simply not been tested against CYP2A13. This work examined such compounds including: phenethyl isothiocyanate (PEITC), 4-dimethylaminobenzaldehyde (DMABA), 8-methoxypsoralen (8-MOP), tranlylcypromine, tryptamine, pilocarpine, (*S*)-nicotine, (*R*)-(+)-menthofuran, and β -nicotyrine. The relative impact of these inhibitors on CYP2A6 and CYP2A13 function was evaluated by determining K_i values and modes of inhibition for each of the compounds against both enzymes, followed by the calculation of a selectivity factor. The results of these studies serve as the first explicit determination of the selectivity of these compounds for enzymes within the CYP2A family and indicate that only (*R*)-(+)-menthofuran and tranlylcypromine demonstrate even a 10-fold preference for CYP2A6 inhibition over CYP2A13. This information can be used as a guide for the selection of inhibitors with the greatest potential for determining whether CYP2A6 or CYP2A13 is responsible for the metabolism or activation of procarcinogenic compounds, such as tobacco-derived NNK in the human respiratory tract.

Collectively, the CYP26 family of P450 enzymes serve as important mediators of retinoic acid (RA) catabolism in the body. In humans, the CYP26 family of enzymes consists of three isoforms: CYP26A1, CYP26B1, and CYP26C1. As a result of RA's endogenous role in regulating cellular growth and differentiation, geometric isomers of RA such as *all-trans*-RA (*at*RA) and 13-*cis*-RA represent attractive targets for cancer therapy and the treatment of dermatological conditions. Unfortunately, RA resistance is often experienced in patients undergoing prolonged RA-based therapy. This failure has been suggested to be the result of up-regulation of P450 enzymes, particularly the enzymes of the CYP26 family, resulting in enhanced RA metabolism *in vivo*. As a result, a significant amount of work has been conducted

for the development of chemical agents that inhibit P450-mediated metabolism of *atRA*, commonly referred to as retinoic acid metabolism blocking agents (RAMBAs). The development of safe and effective RAMBAs could be greatly facilitated by more detailed structural and functional characterizations of the CYP26 family of enzymes, since very little is known about these enzymes aside from their dominant role in *atRA* hydroxylation. However, the fact that the human CYP26 enzymes are membrane-bound proteins, a characteristic shared by all human P450 enzymes, represents a major challenge to the recombinant expression and purification of these enzymes in sufficient quantities to enable detailed biochemical and biophysical characterization studies. To address this challenge, a new method for the production of pure CYP26 enzymes was developed based on techniques that have proven successful in the expression and purification of other membrane-bound P450 enzymes in *E. coli*, while incorporating the use of detergents and stabilizing ligands specific to the CYP26 enzymes. The combination of these approaches led to the successful generation of mouse CYP26A1 and CYP26B1 proteins in yields of 200-400 nmol per 2.25 L of *E. coli* expression media and the ability to recover 20-50 nmol following a single chromatographic step. Unfortunately, this protein appeared to be inactive according to reduced carbon monoxide difference spectrum analysis and assays of RA metabolism. As a result, further optimization will be required to reach the original goal set forth to generate pure recombinant CYP26 enzymes for basic kinetic and structural determination studies.

Acknowledgements

I would like to take a moment to thank all of those individuals who assisted me during my graduate studies here at The University of Kansas. First, for their guidance and camaraderie over the years, I would like to thank all of the past and present Scott lab members: Patrick Porubsky, Dr. Kathy Meneely, Dr. Agnes Walsh, Dr. Natasha DeVore, Dr. Linda Blake, Dr. Andi Skinner, Dr. Fernando Estrada, Elyse Petrunak, Lindsay Astleford, Aaron Bart, Melbien Tinio, and Michelle Jackson. It was a pleasure to work alongside such a wonderful and talented group of individuals. I would also like to thank Dr. Emily Scott, Dr. Barbara Timmermann, and Dr. Jennifer Laurence for serving on my committee. I am particularly grateful to my advisor Dr. Emily Scott for her continuous support and guidance over the course of my graduate career. Finally, I would like to acknowledge the people that I cherish most for their support during both the most rewarding and the most challenging experiences of the last three years: David Hymel, Tamara Vasiljevic, Wilmarie Santana-Rios, Kristina Sahl, Andi Skinner, my sisters Tanne and Tess, and my parents Bruce and Petra Stephens. I wouldn't have been able to accomplish this if it hadn't been for all of your love and encouragement. Funding for this work was provided by NIH grant GM076343.

Table of Contents	Page
Abstract	iii
Acknowledgements	vi
Table of Contents	vii
List of Figures	ix
List of Tables	xi
Chapter 1: Introduction	1
Introduction to Cytochrome P450 Enzymes	1
Features of Cytochrome P450 Enzymes	2
Cytochrome P450 Catalytic Cycle	5
Relevance of Cytochrome P450 Enzymes in Xenobiotic Metabolism	8
The Role of Human Cytochrome P450 2A Enzymes in the Metabolic	10
Activation of Procarcinogens and the Significance of Selective	
Inhibitors	
The Cytochrome P450 26 Family of Enzymes, Retinoic Acid	13
Metabolism, and Relevance to Cancer Therapy	
References	19
Chapter 2: Methods	22
Introduction	22
Plasmid Transformation and Expression of Cytochrome P450	22
Proteins in <i>E. coli</i>	
Cytochrome P450 Protein Purification	24
Spectroscopic Analysis for the Quantitation of Cytochrome P450	26

References	27
Chapter 3: Evaluation of Inhibition Selectivity for Human Cytochrome P450 2A Enzymes	29
Introduction	29
Material and Methods	32
Results	34
Discussion	38
Conclusion	42
References	43
Chapter 4: Expression and Purification of the Cytochrome P450 26 Family of Enzymes	45
Introduction	45
Materials and Methods	48
Results	59
Discussion	76
Conclusion	78
References	80
Chapter 5: Conclusions	83
References	88

List of Figures	Page
Figure 1.1. Ferrous heme thiolate catalytic center of cytochrome P450	4
Figure 1.2. Cytochrome P450-catalyzed monooxygenase reaction	5
Figure 1.3. The cytochrome P450 catalytic cycle	6
Figure 1.4. The procarcinogenic nitrosamines NNN, NNK, NNAL, and the tobacco alkaloid precursor nicotine	11
Figure 1.5. NNK α -hydroxylation and formation of DNA adducts	12
Figure 1.6. The synthesis of retinoic acid from retinol and metabolism by CYP26 enzymes	14
Figure 1.7. Retinoic acid metabolism blocking agents designed for the inhibition of CYP26	16
Figure 3.1. <i>para</i> -Nitrophenol 2-hydroxylation catalyzed by human CYP2A enzymes	31
Figure 3.2. Initial evaluation of the selective inhibition of nine previously described CYP2A6 inhibitors for CYP2A6 versus CYP2A13	35
Figure 3.3. PEITC demonstrates extremes of mixed inhibition for CYP2A6 versus CYP2A13	38
Figure 4.1. Retinoic acid metabolism by CYP26 enzymes	46
Figure 4.2. Sequence alignment of the N-terminal and C-terminal portions of full-length CYP26A1 and modified human enzymes CYP2A6, CYP2A13, CYP2E1, and CYP26A1	50
Figure 4.3. Sequence alignment of CYP26A1, CYP26B1, and CYP26C1 in mouse and human	51
Figure 4.4. Human cytochrome P450 26 protein expression and purification	61
Figure 4.5. Mouse cytochrome P450 26 protein expression and purification	63
Figure 4.6. Representative cell pellet samples of CYP26-expressing TOPP3 <i>E. coli</i> cells	67

Figure 4.7. Reduced carbon monoxide difference spectra of CYP26A1	72
Figure 4.8. Detection of CYP26A1 by Western blot	73
Figure 4.7. Characterization of recombinant CYP26 protein by RA metabolism	75

List of Tables	Page
Table 1-1. Human P450 enzymes categorized by substrate class	3
Table 3-1. Results of steady state kinetic studies for the evaluation of CYP2A activity	36
Table 4-1. Oligonucleotide primer designs for human and mouse CYP26A1, CYP26B1, and CYP26C1	53
Table 4-2. PCR thermal cycling parameters used to generate modified versions of human and mouse CYP26 enzymes	54
Table 4-3. Human cytochrome P450 26 protein expression and purification	60
Table 4-4. Mouse cytochrome P450 26 protein expression and purification	62

Chapter 1

Introduction

Introduction to Cytochrome P450 Enzymes

Cytochrome P450 (P450) enzymes are a superfamily of heme-containing proteins that catalyze mixed-function oxidation reactions and are found within a variety of organisms, including plants, microorganisms, and mammals. The function of P450 enzymes in early forms of life is considered to have primarily involved the regulation of endogenous molecules, such as the metabolism of cholesterol to maintain membrane integrity and for steroid biosynthesis and metabolism.¹ In pharmacology, P450 enzymes are often better known for their metabolism of foreign compounds (xenobiotics). This capacity is believed to have evolved from the role of steroidogenic P450 enzymes in protecting organisms from plant toxins,¹ which expanded today to protection from man-made chemical exposures in the form of drugs, common household products, pollutants, and industrial waste. As a result, P450 enzymes have evolved to metabolize a wide variety of substrates from diverse structural classes, while maintaining an overall conserved tertiary structure that is uniquely adapted to the heme-thiolate chemistry required for oxygen activation.

P450 enzymes are classified by an alphanumerical naming system based on evolutionary relationships.² The name of each enzyme begins with the abbreviation 'CYP' to signify its membership within the cytochrome P450 superfamily. P450 enzymes are further categorized into families and subfamilies according to amino acid sequence homology. Enzymes of the same family share a minimum of 40% sequence identity and are distinguished by the first number following the 'CYP' abbreviation (*i.e.* CYP2). The letter following the family number is shared by members of the same subfamily, requiring an amino acid identity of >55% (*i.e.* CYP2A). The

final number is given to an individual enzyme originating from a single gene (*i.e.* CYP2A6). As a result, enzymes having highly conserved evolutionary relationships can be readily identified based on the similarity of their names.

In humans, the P450 enzymes represent 18 families and 43 subfamilies.³ Of the 57 human P450 enzymes identified to date, 42 have been classified according to the substrate class in which they demonstrate catalytic activity (Table 1-1).⁴ P450 enzymes from families 1-3 are primarily involved in the metabolism of xenobiotics and are generally characterized as having broad, overlapping substrate specificities.⁵ The levels of these P450 enzymes can vary considerably among individuals and are often highly inducible by chemical exposures, leading to large differences in the ability to metabolize many drugs.⁶ Families 4 and higher, by contrast, primarily participate in the metabolism of compounds endogenously found in humans and selectively metabolize a limited number of substrates.⁵ The levels of these P450 enzymes are both relatively consistent among individuals and more tightly regulated, and deficiencies in their expression or catalytic activities can lead to serious human diseases.⁷

Features of Cytochrome P450 Enzymes

Human P450 enzymes are all membrane-bound proteins, the majority of which are localized to the endoplasmic reticulum (ER) of the cell.⁷ The membrane-bound nature of these proteins is thought to reflect the hydrophobic properties of their substrates. Hydrophobic substrates that tend to be concentrated within the membranes are thought to access the P450 active site via the membrane-bound face of the enzyme. Two separate hydrophobic regions are responsible for the close association of human P450 enzymes with the membrane. The first is an N-terminal transmembrane helix consisting of approximately 20 hydrophobic amino acids

Table 1-1. Human P450 enzymes categorized by substrate class.⁴

Xenobiotics		Steroids		Fatty Acids	Vitamins	Eicosanoids		Unknown
1A1	2C19	1B1	19A1	2J2	2R1	4F2	2A7	4V2
1A2	2D6	7A1	21A2	4A11	26A1	4F3	2S1	4X1
2A6	2E1	7B1	27A1	4B1	26B1	4F8	2U1	4Z1
2A13	2F1	8B1	39A1	4F12	26C1	5A1	2W1	20A1
2B6	3A4	11A1	46A1		27B1	8A1	3A43	27C1
2C8	3A5	11B1	51A1		24A1		4A22	
2C9	3A7	11B2					4F11	
2C18		17A1					4F22	

inserted co-translationally into the membrane. The second hydrophobic region is one face of the protein surface proximal to the active site. Together, these two regions represent a significant challenge to the study of human P450 enzymes, as they confer properties that make these proteins particularly challenging to extract from the membrane and to solubilize for purposes of purification and biophysical and biochemical characterization. As a result, almost all of the published crystal structures and many characterizations of highly purified human P450 enzymes are of enzymes from which the N-terminal transmembrane domain has been removed. This truncation not only improves solubility due to the removal of one region that anchors the protein to the membrane, but is also beneficial due to increased expression levels in *E. coli* without altering the catalytic activity of the enzyme.⁸

The catalytic domain of human P450 enzymes is located on the cytoplasmic side of the ER membrane, and contains an iron protoporphyrin IV (commonly referred to as the heme)

prosthetic group (Figure 1.1 A) that is crucial to their function as monooxygenase enzymes. The iron of the heme is coordinated to a phylogenetically-conserved cysteine thiolate. When the sixth coordination position of the reduced heme iron is occupied by carbon monoxide (Figure 1.1 A), the result is a difference spectrum with a maximum at 450 nm (Figure 1.1 B). This characteristic spectrum differs from heme proteins where the heme iron is coordinated to histidine or tyrosine, and thus serves as the origin of the name ‘cytochrome P450’. The reduced carbon monoxide difference spectrum of P450 enzymes is widely used to determine the concentration of active P450 in an enzyme preparation. Perturbations of the bond between the heme iron and the cysteinyl sulphur result in an altered electronic structure upon complexing with carbon monoxide, which corresponds to an observed absorption maximum at 420 nm rather than 450 nm. Although in rare instances P420 has been shown to convert to P450, absorption at 420 nm is usually considered to be an indicator of the irreversible formation of inactive P450 enzyme.

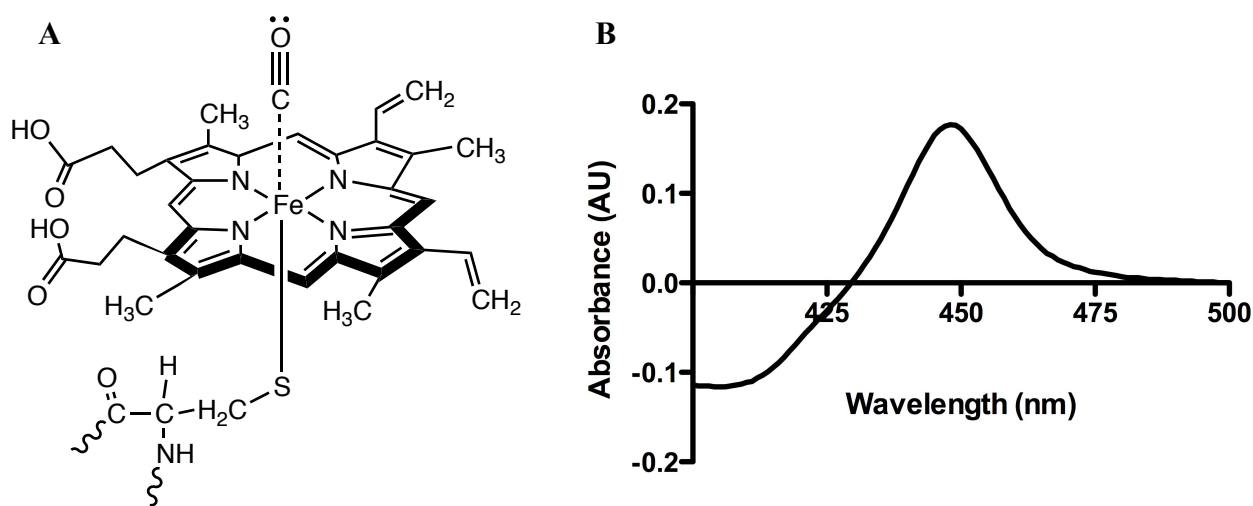


Figure 1.1. Ferrous heme thiolate catalytic center of cytochrome P450. The iron protoporphyrin within the P450 catalytic domain is coordinated to the sulfur of cysteine (A) and has the ability to form a complex with carbon monoxide, yielding a major absorption band at 450 nm (B) in the reduced carbon monoxide difference spectrum.

Cytochrome P450 Catalytic Cycle

The primary function of P450 enzymes as monooxygenases is to introduce an oxygen atom into a usually stable, hydrophobic compound. This is typically accomplished through activation of molecular oxygen and reduction the distal oxygen atom to water followed by incorporation of the remaining oxygen atom into the organic substrate (Figure 1.2). Oxidative metabolism by P450 enzymes results in one or more of the following changes to the molecules that serve as P450 substrates, including: 1) increased hydrophilicity, 2) reduced chemical stability, or 3) generation of a functional group, facilitating subsequent conjugation to a more

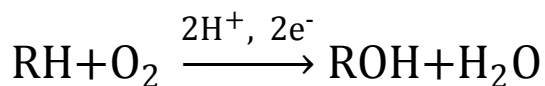


Figure 1.2. Cytochrome P450-catalyzed monooxygenase reaction. The cytochrome P450-mediated reaction involves the combination of oxygen with organic substrate (RH) to produce a molecule of water and a monooxygenated metabolite (ROH).

polar molecule. For the majority of P450 substrates, the result is metabolic

deactivation and elimination from the body. Some substrates, however, become metabolically activated by the very same mechanism, either to a

biologically active therapeutic molecule (prodrug) or to a more harmful chemical species (protoxins, procarcinogens). An example of metabolic activation by P450 enzymes will be discussed later in this chapter in the case of the procarcinogenic tobacco-specific nitrosamine 4-(methylnitrosamino)-1-(3-pyridyl)-1-butanone (NNK) and the closely-related xenobiotic-metabolizing enzymes CYP2A6 and CYP2A13.

Oxidative metabolism by CYP450 enzymes is accomplished through a catalytic cycle⁹ (Figure 1.3) that requires the delivery of two electrons and two protons for every substrate that is oxidized. The electrons are derived from NADPH or NADH and transported to the P450 heme iron via one or more redox partner proteins. For human P450 enzymes localized within the ER,

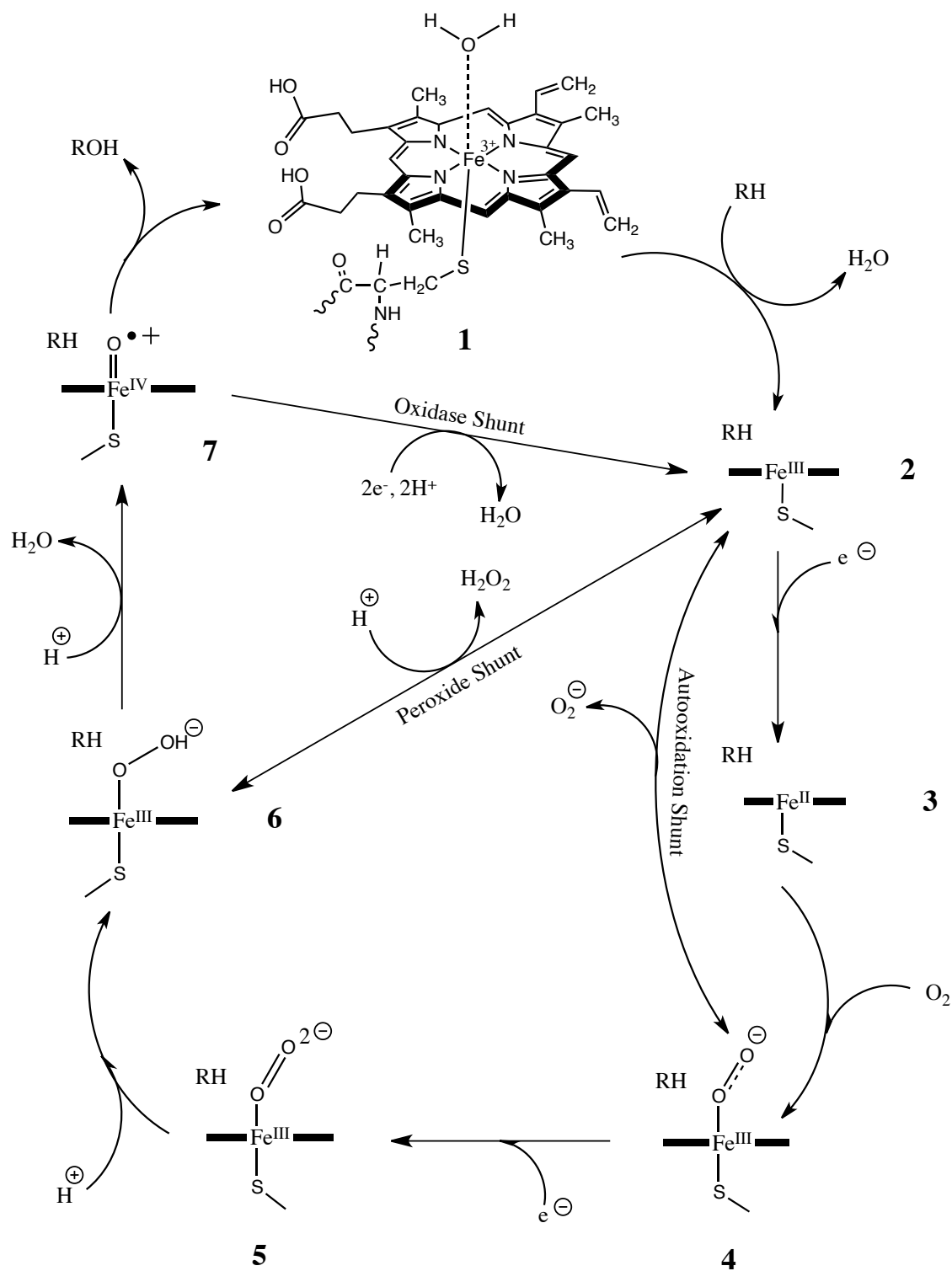


Figure 1.3. The cytochrome P450 catalytic cycle.⁹

this redox partner is NADPH-dependent cytochrome P450 reductase (CPR). CPR is a flavoprotein complex that consists of one FAD (flavin adenine dinucleotide) and one FMN (flavin mononucleotide) per CPR protein. CPR facilitates the transfer of electrons from NADPH to FAD to FMN and finally to P450 for completion of the catalytic cycle. As P450 enzymes are continuously turning over substrates, a constant flow of electrons is necessary to maintain P450-mediated oxidative metabolism.

In the resting state of the P450 enzyme (1), a distal iron-coordinated water molecule occupies the sixth coordination site on the ferric heme iron. The P450 catalytic cycle begins with the reversible binding and orientation of a substrate within the enzyme's active site, which typically displaces the water molecule present during the resting state (2). The transition from a six-coordination state to a five-coordination state means the heme iron converts from low-spin to high-spin, raising the reductive potential from approximately -300 mV to -170 mV and effectively making the complex a good electron acceptor for CPR. This triggers a one electron transfer from the FMN of CPR, reducing the heme iron from high-spin ferric to high-spin ferrous (3). The reduced heme iron readily binds dioxygen as the sixth ligand (4). At this point, the P450 enzyme accepts a second electron from CPR to form a twice-reduced ferric-peroxy species (5), which becomes protonated in the following step to produce a ferric hydroperoxy species (6). A second protonation at the distal oxygen atom and subsequent cleavage of the O-O bond produces a water molecule and a ferryl-oxo intermediate (7). This intermediate, sometime referred to as "Compound I", represents the catalytically active oxygenation species responsible for activating the substrate. Activation proceeds by abstraction of a hydrogen atom from the substrate, and subsequent rebound generates the oxidized product. The cycle ends with dissociation of the product and the re-binding of water to the ferric heme iron (1).

The P450 catalytic cycle contains three branch points where it is possible to prematurely abort the reaction, commonly referred to as ‘shunt’ pathways. The autooxidation shunt involves the autooxidation of the oxy-ferrous enzyme (4) with the concomitant production of a superoxide anion and return of the enzyme to the substrate-bound state (2). The peroxide shunt occurs when the coordinated peroxide (6) dissociates from the iron and forms a hydrogen peroxide to return the enzyme to the substrate-bound state (2). The final uncoupling pathway is the oxidase shunt, in which the ferryl-oxo intermediate (7) is reduced to water by two additional electrons and is returned to the substrate-bound state (2) rather than proceeding to substrate oxidation through hydrogen abstraction.

Relevance of Cytochrome P450 Enzymes in Xenobiotic Metabolism

Of all the enzyme systems present in the human body, P450 enzymes are the most important in terms of drug metabolism. Three quarters of all drug metabolism is mediated by P450 enzymes, and 95% of all drugs are metabolized by just five of the fifteen human P450 enzymes devoted to the metabolism of xenobiotics.⁶ As a result, a significant amount of consideration is given to the activity of these enzymes in drug development.

The development of a successful drug candidate critically depends on four main criteria: absorption, distribution, metabolism, and excretion (ADME).¹⁰ These four criteria influence the levels of exposure of a drug within the body, and therefore the drug’s pharmacological activity and overall effectiveness as a therapeutic agent. P450 enzymes have a major impact on the ADME properties of a drug based on the dominant role they play in xenobiotic metabolism. As a result, the Federal Drug Administration (FDA) requires specific information concerning the ability of a new chemical entity to inhibit, induce, or serve as a substrate to one or more P450 enzymes.⁶ This information is critical to reducing the occurrence of severe clinically-significant

drug interactions as a result of toxicity, understanding pharmacological effectiveness, and evaluating potential drug-drug interactions.

P450 reaction phenotyping studies serve as a primary means of assessing the contribution of individual P450 enzymes to the metabolism of a drug candidate. Multiple *in vitro* approaches have been developed for this purpose, including: the incubation of human liver microsomes in the presence of various inhibitors, the use of recombinant enzyme isoforms, and correlation studies in human liver microsomes to compare the metabolism of a new compound to that of a probe substrate.¹¹ The first of these three approaches is perhaps the most effective and widely used, and depends heavily on the use of inhibitors that are both potent and selective for each of the P450 enzymes present in the microsomes. Since many xenobiotic-metabolizing P450 enzymes can bind and metabolize a wide variety of substrates, it can be difficult to identify compounds that can provide maximal inhibition of one P450 while marginally affecting other isoforms at a given concentration. Nevertheless, broad efforts to this end have successfully identified selective inhibitors for many of the major human hepatic P450 enzymes.¹¹

In addition to their utility in evaluating drug metabolism, selective inhibitors are also fundamental in determining the relative roles that individual P450 enzymes have in the metabolism of potentially harmful compounds to which we are exposed in our daily lives. Fortunately, these same P450 enzymes actively metabolize compounds that we encounter in the air we breathe and in the food we eat. While the liver plays a dominant role in the first-pass clearance of drugs and controls their systemic levels, extrahepatic tissues that serve as portals of entry into the body provide very different settings for the metabolism of potentially harmful foreign compounds. Based on the nature of P450-mediated oxidative metabolism, the activity of these enzymes influences the level of localized tissue exposure to foreign compounds not only by

detoxifying harmful compounds, but also sometimes by activating inert xenobiotics to form toxic or carcinogenic compounds.¹² Though the former is a beneficial process that proceeds relatively unnoticed, the threat imposed by the latter provides an opportunity to exploit the metabolic activity of individual P450 enzymes for purposes of cancer prevention.

The Role of Human Cytochrome P450 2A Enzymes in the Metabolic Activation of Procarcinogens and the Significance of Selective Inhibitors

The first project that will be discussed within this thesis is directly related to evaluating the roles of xenobiotic P450 enzymes that activate procarcinogenesis in extrahepatic tissues. Two closely related xenobiotic-metabolizing P450 enzymes, CYP2A6 and CYP2A13, represent the only two functional enzymes within the human CYP2A subfamily and share an amino acid sequence identity of 94%.¹³ CYP2A6 is primarily a hepatic enzyme, while CYP2A13 is mainly expressed within the respiratory tract.¹⁴ The CYP2A enzymes both metabolize many small, cyclic compounds, including nicotine,¹⁵ *para*-nitrophenol,¹⁶ coumarin,¹⁴ and the nicotine-derived compound cotinine.¹⁵ In addition, there are many other procarcinogenic compounds that CYP2A13 preferentially metabolizes or has the sole ability to activate. CYP2A13 is much more efficient in the metabolism of the tobacco-specific nitrosamine 4-(methylnitrosamino)-1-(3-pyridyl)-1-butanone (NNK)¹⁴ compared to CYP2A6, and has the sole ability to metabolize the tobacco-related procarcinogen 4-aminobiphenyl¹⁷ and activate the mycotoxin aflatoxin B₁¹⁸ to carcinogenic/toxic epoxide metabolites. Of the potentially harmful xenobiotic compounds that CYP2A13 metabolizes, the tobacco-specific nitrosamine 4-(methylnitrosamino)-1-(3-pyridyl)-1-butanone (NNK) continues to cause the greatest concern.

Tobacco use is considered to be the most widespread link between exposure to known carcinogens and death from cancer.¹⁹ Cigarette smoking alone accounts for 90% of lung cancer cases worldwide, although all tobacco products, whether burned or unburned, contain a diverse

array of chemicals that lead to the development of various types of cancers.¹⁹ Cigarette smoke contains more than 60 compounds demonstrating carcinogenic potential, while unburned tobacco products contain more than 16.¹⁹ Among these compounds are nitrosamines such as NNK, N'-nitrosornicotine (NNN), and 4-(methylnitrosamino)-1-(3-pyridyl)-1-butanol (NNAL), which are formed from nicotine during the processing of tobacco and tobacco smoking (Figure 1.4).²⁰ Of these, NNK is the most prevalent and considered by experts to represent one of the

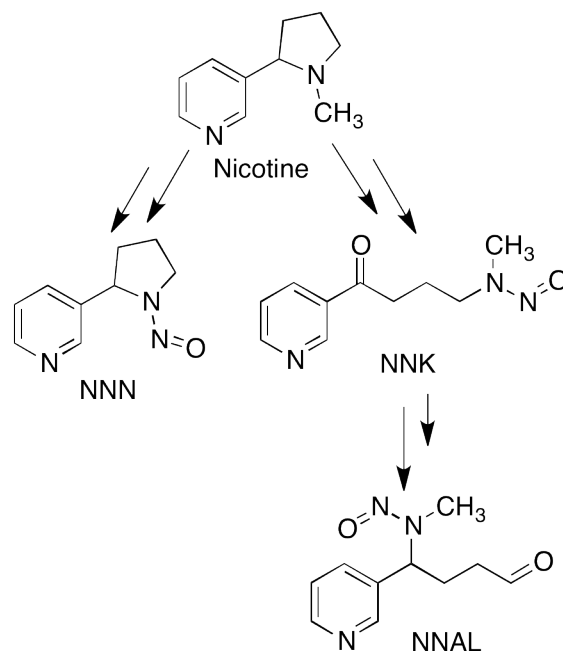


Figure 1.4. The procarcinogenic nitrosamines NNN, NNK, NNAL, and the tobacco alkaloid precursor nicotine.²¹

largest contributing factors to the formation of human tobacco-related lung cancer.¹⁹

NNK is metabolically activated by P450 enzymes to form DNA adducts in lung tissue that can cause cancer. CYP2A6 and CYP2A13 are both able to perform this metabolic activation of NNK, though they do so at very different rates and at different sites. Activation of NNK proceeds through α -hydroxylation of either the methyl or methylene carbon, which generates electrophiles that pyridyloxobutylate or methylate DNA, respectively (Figure 1.5).²¹ CYP2A6 has only been shown to catalyze the α -hydroxylation of the methyl carbon, while CYP2A13 catalyzes the α -hydroxylation of the methyl carbon with much greater catalytic efficiency, in addition to catalyzing α -hydroxylation of the methylene carbon.¹⁴ The greater efficiency of CYP2A13 for NNK activation, coupled with the fact that CYP2A13 is primarily expressed in the

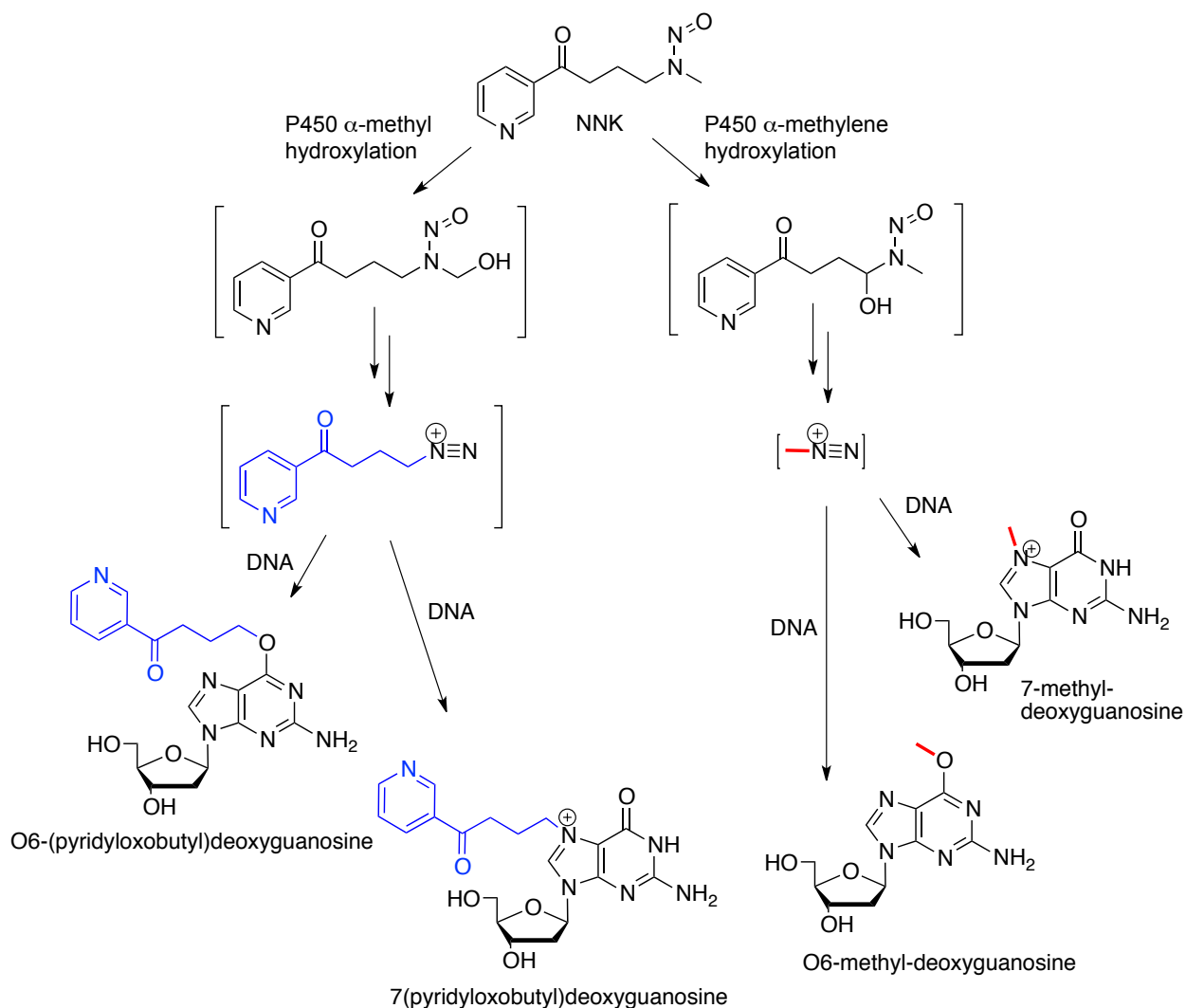


Figure 1.5. NNK α -hydroxylation and formation of DNA adducts. The pyridyl and methyl adduct precursors are colored blue and red, respectively.²¹

respiratory tract where inhaled nitrosamines are most concentrated, makes CYP2A13 a leading target for the prevention of lung cancer as a result of NNK exposure.

Other members of the Scott lab have focused on addressing the immediate, therapeutic need to selectively inhibit CYP2A13 activity in the activation of NNK in the respiratory tract. However, the contribution that CYP2A6 and CYP2A13 have in the metabolism and activation of xenobiotic compounds, in addition to NNK, represents a general need for chemical tools that can be used to determine isozyme-specific metabolic contributions within a given tissue. As a result,

the focus of my project was to evaluate the ability of known CYP2A inhibitors to discriminate between the activity of CYP2A6 and CYP2A13. The data attained from these studies can be used as a guide for the selection of CYP2A-selective inhibitors for CYP phenotyping studies, while contributing to a greater understanding of the biochemical basis for selective interactions between CYP2A enzymes and their ligands.

The Cytochrome P450 26 Family of Enzymes, Retinoic Acid Metabolism, and Relevance to Cancer Therapy

Whereas the CYP2A family of enzymes represent therapeutic targets for the prevention of cancer due to their roles in the metabolic activation of xenobiotics, inhibition of the next family of cytochrome P450 enzymes provides a means for enhancing existing cancer therapies by regulating the concentrations of retinoic acid (RA), the endogenous derivative of vitamin A (retinol) (Figure 1.6). In humans, the CYP26 family of enzymes consists of three isoforms responsible for the metabolism of RA and its structural isomers (collectively referred to as RAs): CYP26A1, CYP26B1, and CYP26C1. In contrast to the xenobiotic-metabolizing enzymes of the CYP2A subfamily, the singular role of the CYP26 family of enzymes is to mediate the levels of endogenous RAs. Consequently, the CYP26 enzymes recognize only this small group of compounds as their substrates. RA plays a major role in regulating growth and differentiation of a wide variety of cell types, and this is involved in several important physiological processes, including reproduction, cell proliferation, differentiation, vision, and embryonic development.²² At the cellular and tissue levels, the need for tight regulation of RA concentrations is well demonstrated by the observations that both deficiency and excess of RA are teratogenic to the embryo during critical developmental periods.²³ This tightly regulated concentration of RA within the body is maintained by both the synthesis of RA from vitamin A and by its metabolism, with the physiologically most prominent pathway being oxidative metabolism of

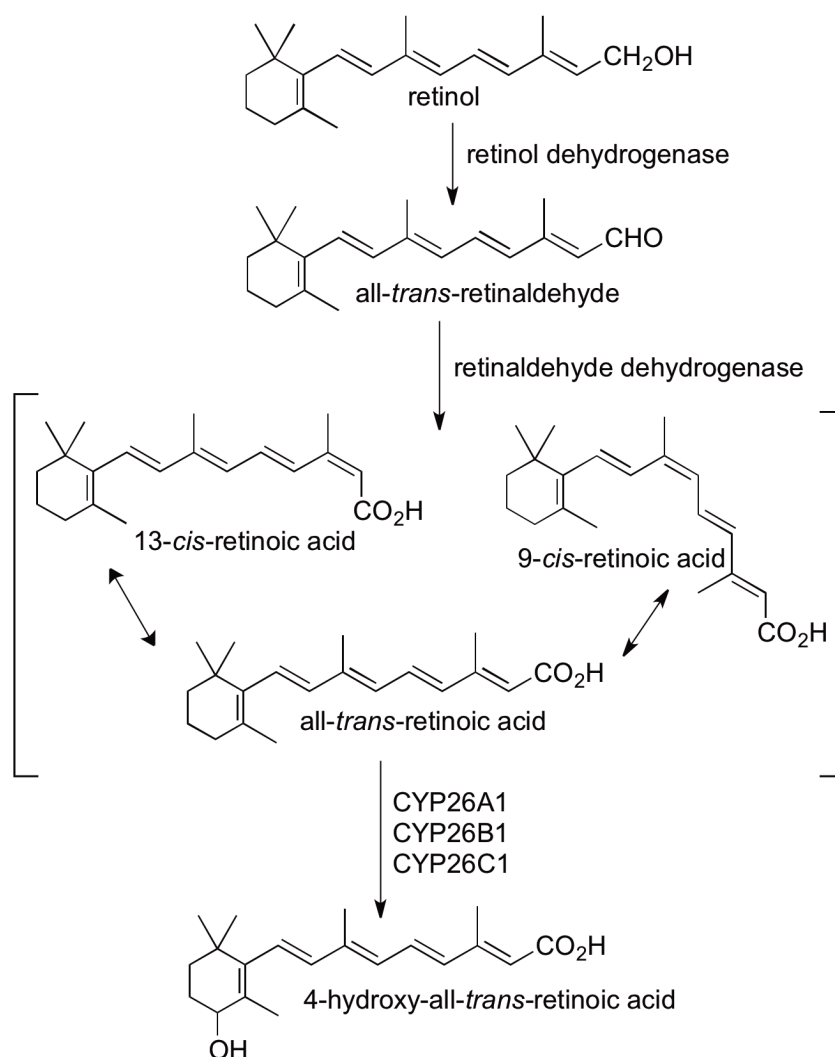


Figure 1.6. The synthesis of retinoic acid from retinol and metabolism by CYP26 enzymes. Retinol (vitamin A) is oxidized to all-*trans*-retinaldehyde by retinol dehydrogenase, which is subsequently oxidized by retinaldehyde dehydrogenase to retinoic acid. Retinoic acid can chemically exist as several different geometric isomers, including 13-*cis*-retinoic acid, 9-*cis*-retinoic acid, and all-*trans*-retinoic acid. All-*trans*-retinoic acid represents the biologically most active metabolite of vitamin A and is metabolized to 4-hydroxy-all-*trans*-retinoic acid by CYP26 enzymes.

atRA to 4-OH-RA. Though several P450 enzymes have been documented for their ability to metabolize RA, the enzymes CYP26A1 and CYP26B1 appear to be the most dedicated to the oxidative metabolism of *atRA* to 4-OH-RA, in addition to being *atRA*-inducible.²⁴⁻²⁶

Pharmacological doses of RAs are useful in the treatment of some types of cancers and dermatological conditions by restoring normal differentiation responses within abnormal cells. *All-trans*-RA (*at*RA or tretinoin) is approved to induce cytodifferentiation and decrease proliferation of acute promyelocytic leukemia, while the RA isomer 13-*cis*-RA (isotretinoin) is used for treatment of severe acne that has been unresponsive to other forms of treatment. Unfortunately, RA resistance is often experienced in patients undergoing prolonged RA-based therapy. Part of this resistance is due to increased plasma clearance of *at*RA, for which P450 enzymes such as the CYP26s are known to play a dominant role. Therefore, an emerging strategy in the field of cancer chemoprevention and treatment is preventing *in vivo* metabolism of *at*RA through inhibition of CYP26 enzymes. P450 inhibitors designed for this purpose are referred to as retinoic acid metabolism blocking agents (RAMBAs).

Liarozole (**1**; Figure 1.7) is the most studied RAMBA and the first RAMBA to be approved for clinical use. It was originally identified as a modest inhibitor of *at*RA hydroxylation *in vitro* (IC_{50} =2.2-6.0 μ M) by researchers at Janssen Research Foundation.²⁷ As a result, it was developed clinically for the treatment of both metastatic prostate cancer and ER-negative metastatic breast cancer, and has additionally been extensively investigated as a potential agent for the treatment of dermatological diseases such as psoriasis and ichthyosis.²⁷ Its development for the treatment of cancer, however, was eventually discontinued due to its lack of P450 enzyme specificity and the fact that it only demonstrates moderate potency as an *at*RA 4-hydroxylase inhibitor.²⁸

Since liarozole's failure in the clinic, significant efforts have been made to obtain RAMBAs that demonstrate enhanced specificity. These efforts have resulted in the development

of several compounds that demonstrate potent, nanomolar inhibition of *atRA* hydroxylation *vitro* with greater selectivity towards *atRA* metabolizing enzymes than liarozole. Examples include the highly potent second generation benzothiazole inhibitors R115866 and R116010 developed by researchers at Johnson and Johnson Pharmaceuticals (previously Janssen Research Foundation). R115866 (**2**; Figure 1.7) is reported to be highly selective for CYP26 and to potently inhibit CYP26A1 with an IC_{50} of 4 nM, which is nearly 1000-fold more potently than liarozole.²⁹ R116011 (**3**; Figure 1.7) is a dimethylamino derivative of R115866 and is reported to potently inhibit *atRA* metabolism catalyzed by CYP26A1 with an IC_{50} of 8.7 nM while

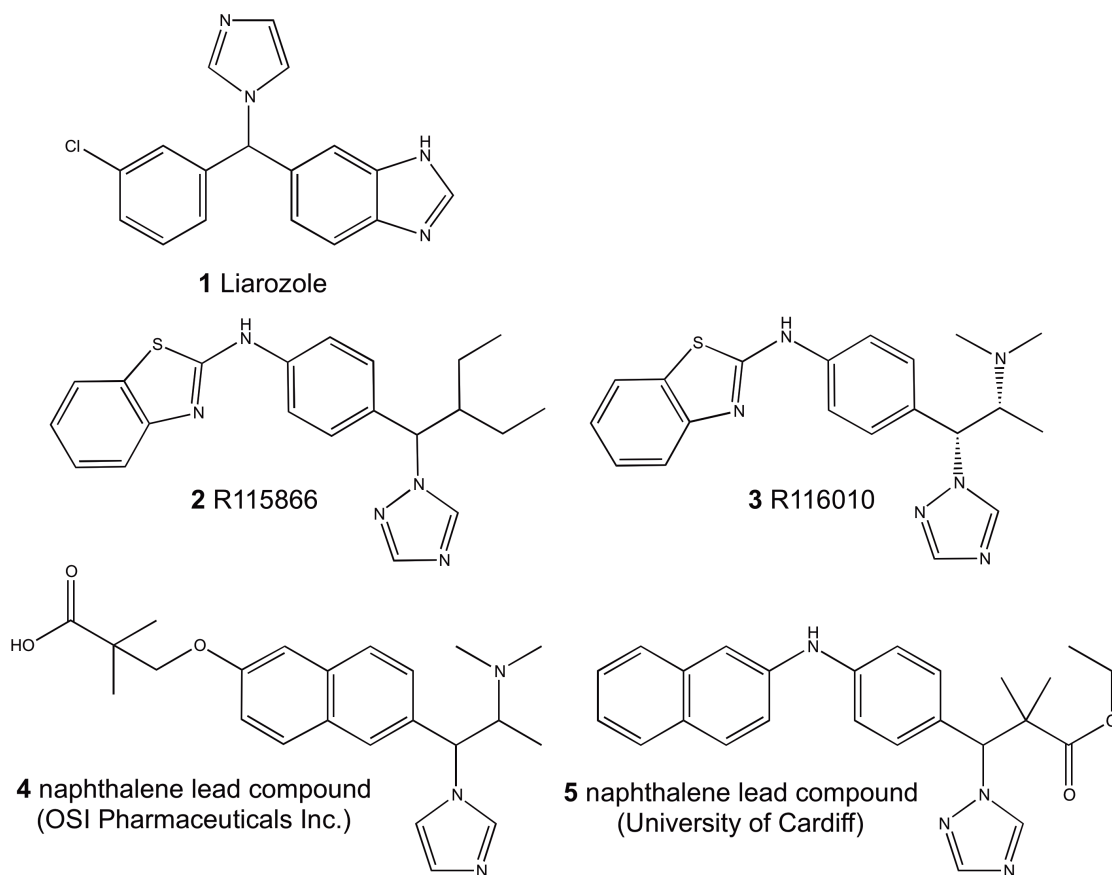


Figure 1.7. Retinoic acid metabolism blocking agents designed for the inhibition of CYP26. Structures of Liarazole (**1**), R115866 (**2**), R116010 (**3**), and naphthalene lead compounds identified by researchers at OSI Pharmaceuticals Inc. (**4**) and University of Cardiff (**5**).

maintaining selectivity against human P450 enzymes CYP19, CYP2C11, CYP2A1, CYP3A, and CYPB1/2.³⁰

The 2,6-disubstituted naphthalenes are one of the newest classes of novel RAMBAs and are based on the fusion of the imidazolyl propylamino moiety of R116010 with a naphthalene core with a substitution at the 6-position. This class of compounds was first introduced by researchers at OSI Pharmaceuticals, whose lead compound (**4**) demonstrated an IC₅₀ of 20 nM against CYP26A1-mediated *atRA* metabolism and favorable selectivity for CYP26 over CYP3A4, CYP1A2, CYP2D6, and CYP2C9.³¹ The most recent naphthyl-based RAMBAS to be reported come from a series of 3-(*1H*-imidazol- and triazol-1-yl) -2,2-dimethyl-3-[4-(naphthalen-2-ylamino)phenyl]propyl derivatives developed by researchers at the University of Cardiff, UK.³² All of these latter derivatives that were tested demonstrated inhibition of CYP26A1 equal to or better than R116010. The leading compound, a triazole ester derivative (**5**), demonstrated nearly 30-fold increased potency (IC₅₀=0.35 nM) compared to R116010, while retaining almost identical P450 selectivity against P450 enzymes CYP1A2, CYP2C9, CYP2C19, and CYP2D6.³²

It remains to be seen how the results of the *in vitro* studies of the various 2,6-disubstituted naphthalene inhibitors translate *in vivo* and to what extent R116010 and R115866 will be developed in the clinic, but the high inhibitory potencies and selectivity for CYP26A1 suggest that they will be less likely to produce the unwanted side effects experienced with lizarozole therapy. However, to facilitate the development of truly selective CYP26 inhibitors and improved RAMBAs, more detailed structural and functional characterization of the CYP26 family of enzymes is needed. Aside from their dominant role as *atRA*-hydroxylases, very little is known about their structures, metabolic pathways, or kinetics. Present limitations in CYP26 research are due, in large part, to that fact that like all P450 enzymes, CYP26 enzymes are

membrane-bound proteins, which makes them both difficult to express recombinantly and to purify. As a result, the majority of CYP26 research conducted to date has relied on assays conducted with transfected cells or microsomal fractions prepared from tissue samples or cultured cells.^{25,32-35} These studies provide only limited structural and functional data based on the scarce quantities and low purity of these types of enzyme preparations. As a result, the immediate goal of this second project was the production of recombinant CYP26 enzyme that exceeded the yield and purity attainable by previous methods.

Our approach to building a new method for the production of pure CYP26 enzymes was to apply techniques that have proven successful in the expression and purification of other membrane-bound P450 enzymes in *E. coli*, including the use of detergents and stabilizing ligands specific to the CYP26 enzymes. In following with literature precedence for the other mammalian P450 enzymes, the amino acid sequences of the CYP26 enzymes were modified to facilitate recombinant expression in *E. coli* and purification by metal affinity chromatography. The detergents sodium cholate and Tergitol NP-10 were used based on their demonstrated utility in the purification of CYP26 enzymes expressed recombinantly in insect cells.^{24,36} Further efforts to optimize CYP26 expression and purification incorporated the use of the endogenous substrate RA, the clinically developed RAMBA liarozole, and representative compounds within the 3-(*1H*-imidazol- and triazol- 1-yl)-2,2-dimethyl-3-[4-(naphthalen-2-ylamino)phenyl]propyl series of inhibitors to facilitate protein stability by occupying the protein's active site. Together, the application of proven methods for the expression and purification of other mammalian truncated P450 enzymes with the use of detergents and stabilizing ligands specific for the CYP26 enzymes provided a rational approach for generating significant amounts of pure protein. It was

envisioned that development of such a protocol would enable basic structural and kinetic studies to facilitate the development of enhanced RAMBAs for the treatment of cancer.

References

1. Williams, D.A. (2008) Drug metabolism. in *Foye's Principles of Medicinal Chemistry*, (ed. Thomas, L.L.) 253-285 (Lippincott Williams & Wilkins, Philadelphia).
2. Nebert, D.W. and Nelson, D.R. (1991) P450 gene nomenclature based on evolution. *Methods Enzymol.* **206**, 3-11.
3. Stark, K. and Guengerich, F.P. (2007) Characterization of orphan human cytochromes P450. *Drug Metab. Rev.* **39**, 627-637.
4. Guengerich, F.P. and Cheng, Q. (2011) Orphans in the human cytochrome P450 superfamily: approaches to discovering functions and relevance in pharmacology. *Pharmacol Rev* **63**, 684-99.
5. Lewis, D.F.V. (2001) Substrate selectivity and metabolism. in *Guide to Cytochromes P450 Structure and Function* 76-117 (Taylor & Francis Inc., New York).
6. Guengerich, F.P. (2003) Cytochromes P450, drugs, and diseases. *Mol. Interventions* **3**, 194-204.
7. Guengerich, F.P. (2005) Human cytochrome P450 enzymes. in *Cytochrome P450: Structure, Mechanism, and Biochemistry*, (ed. Ortiz de Montellano, P.R.) 377-463 (Kluwer Academic/ Plenum Publishers, New York).
8. Williams, P.A., Cosme, J., Ward, A., Angove, H.C., Vinkovic, D.M. and Jhoti, H. (2003) Crystal structure of human cytochrome P450 2C9 with bound warfarin. *Nature (London, U. K.)* **424**, 464-468.
9. Makris, T.M., Denisov, I., Schlichting, I. & Sligar, S.G. (2005) Activation of molecular oxygen by cytochrome P450. in *Cytochrome P450: Structure, Mechanism, and Biochemistry*, (ed. Ortiz de Montellano, P.R.) 149-182 (Kluwer Academic/ Plenum Publishers, New York).
10. Jambhekar, S.S. (2008) Physiochemical and biopharmaceutical properties of drug substances and pharmacokinetics. in *Foye's Principles of Medicinal Chemistry*, (ed. Lemke, T.L.) 210-252 (Lippincott Williams & Wilkins, Philadelphia).
11. Khojasteh, S.C., Prabhu, S., Kenny, J.R., Halladay, J.S. and Lu, A.Y.H. (2011) Chemical inhibitors of cytochrome P450 isoforms in human liver microsomes: a re-evaluation of P450 isoform selectivity. *Eur. J. Drug Metab. Pharmacokinet.* **36**, 1-16.
12. Ding, X. and Kaminsky, L.S. (2003) Human extrahepatic cytochromes P450: function in xenobiotic metabolism and tissue-selective chemical toxicity in the respiratory and gastrointestinal tracts. *Annu. Rev. Pharmacol. Toxicol.* **43**, 149-173.
13. Smith, B.D., Sanders, J.L., Porubsky, P.R., Lushington, G.H., Stout, C.D. and Scott, E.E. (2007) Structure of the human lung cytochrome P 450 2A13. *J. Biol. Chem.* **282**, 17306-17313.
14. Su, T., Bao, Z., Zhang, Q.-Y., Smith, T.J., Hong, J.-Y. and Ding, X. (2000) Human cytochrome P450 CYP2A13: predominant expression in the respiratory tract and its high efficiency metabolic activation of a tobacco-specific carcinogen, 4-(methylnitrosamino)-1-(3-pyridyl)-1-butanone. *Cancer Research* **60**, 5074-5079.

15. Bao, Z., He, X.-Y., Ding, X., Prabhu, S. and Hong, J.-Y. (2005) Metabolism of nicotine and cotinine by human cytochrome P450 2A13. *Drug Metab. Dispos.* **33**, 258-261.
16. Fukami, T., Katoh, M., Yamazaki, H., Yokoi, T. and Nakajima, M. (2008) Human cytochrome P450 2A13 efficiently metabolizes chemicals in air pollutants: naphthalene, styrene, and toluene. *Chem. Res. Toxicol.* **21**, 720-725.
17. Nakajima, M., Itoh, M., Sakai, H., Fukami, T., Katoh, M., Yamazaki, H., Kadlubar, F.F., Imaoka, S., Funae, Y. and Yokoi, T. (2006) CYP2A13 expressed in human bladder metabolically activates 4-aminobiphenyl. *Int. J. Cancer* **119**, 2520-2526.
18. He, X.-Y., Tang, L., Wang, S.-L., Cai, Q.-S., Wang, J.-S. and Hong, J.-Y. (2006) Efficient activation of aflatoxin B1 by cytochrome P450 2A13, an enzyme predominantly expressed in human respiratory tract. *Int. J. Cancer* **118**, 2665-2671.
19. Hecht, S.S. (2003) Tobacco carcinogens, their biomarkers and tobacco-induced cancer. *Nat. Rev. Cancer* **3**, 733-744.
20. Hoffmann, D., Brunnemann, K.D., Prokopczyk, B. and Djordjevic, M.V. (1994) Tobacco-specific N-nitrosamines and areca-derived N-nitrosamines: chemistry, biochemistry, carcinogenicity, and relevance to humans. *J. Toxicol. Environ. Health* **41**, 1-52.
21. Hecht, S.S. (1998) Biochemistry, biology, and carcinogenicity of tobacco-specific N-nitrosamines. *Chem. Res. Toxicol.* **11**, 559-603.
22. Gudas, L.J., Sporn, M.B. and Roberts, A.B. (1994) Cellular biology and biochemistry of the retinoids. 443-520 (Raven).
23. Abu-Abed, S., Dolle, P., Metzger, D., Beckett, B., Chambon, P. and Petkovich, M. (2001) The retinoic acid-metabolizing enzyme, CYP26A1, is essential for normal hindbrain patterning, vertebral identity, and development of posterior structures. *Genes Dev.* **15**, 226-240.
24. Topletz, A.R., Thatcher, J.E., Zelter, A., Lutz, J.D., Tay, S., Nelson, W.L. and Isoherranen, N. (2012) Comparison of the function and expression of CYP26A1 and CYP26B1, the two retinoic acid hydroxylases. *Biochem. Pharmacol.* **83**, 149-163.
25. White, J.A., Guo, Y.D., Baetz, K., Beckett-Jones, B., Bonasoro, J., Hsu, K.E., Dilworth, F.J., Jones, G. and Petkovich, M. (1996) Identification of the retinoic acid-inducible all-trans-retinoic acid 4-hydroxylase. *J Biol Chem* **271**, 29922-7.
26. White, J.A., Ramshaw, H., Taimi, M., Stangle, W., Zhang, A., Everingham, S., Creighton, S., Tam, S.-P., Jones, G. and Petkovich, M. (2000) Identification of the human cytochrome P450, P450RAI-2, which is predominantly expressed in the adult cerebellum and is responsible for all-trans-retinoic acid metabolism. *Proc. Natl. Acad. Sci. U. S. A.* **97**, 6403-6408.
27. Njar, V.C.O. (2008) Retinoids in clinical use. *Methods Princ. Med. Chem.* **39**, 389-407.
28. Njar, V.C.O., Gediya, L., Purushottamachar, P., Chopra, P., Belosay, A. and Patel, J.B. (2006) Retinoids in clinical use. *Med. Chem.* **2**, 431-438.
29. Stoppie, P., Borgers, M., Borghgraef, P., Dillen, L., Goossens, J., Sanz, G., Szel, H., Van, H.C., Van, N.G., Nobels, G., Vanden, B.H., Venet, M., Willemsens, G. and Van, W.J. (2000) R115866 inhibits all-trans-retinoic acid metabolism and exerts retinoidal effects in rodents. *J. Pharmacol. Exp. Ther.* **293**, 304-312.
30. Van, H.J., Van, G.R., Bruwiere, H., Moelans, P., Janssen, B., Floren, W., van, d.L.B.J., van, D.J., Sanz, G., Venet, M., Dillen, L., Van, H.C., Willemsens, G., Janicot, M. and

- Wouters, W. (2002) Inhibition of all-TRANS-retinoic acid metabolism by R116010 induces antitumor activity. *Br. J. Cancer* **86**, 605-611.
31. Mulvihill, M.J., Kan, J.L.C., Beck, P., Bittner, M., Cesario, C., Cooke, A., Keane, D.M., Nigro, A.I., Nillson, C., Smith, V., Srebernak, M., Sun, F.-L., Vrkljan, M., Winski, S.L., Castelhana, A.L., Emerson, D. and Gibson, N. (2005) Potent and selective [2-imidazol-1-yl-2-(6-alkoxy-naphthalen-2-yl)-1-methyl-ethyl]-dimethyl-amines as retinoic acid metabolic blocking agents (RAMBAs). *Bioorg. Med. Chem. Lett.* **15**, 1669-1673.
 32. Gomaa, M.S., Bridgens, C.E., Veal, G.J., Redfern, C.P.F., Brancale, A., Armstrong, J.L. and Simons, C. (2011) Synthesis and biological evaluation of 3-(1H-imidazol- and triazol-1-yl)-2,2-dimethyl-3-[4-(naphthalen-2-ylamino)phenyl]propyl derivatives as small molecule inhibitors of retinoic acid 4-hydroxylase (CYP26). *J. Med. Chem.* **54**, 6803-6811.
 33. Chithalen, J.V., Luu, L., Petkovich, M. and Jones, G. (2002) HPLC-MS/MS analysis of the products generated from all-trans-retinoic acid using recombinant human CYP26A. *J. Lipid Res.* **43**, 1133-1142.
 34. Helvig, C., Taimi, M., Cameron, D., Jones, G. and Petkovich, M. (2011) Functional properties and substrate characterization of human CYP26A1, CYP26B1, and CYP26C1 expressed by recombinant baculovirus in insect cells. *J. Pharmacol. Toxicol. Methods* **64**, 258-263.
 35. White, J.A., Beckett-Jones, B., Guo, Y.-D., Dilworth, F.J., Bonasoro, J., Jones, G. and Petkovich, M. (1997) cDNA cloning of human retinoic acid-metabolizing enzyme (hP450RAI) identifies a novel family of cytochromes P450 (CYP26). *J. Biol. Chem.* **272**, 18538-18541.
 36. Lutz, J.D., Dixit, V., Yeung, C.K., Dickmann, L.J., Zelter, A., Thatcher, J.E., Nelson, W.L. and Isoherranen, N. (2009) Expression and functional characterization of cytochrome P 450 26A1, a retinoic acid hydroxylase. *Biochem. Pharmacol.* **77**, 258-268.

Chapter 2

Methods

Introduction

The studies summarized within Chapters 3 and 4 have several methods in common. For the most part, these methods consist of common biochemical research techniques or have been generated based on established protocols within the cytochrome P450 field. Modifications to these protocols were made according to the enzymes that served as the subjects of these studies and the instrumentation available within the lab. As a result, the methods described within this chapter are applicable to studies of the CYP2A subfamily proteins (Chapter 3) as well as the CYP26 family of proteins (Chapter 4). Methods specific to a single project, in contrast, can be found in the individual project chapters. This includes, but is not limited to, the engineering of plasmid DNA of individual P450 enzymes, optimization of a protocol for the expression and purification of the CYP26 proteins, as well as assays characterizing metabolism by CYP26 enzymes or inhibition of CYP2A enzymes.

Plasmid Transformation and Expression of Cytochrome P450 Proteins in *E. coli*

Transformation

The pKK233-3 plasmids containing the respective modified P450 genes (for CYP2A proteins see references (1,2); for CYP26 proteins see Chapter 4) were transformed into *E. coli* tetracycline-resistant TOPP-3 cells (Stratagene, La Jolla, CA) using the following procedure. To begin, *E. coli* TOPP-3 chemically competent cells (50 μ L) were incubated on ice for 40 minutes with 0.5 μ L pKKP450 plasmid, followed by heat shock at 42 °C for 30 seconds to facilitate uptake of the DNA. Next, super optimal catabolite repressive (SOC) media (1 mL) containing 1.7 μ L of 10% β -mercaptoethanol (BME) was added to the cells, which were then incubated at

37 °C for an hour with shaking at 250 rpm. Following this recovery period, brief centrifugation at 10,000 x g was used to pellet the cells, and all but ~100 µL of supernatant was removed. In the final step, the pelleted cells were resuspended in the remaining supernatant and spread on Lysogeny Broth (LB) plates containing 50 µg/mL ampicillin. Plates were incubated overnight at 37 °C to grow isolated colonies.

Expression

Cytochrome P450 proteins were expressed recombinantly in *E. coli* TOPP-3 cells based on procedures described by others.¹⁻³ To begin, a single colony selected from the overnight plate was used to inoculate 5 mL of LB media containing 50 µg/mL ampicillin and 25 µg/mL tetracycline. This culture was incubated at 37 °C with shaking at 250 rpm for approximately 8 hours. Two larger cultures of LB media were then grown by inoculating 50 µL of the 5 mL culture into 200 mL LB media containing 50 µg/mL ampicillin and 12.5 µg/mL tetracycline. These 200 mL starter cultures were grown at 37 °C with shaking at 250 rpm overnight. The final scale-up was accomplished by introducing 15 mL of the 200 mL overnight starter cultures into each of 18 1L-flasks containing 225 mL of Terrific Broth (TB) media, 25 mL of TB salts, and 50 µg/mL ampicillin. These expression cultures were grown for approximately 2 hours at 37 °C with shaking at 250 rpm until an OD₆₀₀ of 1.0-1.5 was reached. Cytochrome P450 expression was initiated at that point by adding 240 µg/mL isopropyl β-D-1-thiogalactopyranoside, and heme generation was facilitated with the addition of 80 µg/mL δ-aminolevulinic acid (ALA). These expression cultures were incubated for a total of three days at a reduced temperature of 30 °C with shaking at 190 rpm. Following the third day of expression, the cells were harvested by centrifugation at 6,500 x g for 10 minutes. The cell pellets were collected into 50 mL conical tubes and stored at -80 °C until purification.

Cytochrome P450 Protein Purification

CYP2A6 and CYP2A13 were purified using a standard protocol developed and optimized previously.^{1,3} Each of the CYP26 proteins of interest were initially purified using the same protocol used for the purification of CYP2A proteins. This standard protocol was further optimized for the purification of the CYP26 proteins to maximize protein yield. The standard purification protocol is described in detail below, whereas the optimization to the standard protocol for the CYP26 proteins can be found in the methods section of Chapter 4: Expression and Purification of the Cytochrome P450 26 Family of Enzymes.

The isolation of membrane-associated P450 protein was accomplished by a combination of approaches including: enzymatic lysis, flash freezing, homogenization, sonication, detergent solubilization, and centrifugation.⁴ To begin with, the frozen cell pellet was thawed and resuspended in 200 mL of 20 mM potassium phosphate, pH 7.4, containing 20% glycerol. Spheroplasts were then produced by treating the suspension for 30 min with 0.3 mg/mL lysozyme with stirring at 4 °C and adding an equal volume of cold water to the stirring mixture. After stirring at 4 °C for 10 min, these spheroplasts were pelleted by centrifugation at 10,000 x g for 15 min at 4 °C. The spheroplasts were then lysed by freezing the pellets *in situ* using either a liquid nitrogen bath or a dry ice/ethanol slurry. The frozen pellets were thawed, suspended in 100 mL of 500 mM potassium phosphate, pH 7.4, containing 20% glycerol, and homogenized by hand. The resulting suspension was sonicated using three 30 sec pulses with 60 sec of cooling on ice between pulses. The material was then centrifuged at 10,000 x g for 15 min at 4 °C, and the protein within the resulting supernatant fraction was solubilized by treatment with a detergent with stirring at 4 °C for 30 minutes. For the CYP2A proteins, the detergent employed was

Cymal-5 at a concentration of 4.8 mM (twice the critical micellar concentration). Optimization of the standard protocol for CYP26 proteins involved the use of 1% each of Tergitol (type NP-10) and sodium cholate. The solution was then centrifuged at 100,000 x g for 60 min at 4 °C to separate the solubilized P450 protein from the membrane lipids.

Following successful isolation from the membrane, P450 protein was purified using successive chromatographic steps on an ÄKTApurifier 10 FPLC system (GE HealthCare, Umeå, Sweden) by means of immobilized metal affinity chromatography and cation exchange chromatography. While both chromatographic steps were applied to the purification of CYP2A proteins used in kinetic studies, it should be noted that CYP26 protein was rarely recovered from the NiNTA column in high enough yield to allow for a second chromatographic step. The first column in the purification scheme was a nickel nitrilotriacetic acid (NiNTA) immobilized metal affinity column (Qiagen, Valencia, CA), since the 4X-histidine tag engineered onto the C-terminus of the P450 enzymes has a highly selective interaction with Ni^{2+} . This interaction allows for rapid and effective isolation of His-tagged P450 protein from most other proteins. The solubilized P450-containing solution was loaded onto a NiNTA column that had been equilibrated with loading buffer (100 mM potassium phosphate, pH 7.4, 20% glycerol, 0.2 M NaCl, 4.8 mM Cymal-5). Non-specifically bound fractions were removed from the column by a two-column volume wash of loading buffer. Impurities with a weak affinity for the NiNTA column were removed by an 8 mM histidine wash buffer (100 mM potassium phosphate, pH 7.4, 20% glycerol, 0.2 M NaCl, 4.8 mM Cymal-5, 8 mM histidine), although the wash buffer at this step was substituted with loading buffer for the purification of CYP26 proteins. His-tagged P450 protein was eluted from the NiNTA column with an 80 mM histidine elution buffer (10 mM

potassium phosphate, pH 7.4, 20% glycerol, 0.1 M NaCl, 4.8 mM Cymal-5, 80 mM histidine, 2 mM EDTA).

The carboxymethyl (CM) sepharose cation exchange column (GE HealthCare, Umeå, Sweden) employed in the next step served to further purify the P450 proteins based on charge-charge interactions. Given a buffer pH of 7.4 and an isoelectric point (pI) of ~9 for CYP26 and CYP2A proteins, the negatively charged resin of the CM column binds efficiently to the overall positively charged P450 proteins. Fractions containing the most P450 (as evaluated by absorbance at 418 nm) following NiNTA chromatography were pooled, diluted three times with buffer (5 mM potassium phosphate, pH 7.4, with 20% glycerol, 4.8 mM Cymal-5, and 1 mM EDTA) to reduce the ionic strength, and loaded onto a HiTrap CM-Sepharose Fast Flow column that had been equilibrated with the same buffer. A ten-column-volume wash with CM wash buffer (50 mM potassium phosphate pH 7.4, 1 mM EDTA, 20% glycerol) was used to remove impurities and detergent, and the P450 protein was eluted from the column with a buffer containing high salt (50 mM potassium phosphate, pH 7.4, 20% glycerol, 500 mM NaCl, 1 mM EDTA). The final concentrations of P450 proteins were determined using the absolute absorbance at 417 nm and the reduced carbon monoxide difference spectrum.

Spectroscopic Analysis for the Quantitation of Cytochrome P450

The absolute absorption and reduced carbon monoxide difference spectra were both collected using a UV-2101 UV-visible scanning spectrophotometer (Shimadzu Scientific Instruments, Inc., Columbia, MD) and the general methods of Omura and Sato.⁵ To determine the absolute absorption, buffer corresponding to the protein sample (800 μ L) was placed into a cuvette, the absorbance at 700 nm was set to zero, and a baseline was collected from 700-250 nm. Protein sample (100 μ L) was then added to the cuvette and mixed with the buffer by

inversion. The absorbance at 700 nm was set to zero a final time before the sample was scanned from 700-250 nm. The sample was analyzed to determine the concentration of P450 present using Beer's Law: $c = A / \epsilon * l$ where c is the concentration in μM , l is the pathlength (1 cm), A is the absorption, and ϵ is the extinction coefficient ($0.100 \mu\text{M}^{-1} \text{cm}^{-1}$).

To determine the reduced carbon monoxide difference spectrum, 100 μL of protein solution was diluted into 800 μL of buffer corresponding to the protein sample in a 1 cm pathlength cuvette. The protein sample was reduced by the addition of a small amount of dithionite, mixed by inversion, and placed into the spectrophotometer. The absorbance at 500 nm was set to zero, and a baseline was collected from 500-400 nm. The reduced sample was removed from the spectrophotometer and further prepared by introducing ~50 bubbles of carbon monoxide into the solution. The sample was then returned to the spectrophotometer, the absorbance at 500 nm set to zero, and the difference spectrum from 500-400 nm measured. As necessary, the spectrum was measured every few minutes until the increase in absorbance at 450 nm reached a maximum. The sample was analyzed to determine the concentration of P450 present using Beer's Law: $c = A / \epsilon * l$ where c is the concentration in μM , l is the pathlength (1 cm), A is the absorption, and ϵ is the extinction coefficient ($0.091 \mu\text{M}^{-1} \text{cm}^{-1}$).

References

1. DeVore, N.M., Smith, B.D., Urban, M.J. and Scott, E.E. (2008) Key residues controlling phenacetin metabolism by human cytochrome P450 2A enzymes. *Drug Metab. Dispos.* **36**, 2582-2590.
2. Scott, E.E., Spatzenegger, M. and Halpert, J.R. (2001) A truncation of 2B subfamily cytochromes P450 yields increased expression levels, increased solubility, and decreased aggregation while retaining function. *Arch. Biochem. Biophys.* **395**, 57-68.
3. Smith, B.D., Sanders, J.L., Porubsky, P.R., Lushington, G.H., Stout, C.D. and Scott, E.E. (2007) Structure of the human lung cytochrome P 450 2A13. *J. Biol. Chem.* **282**, 17306-17313.
4. Wester, M.R., Stout, C.D. and Johnson, E.F. (2002) Purification and crystallization of N-terminally truncated forms of microsomal cytochrome P450 2C5. *Methods Enzymol.* **357**, 73-79.

5. Omura, T. and Sato, R. (1964) Carbon monoxide-binding pigment of liver microsomes. I. Evidence for its hemoprotein nature. *J. Biol. Chem.* **239**, 2370-8.

Chapter 3

Evaluation of Inhibition Selectivity for Human Cytochrome P450 2A Enzymes

Introduction

While xenobiotic metabolism by cytochrome P450 enzymes is often a detoxifying event, P450 enzymes can also activate toxins and procarcinogens. To evaluate the involvement of individual P450 enzymes in drug metabolism or activation of potentially harmful chemical agents *in vivo*, a test compound is often incubated with human microsomes in the presence and absence of potent and selective inhibitors for the individual P450 enzymes expressed therein. This phenotyping process is widely used, but is critically dependent on the selectivity of the inhibitors employed. Despite the substantial overlapping substrate selectivity demonstrated by xenobiotic-metabolizing P450 enzymes, broad efforts have resulted in the identification of sufficiently selective inhibitors for many of the major human hepatic P450 enzymes, including CYP1A2, CYP2B6, CYP2C8, CYP2C9, CYP2C19, CYP2D6, and CYP3A4.¹

In *extrahepatic* tissues, however, discrimination between the roles of individual P450 enzymes is much more difficult for two reasons: 1) information about the expression of individual P450 proteins in the given tissue is often incomplete and 2) selective inhibitors are not well developed for most non-hepatic P450 enzymes. This is particularly true in the human lung and respiratory tract, where at least 16 human P450 enzymes may play a crucial role in the balance between the detoxification and activation of inhaled compounds including environmental pollutants, industrial chemicals, therapeutic agents, and chemicals in cigarette smoke.^{2,3}

In lung tissue, the dissection of individual P450 contributions can be difficult because more than one protein from the same P450 subfamily is often present and their activities can be very similar. This is the case with the CYP2A6 and CYP2A13 enzymes of the CYP2A family,

whose detection is complicated by the cross-reactive nature of commercially available CYP2A antibodies.⁴ As a result, reliable information about relative CYP2A expression has been derived from mRNA. CYP2A13 is expressed to a greater extent in the respiratory tract, with ~5-fold higher mRNA levels in nasal mucosa and ~9-fold higher mRNA levels in lung compared to CYP2A6.⁴ In contrast, CYP2A6 expression is higher in human liver, with mRNA levels exceeding CYP2A13 by ~1900-fold.⁴ Thus, the relative contribution of CYP2A13 metabolism and inhibition is likely to be negligible in human liver microsomes, while both CYP2A enzymes may have substantial contribution in respiratory tract microsomes depending on the substrate or inhibitor chosen.

Dissecting the relative metabolic roles of the CYP2A enzymes is further complicated by the fact that CYP2A6 and CYP2A13 share an amino acid sequence identity of 94%.⁵ Although such a high identity lends itself to substantial overlapping substrate selectivity, the CYP2A enzymes also exhibit key functional differences.^{4,6-8} For example, while CYP2A6 has a ten-fold higher enzymatic efficiency (k_{cat}/K_m) compared to CYP2A13 for 7-hydroxylation of coumarin, CYP2A13 much more efficiently metabolizes nicotine and activates the tobacco-related procarcinogen 4-(methylnitrosamino)-1-(3-pyridyl)-1-butanone (NNK) *in vitro*.^{4,6} Thus, CYP2A13- and CYP2A6-selective inhibitors are not only needed to evaluate the metabolism of drugs and other xenobiotic compounds delivered via inhalation, but may also be relevant to studying the tissue-specific activation of procarcinogens in the lung.

To evaluate the respective roles of the CYP2A enzymes in tissues such as the lung where both enzymes are expressed, CYP2A13- and CYP2A6-selective inhibitors are needed. A number of compounds were reported to selectively inhibit CYP2A6 before CYP2A13 was determined to be a functional member of the CYP2A family, or have simply not been tested against CYP2A13.

These compounds include: phenethyl isothiocyanate (PEITC), 4-dimethylaminobenzaldehyde (DMABA), 8-methoxypsoralen (8-MOP), tranylcypromine, tryptamine, pilocarpine, (*S*)-nicotine, (*R*)-(+)-menthofuran, and β -nicotyrine.⁹⁻¹⁴ Although a few of these inhibitors have now been tested for their ability to inhibit CYP2A13, these studies were conducted using a variety of experimental methods and protein preparations that make it difficult to directly compare CYP2A inhibition selectivity.^{6,15,16} More recent work has identified several additional inhibitors reportedly selective for CYP2A6, but which have not been evaluated for their ability to inhibit CYP2A13.¹⁷

To address this gap in knowledge, the following study was designed to evaluate traditionally employed CYP2A6-selective inhibitors for their ability to discriminate between CYP2A6 and CYP2A13 using parallel assays for the inhibition of *para*-nitrophenol (*p*NP) 2-hydroxylation (Figure 3.1). The relative impact of these inhibitors on CYP2A6 and CYP2A13 function was evaluated by determining K_i values and modes of

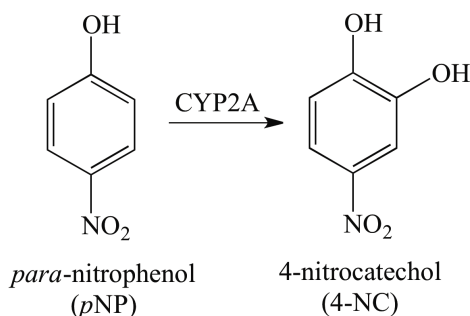


Figure 3.1 *para*-Nitrophenol 2-hydroxylation catalyzed by human CYP2A enzymes. Oxidative metabolism of *p*NP by CYP2A enzymes produces the metabolite 4-NC.

inhibition for each of the compounds against both enzymes, followed by the calculation of a selectivity factor. The results of these studies serve as the first explicit determination of the selectivity of these compounds for enzymes within the CYP2A family. This information can be used to identify inhibitors with the greatest potential for determining whether CYP2A6 or CYP2A13 is responsible for the metabolism or activation of compounds, such as tobacco-derived NNK in the human respiratory tract.

Materials and Methods

Inhibition Assays

The compound *para*-nitrophenol (*p*NP) was the substrate for inhibition assays used to evaluate the selectivity of CYP2A inhibitors. *p*NP was employed instead of the more traditional CYP2A substrate coumarin because the CYP2A enzymes catalyze the metabolism of *p*NP with more similar catalytic efficiency compared to that of coumarin. CYP2A6 and CYP2A13 have respective catalytic efficiencies (k_{cat}/K_m) of $0.12 \mu\text{M}^{-1}\text{min}^{-1}$ and $0.19 \mu\text{M}^{-1}\text{min}^{-1}$ for the metabolism of *p*NP. In contrast, the catalytic efficiency for the metabolism of coumarin by CYP2A6 ($0.53 \mu\text{M}^{-1}\text{min}^{-1}$) is nearly 5-fold higher than that of CYP2A13 for the same reaction ($0.11 \mu\text{M}^{-1}\text{min}^{-1}$). The more similar catalytic efficiency that both enzymes demonstrate for the metabolism of *p*NP allows for a more straightforward analysis of the ability of each compound to inhibit CYP2A6 versus CYP2A13.

*p*NP is converted to 4-nitrocatechol (4-NC) by both CYP2A6 and CYP2A13 (Figure 3.1). Inhibition assays used a reconstituted protein system (RPS) consisting of 50 pmol of purified CYP2A protein incubated with 200 pmol NADPH-cytochrome P450 reductase and 100 pmol cytochrome b_5 for 20 minutes at room temperature prior to use. RPS was added to 100 mM potassium phosphate, pH 6.8, with the substrate *p*NP and the desired inhibitor for a total volume of 500 μL . Samples were pre-incubated at 37 °C for 3 minutes before initiating the reactions by the addition of 1 mM NADPH. Reactions were allowed to proceed for 10 minutes at 37 °C and were quenched with 300 μL of 20% trichloroacetic acid and placed on ice. Samples were centrifuged at $4,500 \times g$ for 6 minutes to pellet the protein, and the amount of the 4-nitrocatechol (4-NC) product in the supernatant was determined by absorbance following HPLC separation on a Luna 5 μm C-18 column (Phenomenex, Torrance, CA). A mobile phase of 29% acetonitrile

and 0.2% acetic acid at 0.8 mL/min was used for separation, except for assays with the inhibitor DMABA, which required 26% methanol and 0.2% acetic acid. Detection of absorption at 345 nm revealed elution of the 4-NC product at a retention time of ~6 minutes, while the *p*NP substrate eluted at ~9 minutes. The amount of metabolite was determined by comparing the product peak area to a standard curve of 4-NC (0 μ M - 30 μ M). For preliminary IC₅₀ determinations, CYP2A activity was tested at a range of eight to twelve inhibitor concentrations from 0-1000 μ M at a substrate concentration of 800 μ M. IC₅₀ values were then used to determine the range of concentrations to be used for full kinetic analysis of each inhibitor. For K_i determination, incubations were performed with at least four different concentrations of inhibitor and at least eight different concentrations of substrate (0 μ M - 800 μ M). K_i values are the global fit to at least two separate inhibition experiments.

Kinetic Analysis

The rate of metabolite formation (pmol of metabolite/min/pmol of P450) was plotted against substrate concentration (μ M), and the data were initially fit to the Michaelis-Menten equation using GraphPad Prism 5 (GraphPad Software Inc., San Diego, CA). K_m and V_{max} values were determined and used to assess the mode of inhibition for each compound. Following this analysis, the data was re-fit to the appropriate inhibition equation to determine K_i values (Eq. 3 for competitive inhibition, Eq. 4 for uncompetitive inhibition, and Eq. 5 for mixed inhibition).

$$(3) \quad K_m^{Obs} = K_m \times (1 + [I] / K_i)$$

$$(4) \quad V_{max}^{App} = V_{max} / (1 + I / \text{Alpha} K_i)$$

$$(5) \quad V_{max}^{App} = V_{max} / (1 + I / (\text{Alpha} \times K_i))$$

Goodness of fit was determined using the global R^2 value of the nonlinear regression analysis and inspection of the residuals. A selectivity factor indicating preference for CYP2A6 versus CYP2A13 was calculated by taking the ratio of CYP2A13 K_i / CYP2A6 K_i .

Results

Enzyme Inhibition

Nine compounds have been reported by others to selectively inhibit CYP2A6. These compounds include PEITC, DMABA, 8-MOP, tranlycypromine, tryptamine, pilocarpine, (*S*)-nicotine, (*R*)-(+)-menthofuran, and β -nicotyrine,⁹⁻¹⁴ and were either identified before CYP2A13 was determined to be a functional enzyme of the CYP2A subfamily or have simply not been tested against CYP2A13. As a result, parallel assays for the inhibition of *p*NP 2-hydroxylation were conducted with purified, recombinant CYP2A enzymes to evaluate the ability of each of these compounds to differentially inhibit CYP2A6 and CYP2A13.

Each compound was initially evaluated based on its ability to inhibit CYP2A6 or CYP2A13 at a single concentration. The percentage of enzyme activity remaining in the presence of 800 μ M *p*NP and 400 μ M inhibitor is shown for the different inhibitors in Figure 3.2. Seven of the eight inhibitors tested under these conditions inhibited CYP2A6 and CYP2A13 within a range of 2.2% to 64% remaining activity. The last inhibitor 8-MOP was not soluble at 400 μ M for this comparison, but 3 μ M 8-MOP effectively reduced the function of CYP2A6 to 24% remaining activity and CYP2A13 to 3.1% remaining activity. Aside from 8-MOP, the lowest activity remaining was observed in the presence of tranlycypromine for CYP2A6 and with pilocarpine for CYP2A13. The most activity remaining for both enzymes was observed in the presence of (*S*)-nicotine. In addition, (*S*)-nicotine, DMABA, pilocarpine, PEITC, and β -nicotyrine inhibited both CYP2A enzymes to similar extents, while 8-MOP, tryptamine, tranlycypromine, and

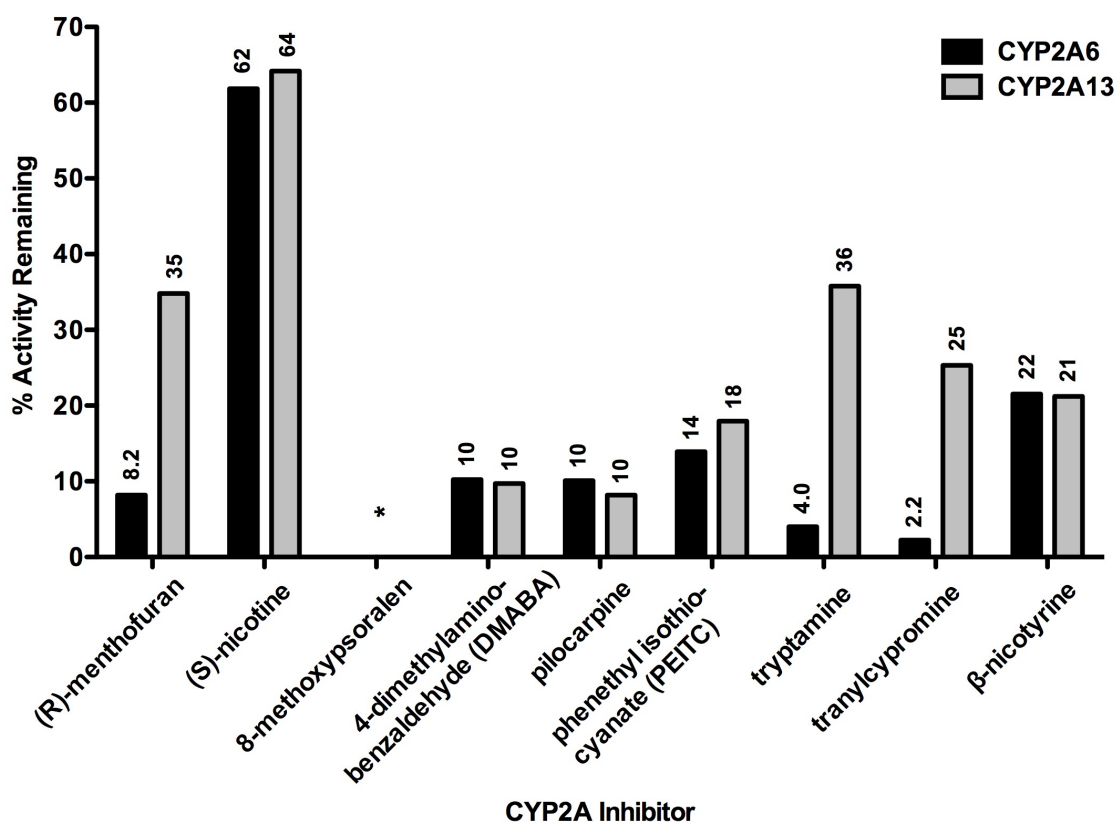
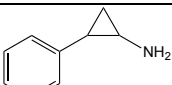
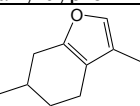
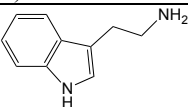
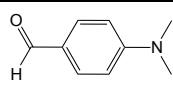
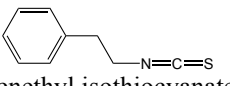
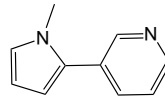
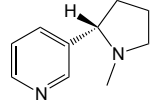
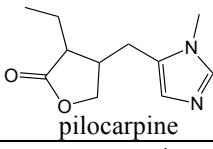
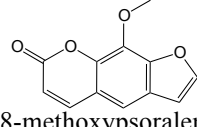


Figure 3.2 Initial evaluation of the selective inhibition of nine previously described CYP2A6 inhibitors for CYP2A6 versus CYP2A13. Percentage of remaining activity is based on the amount of *p*NP (800 μ M) metabolism to 4-NC in the presence of 400 μ M of the various inhibitors shown. The symbol * indicates that the compound was not soluble at 400 μ M in assay buffer. The compound 8-MOP was tested at a maximal concentration of 3 mM, at which point CYP2A6 and CYP2A13 were reduced to 24% and 3.1% of maximal activity, respectively.

menthofuran showed varying selectivity for inhibition of CYP2A6 activity over CYP2A13 activity.

Comparison of each compound's potency for inhibition of CYP2A6 versus CYP2A13 at a single concentration may not be reflective of inhibition over a range of concentrations due to the fact that the modality of inhibition may differ among these inhibitors and between the two enzymes examined. Thus, steady state kinetics were evaluated for both CYP2A6 and CYP2A13 in the presence of each inhibitor and K_i values were determined (Table 3-1). For CYP2A6, K_i values varied from 0.13 to 130 μ M, while K_i values for CYP2A13 ranged from 0.04 to 72 μ M.

Table 3-1. Results of steady state kinetic studies for the evaluation of CYP2A selectivity. Incubations were performed with recombinant, purified CYP2A6 or CYP2A13 reconstituted in a 1:4:2 ratio with P450 reductase and cytochrome b₅ in the presence of four or more different concentrations of inhibitor and eight or more different concentrations of substrate (0 μ M - 800 μ M). K_i values are the global fit to at least two separate inhibition experiments.

Inhibitor	P450	K_i (μ M)	Mechanism (α)	$\frac{2A13 K_i}{2A6 K_i}$
 tranylcypromine	2A13	6.5 ± 1.2	competitive	49
	2A6	0.13 ± 0.02	mixed ($\alpha=10$)	
 (R)-menthofuran	2A13	54 ± 12	mixed ($\alpha=4.3$)	27
	2A6	2.0 ± 0.44	mixed ($\alpha=4.3$)	
 tryptamine	2A13	16 ± 3.5	competitive	9.4
	2A6	1.7 ± 0.12	competitive	
 4-dimethylamino-benzaldehyde (DMABA)	2A13	17 ± 5.0	mixed ($\alpha=13$)	4.6
	2A6	3.6 ± 0.83	mixed ($\alpha=5.5$)	
 phenethyl isothiocyanate (PEITC)	2A13	3.8 ± 1.6	mixed ($\alpha=0.20$)	2.2
	2A6	1.7 ± 0.28	mixed ($\alpha=270$)	
 β -nicotryne	2A13	5.6 ± 0.86	mixed ($\alpha=6.6$)	0.74
	2A6	7.5 ± 2.9	mixed ($\alpha=3.5$)	
 (S)-nicotine	2A13	72 ± 4.6	competitive	0.55
	2A6	130 ± 8.8	competitive	
 pilocarpine	2A13	1.4 ± 0.12	competitive	0.47
	2A6	3.0 ± 0.45	mixed ($\alpha=25$)	
 8-methoxypsoralen (8-MOP)	2A13	0.040 ± 0.009	mixed ($\alpha=1.9$)	0.16
	2A6	0.25 ± 0.10	mixed ($\alpha=3.3$)	

The strongest inhibitors of CYP2A6 are tranlycypromine ($K_i = 0.13 \pm 0.02 \mu\text{M}$) and 8-MOP ($K_i = 0.25 \pm 0.10 \mu\text{M}$), both displaying submicromolar K_i values. The inhibitor 8-MOP was the only inhibitor with a submicromolar K_i value for CYP2A13 ($K_i = 0.04 \pm 0.009 \mu\text{M}$), with the next closest as PEITC ($K_i = 3.8 \pm 1.6 \mu\text{M}$). The least potent inhibitor for CYP2A6 is (*S*)-nicotine ($K_i = 130 \pm 8.8 \mu\text{M}$). For CYP2A13 both (*S*)-nicotine ($K_i = 72 \pm 4.6 \mu\text{M}$) and (*R*)-(+)-menthofuran ($K_i = 54 \pm 12 \mu\text{M}$) are the least effective inhibitors.

Each of the compounds exhibited either competitive or mixed modes of inhibition, and most of the compounds exhibited the same mode of inhibition for both enzymes. (*S*)-Nicotine and tryptamine exhibited competitive modes of inhibition against both CYP2A6 and CYP2A13. Tranlycypromine and pilocarpine both exhibited competitive inhibition with CYP2A13, while mixed inhibition was the best model for these compounds with CYP2A6. The remaining compounds ((*R*)-(+)-menthofuran, DMABA, PEITC, β -nicotyrine, and 8-MOP) demonstrated mixed inhibition for both enzymes. While the alpha values for the mixed inhibitors (*R*)-(+)-menthofuran, DMABA, β -nicotyrine and 8-MOP are fairly close in value for the two enzymes, a large difference in the alpha values were observed for PEITC. An alpha value of 270 in the case of CYP2A6 suggests that PEITC binds primarily to the free enzyme (E state), while a much smaller alpha value of 0.20 in the case of CYP2A13 indicates that PEITC binds primarily to the enzyme-substrate complex (ES state). The contrasting modes of inhibition that PEITC demonstrates for CYP2A6 versus CYP2A13 are illustrated in Figure 3.3. The selectivity of these compounds to inhibit enzyme activity was determined by calculating the ratio of the CYP2A13 K_i to the CYP2A6 K_i (Table 1). Of the nine compounds examined, only (*R*)-(+)-menthofuran and tranlycypromine have a greater than 10-fold preference for CYP2A6 inhibition over CYP2A13. Tranlycypromine demonstrates the highest preference for CYP2A6 with a selectivity factor of

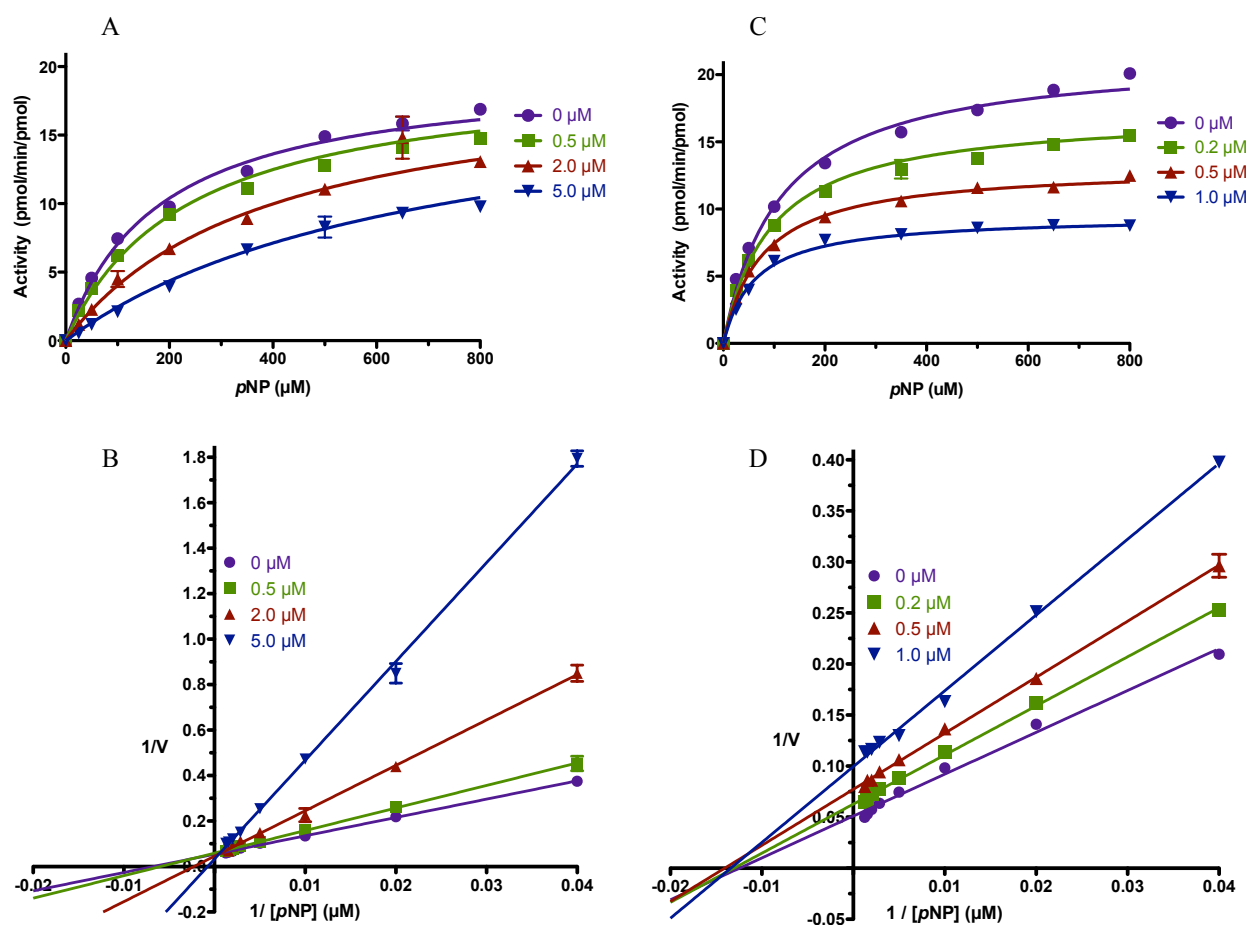


Figure 3.3. PEITC demonstrates extremes of mixed inhibition for CYP2A6 versus CYP2A13. CYP2A6 inhibition by PEITC results in a much larger effect on the K_m values, as shown in the Michaelis-Menten (A) and Lineweaver-Burk (B) plots, suggesting much higher affinity for the E state ($\alpha=270$). For CYP2A13, however, Michaelis-Menten (C) and Lineweaver-Burk (D) plots illustrate that PEITC inhibition has a larger effect on the V_{max} , suggesting much tighter binding to the ES state ($\alpha=0.20$).

49, followed by (*R*)-(+)-menthofuran with a selectivity factor of 27. DMABA and tryptamine have more moderate selectivity for CYP2A6, with selectivity factors of ~5-10. The remaining inhibitors have less than ~2-fold preference for either of the CYP2A enzymes, with the exception of 8-MOP. 8-MOP demonstrated a 6-fold preference for inhibition of CYP2A13 over CYP2A6.

Discussion

Kinetic analysis for the inhibition of *p*NP 2-hydroxylation was used to evaluate a chemically diverse set of known CYP2A6 inhibitors to determine which are able to discriminate effectively between CYP2A6 and CYP2A13. The evaluation of the selectivity of these

compounds for both enzymes within the human CYP2A family employed parallel assays under identical experimental conditions with recombinant, purified proteins. Among the most selective enzyme inhibitors tested were tranlycypromine and (*R*)-(+)-menthofuran, which demonstrate a 49-fold and 27-fold preference for CYP2A6 inhibition over CYP2A13, respectively. Tryptamine and DMABA were only moderately (5- to 10-fold, respectively) selective for CYP2A6 inhibition.

The monoamine oxidase inhibitor tranlycypromine is a potent inhibitor of CYP2A6 and is commonly used for P450 phenotyping, but the selectivity of the compound has been reported by several others as less than ideal.¹ In a study conducted to characterize the inhibitory selectivity of tranlycypromine in human liver microsomes, Taavitsainen and colleagues determined that the K_i value of tranlycypromine for CYP2A6 is 16- to 17-times lower than the next most potently inhibited enzymes, CYP2C19 and CYP2E1.¹⁸ This is a much narrower range than the 49-fold difference in CYP2A6 K_i versus CYP2A13 K_i reported herein. Thus, tranlycypromine may have utility in studies that seek to discriminate between CYP2A6 and CYP2A13 activity, but the compound fails to discriminate sufficiently among liver CYP450 enzymes, as demonstrated previously.

(*R*)-(+)-Menthofuran was first reported in 1998 by Khojasteh-Bakht and colleagues as a potent, mechanism-based highly selective inhibitor of human CYP2A6.¹⁰ Since then, it has been used in various P450 phenotyping studies to selectively inhibit CYP2A6.^{19,20} The K_i value of $2.0 \pm 0.44 \mu\text{M}$ herein agrees well with $2.5 \mu\text{M}$ reported for CYP2A6 in human liver microsomes by Khojasteh-Bakht and colleagues, but is slightly higher than the K_i value of $0.84 \mu\text{M}$ reported elsewhere for reconstituted purified CYP2A6 enzyme.¹⁰ Based on inhibition of *p*NP 2-hydroxylation in reactions similar to those typically used for P450 phenotyping, menthofuran

was one of the more selective of the traditionally employed CYP2A6 inhibitors when specifically discriminating enzyme activity within CYP2A family.

Tryptamine is a trace amine found in the brain that serves as a precursor to the neurotransmitter serotonin and the hormone melatonin. Tryptamine demonstrated a competitive mode of inhibition for both CYP2A6 and CYP2A13. The K_i value of tryptamine for CYP2A6 of 1.7 μM is identical to the value reported by Zhang and colleagues in cDNA-expressing microsomes using coumarin 7-hydroxylase activity.¹⁴ However, the preference of tryptamine for the inhibition of CYP2A6 over CYP2A13 difference is less than ten-fold, making it an undesirable candidate for effectively distinguishing between the activities of the two enzymes.

DMABA is an inhibitor reported to be selective for CYP2A6.¹³ Inhibition studies of this compound using human liver microsomes indicated >20-fold selectivity for CYP2A6 over all other hepatic cytochrome P450 enzymes, with the exception of CYP2E1 where the DMABA is only 13-fold selective for CYP2A6.¹³ The reported IC_{50} for CYP2A6 was 0.45 μM , but CYP2A13 was not evaluated in that work. We observed only a very moderate 4.6-fold selectivity for CYP2A6 over CYP2A13, making DMABA an inappropriate inhibitor for distinguishing between the activities of CYP2A6 and CYP2A13 in respiratory tract and other tissues that express both enzymes.

The remaining compounds preferentially inhibited CYP2A13 or demonstrated relatively little preference for either CYP2A6 or CYP2A13. PEITC, (S)-nicotine, β -nicotyrine, pilocarpine, and 8-MOP all have selectivity factors ranging from 0.16 to 2.2.

PEITC is one of the most extensively studied compounds of the isothiocyanate class of compounds. Isothiocyanates such as PEITC are found in high levels in cruciferous vegetables such as cauliflower, Brussels sprouts, and watercress. PEITC is considered to act as a

chemopreventative agent through the inhibition of P450 enzymes involved in the activation of procarcinogens, such as the activation of the tobacco-derived procarcinogen NNK by enzymes of the CYP2A family.^{12,21,22} PEITC has been reported to potently inhibit both CYP2A6 and CYP2A13 with sub-micromolar K_i values,¹⁵ and was found in this study to demonstrate a two-fold preference for the inhibition of CYP2A13 over CYP2A6 with K_i values of 3.8 μ M and 1.7 μ M for the two enzymes, respectively.

The tobacco alkaloids (*S*)-nicotine and β -nicotyrine are structurally similar and demonstrate a similar lack of selectivity among human CYP2A enzymes. The major tobacco alkaloid (*S*)-nicotine is the primary mediator of the pharmacological effects and addiction liability of smoking and is a known substrate for both CYP2A enzymes. The competitive mode of inhibition that (*S*)-nicotine demonstrates is consistent with the fact that it is a known substrate for both CYP2A enzymes. The nicotine-related tobacco alkaloid β -nicotyrine is a potent, mechanism-based inactivator of CYP2A6, although its inhibitory activity is not selective for CYP2A6.⁹ Both compounds demonstrate a slight preference for the inhibition of CYP2A13 over CYP2A6, but the difference in K_i values for both compounds are less than two fold.

Pilocarpine is a natural alkaloid found in the leaves of *P. microphyllus* and is used therapeutically as a non-selective muscarinic receptor agonist to control elevated intraocular pressure associated with glaucoma. It has been previously determined by others to inhibit CYP2A and CYP2B activities more efficiently than other P450 activities *in vitro*.²³ Our studies confirm that pilocarpine is a potent inhibitor of CYP2A enzymes, with K_i values of 3.0 μ M and 1.4 μ M for CYP2A6 and CYP2A13, respectively. Pilocarpine inhibits the two closely related CYP2A enzymes using similar but not identical mechanisms of inhibition, acting as a

competitive inhibitor for CYP2A13 and as a mixed inhibitor for CYP2A6 with higher affinity for the E state ($\alpha=25$).

The compound that demonstrated the most selectivity for CYP2A13 inhibition with a selectivity factor of 0.16 is 8-MOP (also known as methoxsalen or xanthotoxin). Inhibition of CYP2A6 and CYP2A13 resulted in a decrease in the V_{\max} and an increase in the K_m , suggesting a mixed mode of inhibition for both enzymes, with alpha values of 3.3 and 1.9 for CYP2A6 and CYP2A13, respectively. Previous reports have identified 8-MOP as a noncompetitive inhibitor for both CYP2A enzymes.^{14,16} Our study also confirms that 8-MOP more potently inhibits CYP2A13, with a K_i value of 0.04 μM versus 0.25 μM for CYP2A6. This 6-fold degree of selectivity is greater than the 1.8-fold difference previously indicated according to results published in separate studies.^{14,16}

Conclusion

The goal of this study was to compare, side-by-side, a set of reportedly CYP2A6-selective inhibitors to determine their relative ability to discriminate between CYP2A6 and the 94% identical enzyme CYP2A13, and thus their utility in distinguishing between CYP2A activities in tissues where both enzymes are present. The ratio of CYP2A13 K_i / CYP2A6 K_i for each compound revealed that tranlycypromine and (*R*)-(+)-menthofuran are the most selective inhibitors for CYP2A6, but that they have only 49- and 27-fold selectivity for CYP2A6 over CYP2A13, respectively. Even though the ability of tranlycypromine to distinguish between CYP2A enzymes is not ideal, this compound can be used as a benchmark for the development of more selective inhibitors. Six of the compounds tested demonstrated only moderate or no real selectivity between the human CYP2A enzymes. Thus, these compounds should not be employed to evaluate individual CYP2A enzyme contributions to metabolism in tissues where

both enzymes may be present. This study did not identify a suitably selective inhibitor for CYP2A13. The 6-fold selectivity of 8-MOP for CYP2A13 over CYP2A6 is marginal at best, but does provide a starting point for the development of a more selective inhibitor. Altogether, these results can be used as a guide for the selection of CYP2A-selective inhibitors in studies that seek to accurately distinguish between CYP2A6 and CYP2A13 activity. Such efforts are particularly relevant in evaluations of the *in vivo* activation of compounds that give rise to tissue-specific carcinogenesis, such as tobacco-derived NNK in the human respiratory tract.

References

1. Khojasteh, S.C., Prabhu, S., Kenny, J.R., Halladay, J.S. and Lu, A.Y.H. (2011) Chemical inhibitors of cytochrome P450 isoforms in human liver microsomes: a re-evaluation of P450 isoform selectivity. *Eur. J. Drug Metab. Pharmacokinet.* **36**, 1-16.
2. Pavak, P. and Dvorak, Z. (2008) Xenobiotic-induced transcriptional regulation of xenobiotic metabolizing enzymes of the cytochrome P450 superfamily in human extrahepatic tissues. *Curr. Drug Metab.* **9**, 129-143.
3. Zhang, J.Y., Wang, Y. and Prakash, C. (2006) Xenobiotic-metabolizing enzymes in human lung. *Curr. Drug Metab.* **7**, 939-948.
4. Su, T., Bao, Z., Zhang, Q.-Y., Smith, T.J., Hong, J.-Y. and Ding, X. (2000) Human cytochrome P450 CYP2A13: predominant expression in the respiratory tract and its high efficiency metabolic activation of a tobacco-specific carcinogen, 4-(methylnitrosamino)-1-(3-pyridyl)-1-butanone. *Cancer Research* **60**, 5074-5079.
5. Smith, B.D., Sanders, J.L., Porubsky, P.R., Lushington, G.H., Stout, C.D. and Scott, E.E. (2007) Structure of the human lung cytochrome P 450 2A13. *J. Biol. Chem.* **282**, 17306-17313.
6. Bao, Z., He, X.-Y., Ding, X., Prabhu, S. and Hong, J.-Y. (2005) Metabolism of nicotine and cotinine by human cytochrome P450 2A13. *Drug Metab. Dispos.* **33**, 258-261.
7. Fukami, T., Katoh, M., Yamazaki, H., Yokoi, T. and Nakajima, M. (2008) Human cytochrome P450 2A13 efficiently metabolizes chemicals in air pollutants: naphthalene, styrene, and toluene. *Chem. Res. Toxicol.* **21**, 720-725.
8. Fukami, T., Nakajima, M., Sakai, H., Katoh, M. and Yokoi, T. (2007) CYP2A13 metabolizes the substrates of human CYP1A2, phenacetin, and theophylline. *Drug Metab. Dispos.* **35**, 335-339.
9. Denton, T.T., Zhang, X. and Cashman, J.R. (2004) Nicotine-related alkaloids and metabolites as inhibitors of human cytochrome P-450 2A6. *Biochem. Pharmacol.* **67**, 751-756.
10. Khojasteh-Bakht, S.C., Koenigs, L.L., Peter, R.M., Trager, W.F. and Nelson, S.D. (1998) (R)-(+)-menthofuran is a potent, mechanism-based inactivator of human liver cytochrome P450 2A6. *Drug Metab. Dispos.* **26**, 701-704.

11. Koenigs, L.L., Peter, R.M., Thompson, S.J., Rettie, A.E. and Trager, W.F. (1997) Mechanism-based inactivation of human liver cytochrome P450 2A6 by 8-methoxypsoralen. *Drug Metab Dispos* **25**, 1407-15.
12. Nakajima, M., Yoshida, R., Shimada, N., Yamazaki, H. and Yokoi, T. (2001) Inhibition and inactivation of human cytochrome P450 isoforms by phenethyl isothiocyanate. *Drug Metab. Dispos.* **29**, 1110-1113.
13. Rahnasto, M., Wittekindt, C., Juvonen, R.O., Turpeinen, M., Petsalo, A., Pelkonen, O., Poso, A., Stahl, G., Hoeltje, H.D. and Raunio, H. (2008) Identification of inhibitors of the nicotine metabolising CYP2A6 enzyme - an in silico approach. *Pharmacogenomics J.* **8**, 328-338.
14. Zhang, W., Kilicarslan, T., Tyndale, R.F. and Sellers, E.M. (2001) Evaluation of methoxsalen, tranlylcypromine, and tryptamine as specific and selective CYP2A6 inhibitors in vitro. *Drug Metab. Dispos.* **29**, 897-902.
15. von Weymarn, L.B., Chun, J.A. and Hollenberg, P.F. (2006) Effects of benzyl and phenethyl isothiocyanate on P450s 2A6 and 2A13: potential for chemoprevention in smokers. *Carcinogenesis* **27**, 782-790.
16. von Weymarn, L.B., Zhang, Q.-Y., Ding, X. and Hollenberg, P.F. (2005) Effects of 8-methoxypsoralen on cytochrome P450 2A13. *Carcinogenesis* **26**, 621-9.
17. Yano, J.K., Denton, T.T., Cerny, M.A., Zhang, X., Johnson, E.F. and Cashman, J.R. (2006) Synthetic inhibitors of cytochrome P-450 2A6: inhibitory activity, difference spectra, mechanism of inhibition, and protein cocrystallization. *J. Med. Chem.* **49**, 6987-7001.
18. Taavitsainen, P., Juvonen, R. and Pelkonen, O. (2001) In vitro inhibition of cytochrome P450 enzymes in human liver microsomes by a potent CYP2A6 inhibitor, trans-2-phenylcyclopropylamine (tranlylcypromine), and its nonamine analog, cyclopropylbenzene. *Drug Metab. Dispos.* **29**, 217-222.
19. Diaz, G.J. and Squires, E.J. (2000) Metabolism of 3-methylindole by porcine liver microsomes: responsible cytochrome P450 enzymes. *Toxicol. Sci.* **55**, 284-292.
20. Miyazawa, M. and Haigou, R. (2011) Determination of cytochrome P450 enzymes involved in the metabolism of (-)-terpinen-4-ol by human liver microsomes. *Xenobiotica* **41**, 1056-1062.
21. Hecht, S.S. (1998) Biochemistry, biology, and carcinogenicity of tobacco-specific N-nitrosamines. *Chem. Res. Toxicol.* **11**, 559-603.
22. Smith, T.J., Guo, Z., Thomas, P.E., Chung, F.L., Morse, M.A., Elkind, K. and Yang, C.S. (1990) Metabolism of 4-(methylnitrosamino)-1-(3-pyridyl)-1-butanone in mouse lung microsomes and its inhibition by isothiocyanates. *Cancer Res.* **50**, 6817-22.
23. Kimonen, T., Juvonen, R.O., Alhava, E. and Pasanen, M. (1995) The inhibition of CYP enzymes in mouse and human liver by pilocarpine. *Br. J. Pharmacol.* **114**, 832-6.

Chapter 4

Expression and Purification of the Cytochrome P450 26 Family of Enzymes

Introduction

The CYP26 family of cytochrome P450 enzymes are important mediators of retinoic acid (RA) catabolism in the body. Biologically active retinoids are essential signaling molecules that control various developmental pathways and influence the proliferation and differentiation of a variety of cell types.^{1,2} The proper function of these pathways relies upon the body's ability to maintain precise control of retinoic acid levels, particularly the biologically most active isomer *all-trans*-retinoic acid (*atRA*).³

The human CYP26 family consists of three enzymes that share an amino acid sequence identity of 42-51%: CYP26A1, CYP26B1, and CYP26C1.⁴ All three members of the CYP26 family are capable of metabolizing *atRA* to the major oxidative metabolites 4-hydroxy-*atRA*, 4-oxo-*atRA*, and 18-hydroxy-*atRA* (Figure 4.1).⁵⁻⁷ CYP26A1 and CYP26B1 share similar substrate specificities, with high catalytic activity toward *atRA* and much lower activity towards 9-*cis*-RA and 13-*cis*-RA.⁸ The expression and metabolic function of these two enzymes are also inducible by the presence of *atRA*, likely serving as a feedback loop for the auto-regulation of RA levels.^{8,9} In contrast, CYP26C1 has the ability to bind and oxidize both 9-*cis*-RA and *atRA* equally and is much more effectively induced by 9-*cis*-RA than *atRA*.¹⁰

Retinoids such as *atRA* represent attractive targets for medicinal intervention due to their capacity to serve as differentiating agents, redirecting cells toward their normal phenotype. *atRA* itself has been successfully used for cancer chemoprevention, chemotherapy, differentiation therapy, and for the treatment of acne.³ One of the most impressive effects of *atRA* therapy is in respect to promyelocytic leukemia, with patients achieving full remission after treatment with

high doses of *atRA*.¹¹ Unfortunately, *atRA*-based therapies tend to fail with continuous use due to the development of resistance.¹² This failure has been suggested to be the result of up-regulation of P450 enzymes, particularly the enzymes of the CYP26 family,^{9,13} resulting in

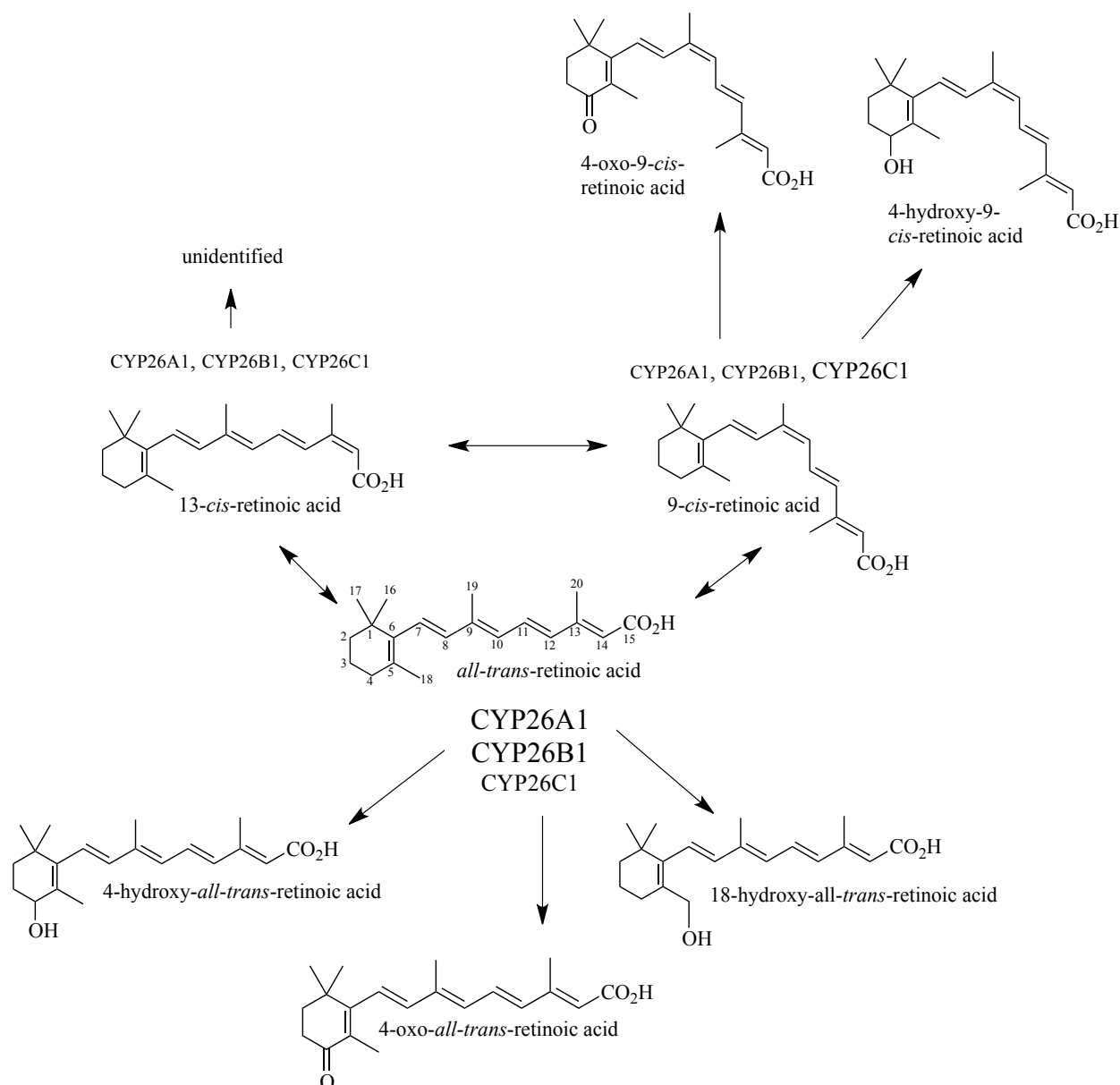


Figure. 4.1 Retinoic acid metabolism by CYP26 enzymes. All three members of the human CYP26 family are able to convert *atRA* to 4-hydroxy-*atRA*, 4-oxo-*atRA*, and 18-hydroxy-*atRA*. CYP26A1 and CYP26B1 exhibit very high catalytic activity toward *atRA* and much lower activity toward 9-*cis*-RA and 13-*cis*-RA, while CYP26C1 demonstrates an equal ability to catalyze the oxidation of 9-*cis*-RA and *atRA*.

enhanced *in vivo* *atRA* metabolism.^{14,15} As a result, a significant amount of work has been conducted for the development of chemical agents that inhibit P450-mediated metabolism of *atRA*, commonly referred to as retinoic acid metabolism blocking agents (RAMBAs).^{3,16-18}

Unfortunately, the exact metabolic pathway and kinetics of RA metabolism, as well as specific structural information of CYP26 enzymes, are lacking due to the inability to generate sufficient amounts of recombinant enzyme necessary for characterization. As members of the P450 family, the CYP26 proteins are membrane-bound proteins localized within the endoplasmic reticulum. This characteristic makes them particularly difficult to express and isolate on a large scale. As a result, a majority of studies have relied on assays conducted with transfected cells or microsomal fractions prepared from tissue samples or cultured cells.^{5,19-22} The scarce quantities and heterogeneous nature of these P450 preparations significantly limit the extent of structural and functional information that can be determined.

Thus, the immediate goal of this project was to construct a method that would enable the production of a recombinant CYP26 enzyme with yield and purity that exceeded current approaches. Although human CYP26A1 represented the original target, the studies were soon expanded to include all three CYP26 enzymes in human and in mouse in hopes that an expanded investigation would increase the chances of successfully generating any one CYP26 enzyme for characterization studies. With limited precedence in the literature for the generation of CYP26 proteins, the techniques used were heavily based on methods applied to the successful expression and purification of other P450 proteins,²³ including those of the CYP2A family.^{24,25} As a result, *E. coli* was selected as an expression host, and the amino acid sequence of each of the CYP26 proteins was specifically modified to facilitate expression via truncation of the N-terminal transmembrane helix. Additional modifications were made to enhance the solubility of the

CYP26 proteins and make them amenable to metal affinity chromatography, thereby promoting ease of purification. Finally, optimization of the purification of the CYP26 proteins involved careful selection of the most promising detergents and stabilizing ligands based on available information in the literature. Altogether, the combination of these approaches had the potential to facilitate basic structural and kinetic determination studies, ultimately serving as a basis for improved modulation of *atRA* levels as a form of cancer treatment.

Materials and Methods

Engineering of Plasmid DNA

The cDNAs coding for each of the CYP26 enzymes were acquired from a variety of sources. Each of the cDNAs coded for the full-length, wild-type versions of the CYP26 proteins, except for the human CYP26A1 cDNA which was synthesized with the modifications described below already in place. A synthetic, codon optimized gene coding for human CYP26A1 was purchased from Blue Heron Biotechnology (Bothell, WA) and received in a pUCminusMCS plasmid. Human CYP26B1 cDNA was purchased from Open Biosystems (Lafayette, CO) and received in a pPCR-Script Amp SK(+) plasmid. Human CYP26C1 cDNA was acquired as a generous gift from Dr. Christian Helvig at Cytochroma in a pcDNA3.1+ plasmid. Mouse CYP26A1, CYP26B1, and CYP26C1 cDNA were all acquired as a generous gift from Dr. Alex Moise at The University of Kansas in a pcDNA3.1/V5-His-TOPO plasmid.

The cDNAs for each of the CYP26 enzymes were transformed into chemically competent DH5 α *E. coli* cells by heat shock for 40 seconds at 42 °C in 1.5 mL microcentrifuge tubes following a 40 minute incubation with the plasmid DNA on ice. The cells were then allowed to recover on ice for a few minutes before they were plated on Lysogeny Broth (LB)-ampicillin agar plates containing 50 μ g/mL ampicillin and grown overnight. The next day, individual

colonies containing full length CYP26 plasmid DNA were isolated from the LB-ampicillin agar plates and grown overnight at 37 °C in 5 mL LB cultures containing 50 µg/mL ampicillin. The cells from the overnight 5 mL LB-ampicillin cultures were pelleted by centrifugation and the supernatant was decanted. Plasmid DNA was purified using the QIAprep Spin Miniprep Kit from Qiagen, according to the manufacturer's protocol.

CYP26 Protein Modification and Cloning

Mammalian membrane cytochrome P450 enzymes have a single N-terminal transmembrane helix followed by a proline-rich region and membrane-bound catalytic domain. While the transmembrane helix can often be truncated, the proline-rich region is often necessary for protein stability. The CYP26 proteins were each engineered for enhanced expression in *E. coli* and ease of purification through truncation of the N-terminal transmembrane sequence, modification of the N-terminus with the addition of a short hydrophilic sequence, and addition of four histidine residues to the C-terminus. To determine the extent of the desired N-terminal truncation for the CYP26 enzymes, an alignment was performed using CLC sequence viewer 6.5.4 with human CYP26A1 and several other human P450 proteins that have been successfully truncated, expressed, and purified by previous members of the research group: CYP2A6, CYP2A13, and CYP2E1 (Figure. 4.2). The same truncation was applied to all six human and mouse CYP26 cDNAs. All work described herein has been conducted with these truncated, His-tagged versions of the CYP26 enzymes. An alignment of all six full-length CYP26 proteins prior to modification is shown in Figure. 4.3.

Synthetic oligonucleotide primers were designed to confer the desired modifications upon each full-length CYP26 cDNA. The forward and reverse oligonucleotide primers shown in Table 4-1 contain nucleotides encoding the desired amino acid changes as well as a region of complementary sequence. Each forward primer was designed to add the hydrophilic tag ‘MAKKTSSKGK’ to the truncated N-terminus, while each reverse primer was designed to add a four-histidine tag after the last native residue. All forward and reverse primers also included specific restriction sites for insertion into the P450 expression plasmid pKK233-2 (Pharmacia, Stockholm, Sweden). For every CYP26 cDNA other than human CYP26A1, this required deletion of an intrinsic and undesired NcoI restriction enzyme recognition site and the simultaneous generation of a new NcoI site.

The oligonucleotide primers were annealed to the respective full-length cDNAs and extended to generate truncated, His-tagged versions of the CYP26 genes using Finnzymes Phusion High-Fidelity DNA Polymerase (Thermo Scientific Inc., Waltham, MA) during PCR using a PCR Sprint Thermal Cycler (Thermo Scientific Inc., Waltham, MA). Each reaction was divided into 3 segments (see Table 4-2). The same thermal cycling conditions were used for the successful modification of each of the CYP26 genes except for human CYP26C1. For human CYP26C1, a lack of product formation could possibly be a result of the very strong secondary structure of the forward primer. To troubleshoot this issue, several modifications were made to the initial thermal cycling conditions, including: the use of a modified polymerase buffer designated for GC rich templates, the addition of a longer initial denaturing cycle of 3 minutes, extended denaturing and extension steps in the second segment, and 40 repeats of the second segment of cycling instead of 30.

Table 4-1: Oligonucleotide primer designs for human and mouse CYP26A1, CYP26B1, and CYP26C1. Forward (fwd) and reverse (rev) primers for each of the CYP26 enzymes were designed to be complementary to opposite strands of the genetic sequence, with the forward primer encoding a hydrophilic tag (**blue**) to the truncated N-terminus and the reverse primer encoding a four-histidine tag (**green**). The portion of the oligonucleotide primer that is complementary to the full-length CYP26 gene is shown in **bold**. The addition or removal of a restriction site for cloning purposes is reported by (+) or (-) respectively, with the single nucleotide change corresponding to restriction site obliteration **highlighted**.

Primer	Sequence (5' to 3')	Restriction site altered	Length (b.p.)	T _m (°C)	GC (%)	Secondary Structure	Primer Dimer
Human CYP26A1 fwd	TTTACCATGGCTAAGAAAACGAGCAGCAAAAGGGAAGCTTCCGTTACCCC CTGGTACTATGGGC	+ NcoI	63	74	59	Strong	No
Human CYP26A1 rev	GATACGGAAGCTTCGGATATCAATGGTGG	+ EcoRV	28	66	45	Weak	No
Human CYP26B1 fwd	TTTACCATGGCTAAGAAAACGAGCAGCAAAAGGGAAGCTGCCGATCCCGA AGGGTCTATGGGCTTCCCGCTCATCGGAGAGACC	- NcoI + NcoI	84	80	63	Strong	No
Human CYP26B1 rev	AAAGATATCAAGCTTCTAATGGTGGTGGTGGGCTCAGCATG GCC	+ HindIII + EcoRV	52	77	68	Moderate	No
Human CYP26C1 fwd	TTTACCATGGCTAAGAAAACGAGCAGCAAAAGGGAAGCTGCCGCTGCCGA AGGGTCTATGGGCTGGCCCTTCTTCGGCGAACC	- NcoI + NcoI	84	83	63	Very Strong	No
Human CYP26C1 rev	AAAGATATCAAGCTTCTAATGGTGGTGGTGGGCTAGCCCATTCCTCCC GCAACCG	+ HindIII + EcoRV	56	81	65	Moderate	No
Mouse CYP26A1 fwd	TTTACCATGGCTAAGAAAACGAGCAGCAAAAGGGAAGCTCCCGTTGCCGC CGGGTACTATGGGCTTCCCATCTTTGGGG	- NcoI + NcoI	79	72	54	Very Strong	No
Mouse CYP26A1 rev	AAAGATATCAAGCTTCTAATGGTGGTGGTGGATGATATCTCCCTGGAACTGG G	+ HindIII + EcoRV	50	62	55	Moderate	No
Mouse CYP26B1 fwd	TTTACCATGGCTAAGAAAACGAGCAGCAAAAGGGAAGCTGCCGATCCCGA AGGGTCTATGGGATTCCTCGCTCATCGGAGAGACTGG	- NcoI + NcoI	86	80	59	Strong	No
Mouse CYP26B1 rev	AAAGATATCAAGCTTCTAATGGTGGTGGTGGTGGTGGTGGTGGTGGTGGTGG GC	+ HindIII + EcoRV	51	68	57	Strong	No
Mouse CYP26C1 fwd	TTTACCATGGCTAAGAAAACGAGCAGCAAAAGGGAAGTTGCCGCTGCCGA AGGGTCTATGGGCTGGCCATCTTCCGTTGAACGC	- NcoI + NcoI	85	81	57	Strong	No
Mouse CYP26C1 rev	AAAGATATCAAGCTTCTAATGGTGGTGGTGGTGGTGGTGGTGGTGGTGGTGG GCAACCG	+ HindIII + EcoRV	56	79	65	Strong	No

Table 4-2: PCR thermal cycling parameters used to generate modified versions of human and mouse CYP26 enzymes.

Segment	Number of Cycles	Temperature	Time
1	1	98°C	1 min 40 sec
2	30	98°C	10 sec
		$T_m + 3^{\circ}\text{C}$	30 sec
		72°C	15 sec/kb
3	1	$T_m + 3^{\circ}\text{C}$	10 min

Following PCR, the ~1.5 kb fragment containing each modified CYP26 cDNA template was cut with the restriction enzymes NcoI and EcoRV or NcoI and HindIII in preparation for ligation into similarly digested pKK233-2. Each CYP26 DNA fragment was ligated into pKK233-2 in a 5 minute reaction conducted at room temperature using Roche's 'Rapid DNA Ligation Kit' with pKK233-2:CYP26 ratios ranging from 1:1 to 1:6. Following the brief ligation reaction, 1.5 μL of each reaction mixture was used to transform into chemically competent DH5 α *E. coli* cells using the transformation procedure described earlier, and the transformed cells were plated on LB-ampicillin agar plates and grown overnight at 37 °C.

To screen the results of the ligation reactions, plasmid DNA from the resulting colonies was purified as described above and submitted to restriction enzyme digest using a restriction enzyme unique to the CYP26 insert but not present in the pKK233-2 plasmid itself. Following the restriction enzyme digestion, the DNA was analyzed by gel electrophoresis (0.8% agarose) to determine whether the DNA had been cut as a result of the digestion and thus contained the desired CYP26 DNA insert. Each gel also included a 1 kb DNA ladder as a size reference and a negative control (uncut plasmid). Plasmid DNA that tested positive for the CYP26 DNA insert was subsequently sent to Idaho State University to verify the faithful incorporation of all intended modifications and the absence of any undesired mutations using DNA sequencing of the complete gene.

CYP26 Expression

Each of the CYP26 proteins of interest were expressed using the procedure described in Chapter 2: Methods, with certain modifications. As indicated by the data summarized in Tables 4-3 and 4-4, these modifications included the use of the chaperone plasmid pGro7 and the incorporation of a stabilizing ligand during expression. The pGro7 plasmid encodes the protein folding chaperone team groES-groEL. Molecular chaperones such as groES and groEL are known to be involved in the protein folding process, and have been demonstrated to enhance bacterial expression of several mammalian P450 enzymes.²⁶ Coexpression of CYP26 proteins with the groES-groEL chaperone team required the addition of L-arabinose and chloramphenicol for induction of expression and antibiotic selection of the pGro7 plasmid, respectively. In addition, all expressions utilizing the pGro7 chaperone plasmid, aside from the initial expression, were conducted over the course of two days rather than three to reduce cell death, which was indicated by the accumulation of a ring of cells along the wall of the flask. For expressions that utilized stabilizing ligands, a final concentration of 100-1000 times the published IC₅₀ value was incorporated into the expression culture. These stabilizing ligands included the natural substrate retinoic acid (Sigma), the clinically-developed RAMBA liarozole (Tocris Bioscience), or an inhibitor of the recently published 3-(*1H*-imidazol- and triazol-1-yl) -2,2-dimethyl-3-[4-(naphthalen-2-ylamino)phenyl]propyl series of derivatives. The latter series of compounds, designated in these studies by ‘MCC’, was recently reported to inhibit CYP26A1 with low nanomolar potency in microsomal assays.¹⁹

CYP26 Purification

Each of the CYP26 proteins of interest were initially purified using the cytochrome P450 protein purification protocol described in Chapter 2: Methods. This standard protocol was further

optimized for selected CYP26 proteins to maximize protein yield. The greatest amount of optimization was conducted for human CYP26A1, as it represents the original protein of interest. As the poor stability and overall yield of purified human CYP26A1 became apparent, the cloning and purification of five other CYP26 proteins were pursued: human CYP26B1 and CYP26C1 and mouse CYP26A1, CYP26B1, and CYP26C1. Based on total nanomoles of protein recovered following the first chromatographic step of the purification, optimization of mouse CYP26A1 and mouse CYP26B1 were pursued as secondary targets of interest while further purification attempts of mouse CYP26C1, human CYP26C1, and human CYP26B1 were abandoned due to low protein yield.

Preparation of Microsomal Mouse CYP26A1 for Metabolism Studies

Mouse CYP26A1 was expressed for three days and harvested as described in Chapter 2: Methods. Following harvest, the cell pellet was re-suspended in 200 mL of 100 mM potassium phosphate, pH 7.4, containing 20% glycerol. Spheroplasts were then produced by treating the suspension for 30 min with 0.3 mg/mL lysozyme with stirring at 4 °C. Following lysozyme treatment, an equal volume of cold water was slowly added to the spheroplasts. After an additional incubation at 4 °C with stirring for 10 min, the spheroplasts were pelleted by centrifugation at 12,000 x g for 10 min at 4 °C. The spheroplasts were then lysed by freezing the pellet using either a liquid nitrogen bath or a dry ice/ethanol slurry. The frozen pellet was thawed and resuspended in 100 mL of 100 mM potassium phosphate, pH 7.4, containing 20% glycerol using manual homogenization on ice. To inhibit proteolysis, the cellular resuspension was supplemented with 0.5 µM PMSF and 10 µg/mL aprotinin. Following homogenization, the suspension was separated into approximately 50 mL aliquots and sonicated on ice using six 20 sec pulses with 40 sec of cooling between pulses. The material was then centrifuged at 12,000 x

g for 10 min at 4 °C to remove cellular debris. Following this process, the supernatant was submitted to ultracentrifugation at 100,000 x g for 60 min at 4 °C. The final pellet was resuspended in 5 mL of retinoic acid metabolism assay buffer (100 mM potassium phosphate, pH 6.8, containing 20% glycerol) using manual homogenization on ice. The concentration of mouse CYP26A1 was analyzed by evaluating the reduced carbon monoxide difference spectrum and then aliquoted for metabolism assays with retinoic acid.

Assay to Detect Retinoic Acid Metabolism by Recombinantly Expressed CYP26 protein

As the primary substrate of the CYP26 enzyme family, retinoic acid was the natural choice for metabolism assays designed to investigate the catalytic function of the CYP26 proteins. Due to the limited success in generating large quantities of pure, stable P450 protein following NiNTA chromatography, metabolism assays were conducted with a microsomal preparation of CYP26A1 in addition to NiNTA-purified CYP26A1. Concentrations of 1 μ M or 10 μ M RA were employed to evaluate the presence or absence of metabolic function for the various preparations of protein. CYP2E1 was employed as a positive reaction control because evidence in the literature indicated that it may be involved in modifications to *in vivo* retinoic acid levels in response to treatment with ethanol.²⁷ A number of negative controls were also included to verify that any observed activity was specific to the presence of CYP26 enzyme and included samples that were 1) stopped with acetonitrile prior to initiation by the addition of NADPH, 2) not initiated by the addition of the obligatory electron donor NADPH, and 3) did not contain the obligatory redox partner protein cytochrome P450 reductase.

Metabolism assays used a reconstituted system (RPS) consisting of 50 pmol of purified or microsomal CYP26A1 incubated with 200 pmol NADPH-cytochrome P450 reductase and 100 pmol cytochrome b₅ for 45 minutes on ice prior to use. RPS was added to 100 mM potassium

phosphate, pH 6.8, and 10 μ M retinoic acid for a total volume of 250 μ L. Samples were pre-incubated at 37 °C for 3 minutes before initiating the reactions by the addition of 1 mM NADPH. Reactions were allowed to proceed for 30 minutes at 37 °C and were quenched with 250 μ L acetonitrile and placed on ice. Samples were centrifuged at 4,500 x g for 6 minutes, and the amount of retinoic acid remaining was determined following HPLC separation. Separation of the reaction mixture was conducted by reverse phase HPLC with an isocratic mobile phase A of 80% acetonitrile, 10 mM ammonium acetate, 1% acetic acid, and a flow rate of 1.6 mL/min held for 15 min. After each run, the column was washed with mobile phase B of 60% tert-butylmethyl ether and 40% methanol for 10 minutes at 1.6 mL/min, followed by re-equilibration in phase A. The elution of retinoic acid was monitored at 350 nm, and the identity of the peak was verified by comparison to the elution time of a standard of either 1 μ M or 10 μ M retinoic acid. The presence or absence in metabolic activity was determined based on comparison of the peak area to a retinoic acid standard in reaction buffer.

Western Blotting

In preparation for SDS-PAGE, CYP26 protein samples were denatured by the addition of an equal volume of 2X SDS-PAGE loading dye (100 mM Tris-HCl, pH 6.8, 4% SDS, 0.2% bromophenol blue, 20% glycerol, 20 mM DTT) and heating at 100 °C for 3 minutes. Samples were then electrophoresed on 10% SDS-PAGE gels in reducing conditions. Protein was transferred to a polyvinylidene fluoride (PVDF) membrane by electrophoresis at 200 mV over 1 hour at room temperature or overnight at 100 mA at 4 °C. Following transfer, the membrane was washed twice for 10 minutes with TBS buffer (10 mM Tris-HCl, 150 mM NaCl, pH 7.5) at room temperature and once for 10 minutes with TBS-TX buffer (20 mM Tris-HCl, 500 mM NaCl, 0.05% Tween 20, 0.2% Triton X-100). Non-specific protein binding was blocked over the course

of a 1-hour incubation period conducted at room temperature with TBS buffer containing 3% bovine serum albumin. Excess bovine serum albumin was removed using two 10-minute washes with TBS-TX buffer and one 10-minute wash with TBS buffer at room temperature. Primary antibody (rabbit polyclonal IgG to human CYP26A1) was diluted into 3% bovine serum albumin in TBS at a 1:1,000 ratio and allowed to react for 1 hour at room temperature. The membrane was then washed twice for 10 minutes each with TBS-TX buffer and once for 10 minutes with TBS buffer at room temperature. A secondary antibody (anti-rabbit IgG) conjugated with alkaline phosphatase was diluted into 3% bovine serum albumin in TBS at a 1:2,000 ratio and allowed to react for 1 hour at room temperature. The membrane was then washed twice for 10 minutes each with TBS-TX buffer and once for 10 minutes with TBS buffer at room temperature. The Western blot was developed with 5-bromo-4-chloro-3-indolyl phosphate/nitro blue tetrazolium (BCIP/NBT) developing solution until the signal was clearly visible. Upon reaching the desired endpoint, the reaction was stopped by rinsing with 1% acetic acid in water.

Results

Expression of CYP26 Proteins

All attempts to express and purify human and mouse CYP26 proteins are summarized in Tables 4-3 and 4-4, respectively. A more visual representation of select data from these tables is also available in Figures 4.4 (human CYP26 expression and purification) and 4.5 (mouse CYP26 expression and purification). Following either a two- or three-day expression period, a typical human CYP26A1 cell pellet exhibited medium-to-light brown coloration with a slightly darker brown top layer and a mass of approximately 25-30 grams per 2.25 L of expression culture (Table 4-3, Row A). This degree of coloration is notably lighter compared to what is observed following an expression of CYP2A enzymes in *E. coli*. Additionally, the cell mass was less than

Table 4-3: Human cytochrome P450 26 protein expression and purification.

Trial	Protein	Cell Line	Cell Pellet Mass (g) / Expression Volume (L)	Wash or Elution Buffer Modifications	Stabilizing Ligand (E)(P)^b	Detergent	Protein yield pre-NiNTA (nmol)	Protein yield post-NiNTA (nmol)
A	CYP26A1	TOPP3	26.58 / 2.25	no modification	none	4.8 mM Cymal-5	114 (P420)	0
B	CYP26A1	TOPP3 pGro7	16.19 / 2.25	no wash buffer	none	4.8 mM Cymal-5	137 (P420)	11 (P420)
C	CYP26A1	TOPP3 pGro7	26.97 / 2.25	no wash buffer	none	Sodium Cholate (1%) Tergitol (NP-10) (1%)	110 (P420) 62 (P450)	15 (P420)
D	CYP26A1	TOPP3 pGro7	25.51 / 2.25	no wash buffer	5 μ M RA (E)(P)	Sodium Cholate (1%) Tergitol (NP-10) (1%)	102 (P420) 22 (P450)	21 (P420) 6 (P450)
E	CYP26A1	TOPP3 pGro7	27.04 / 2.25	no wash buffer; elution buffer NaCl increased to 0.2 M	5 μ M RA (E)(P)	Sodium Cholate (1%) Tergitol (NP-10) (1%)	96 (P420) 19 (P450)	6 (P420) <1 (P450)
F	CYP26A1	TOPP3 pGro7	46.82 / 4.5	no wash buffer; elution buffer NaCl increased to 0.2 M	5 μ M RA (E)(P)	Sodium Cholate (1%) Tergitol (NP-10) (1%)	~770 ^a	1 (P420) <1 (P450)
G	CYP26A1	TOPP3 pGro7	30.44 / 2.25	no wash buffer; elution buffer NaCl increased to 0.2 M and protein diluted with additional buffer upon elution	5 μ M RA (E)(P)	Sodium Cholate (1%) Tergitol (NP-10) (1%)	~880 ^a	14 (P420) <1 (P450)
H	CYP26A1	TOPP3	31.37 / 2.25	no wash buffer	0.8 μ M MCC 187 (E)(P)	Sodium Cholate (1%) Tergitol (NP-10) (1%)	242 (P420) 60 (P450)	25 (P420) 11 (P450)
I	CYP26B1	TOPP3	33.11 / 2.25	no wash buffer	none	4.8 mM Cymal-5	~1400 ^a	24 (P420)
J	CYP26C1	TOPP3	28.05 / 2.25	no wash buffer	5 μ M RA (P)	4.8 mM Cymal-5	43 (P420)	14 (P420)

^aReduced carbon monoxide difference spectrum was not collected, so value shown is an estimation using absolute spectral determination at $\lambda_{\text{max}} \sim 408\text{-}412 \text{ nm}$

^bReports whether ligand was present during expression (E) and/or purification (P)

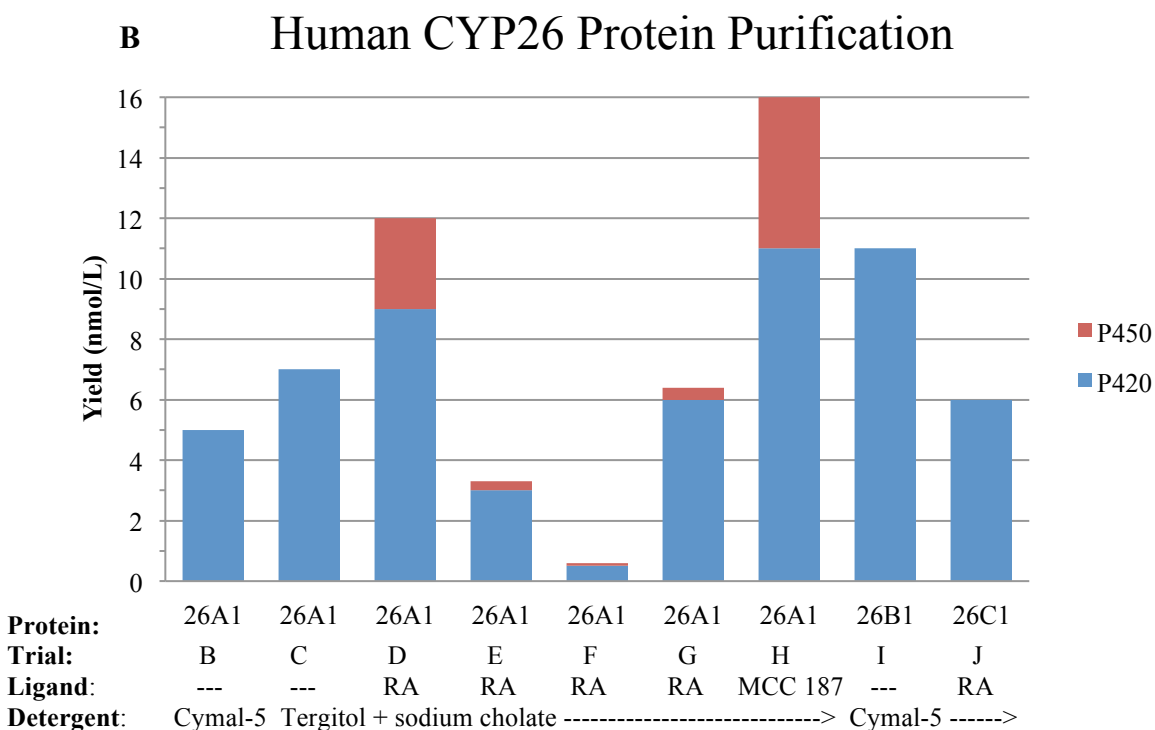
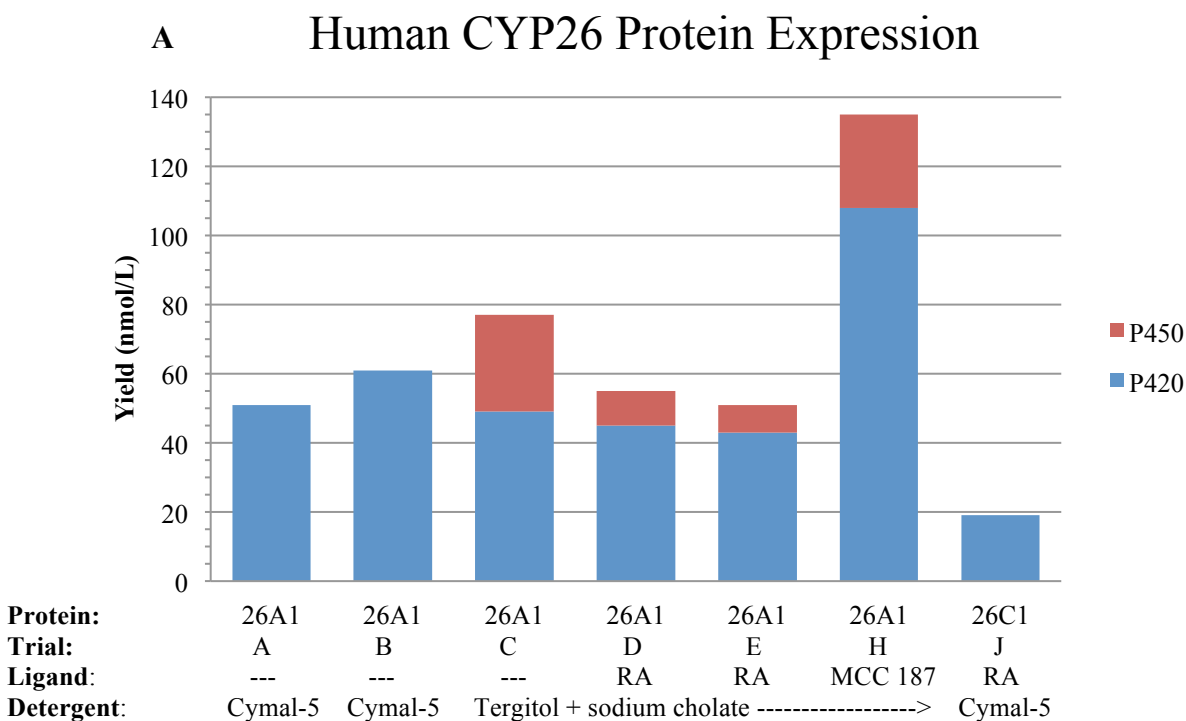


Figure 4.4. Human cytochrome P450 26 protein expression (A) and purification (B). Protein yields reported as nanomoles of protein per liter of expression media and determined by reduced carbon monoxide difference following expression and NiNTA chromatography. Data not shown from expression trials F, G, I and purification trial A because reduced carbon monoxide difference spectrum was not collected or protein was not recovered.

Table 4-4: Mouse cytochrome P450 26 protein expression and purification.

Trial	Protein	Cell Line	Cell Pellet Mass (g) / Expression Volume (L)	Wash or Elution Buffer Modifications	Stabilizing Ligand (E)(P)^b	Detergent	Protein yield pre-NiNTA (nmol)	Protein yield post-NiNTA (nmol)
A	CYP26A1	TOPP3	30.52 / 2.25	no wash buffer	none	4.8 mM Cymal-5	332 (P420)	42 (P420)
B	CYP26A1	TOPP3	60.84 / 4.5	no wash buffer	none	Sodium Cholate (1%) Tergitol (NP-10) (1%)	218 (P420)	17 (P420) 2 (P450)
C	CYP26A1	TOPP3	33.09 / 2.25	no wash buffer	5 μ M liarazole (P)	Sodium Cholate (1%) Tergitol (NP-10) (1%)	65 (P420) 22 (P450)	n.d. ^c
D	CYP26A1	TOPP3	28.34 / 2.25	no wash buffer	0.3 μ M MCC 154 (E)(P)	Sodium Cholate (1%) Tergitol (NP-10) (1%)	136 (P420) 2 (P450)	16 (P420) 7 (P450)
E	CYP26B1	TOPP3	30.37 / 2.25	no modification	5 μ M RA (E)(P)	4.8 mM Cymal-5	420 (P420)	50 (P420)
F	CYP26B1	TOPP3	39.19 / 2.25	8 mM His replaced by 100 mM Gly in wash buffer	5 μ M RA (E)(P)	4.8 mM Cymal-5	234 (P420)	24 (P420)
G	CYP26B1	TOPP3	38.50 / 2.25	Tris-HCl ^d	none	Emulgen-913 (0.2%)	276 (P420)	32 (P420)
H	CYP26B1	TOPP3	23.89 / 2.25	no wash buffer	0.3 μ M MCC 154 (E)(P)	Sodium Cholate (1%) Tergitol (NP-10) (1%)	135 (P420) 7 (P450)	13 (P420)
I	CYP26C1	TOPP3	29.80 / 2.25	no wash buffer	5 μ M RA	4.8 mM Cymal-5	~870 ^d	33 (P420)

^aReduced carbon monoxide difference spectrum was not collected, so value shown is an estimation using absolute spectral determination at λ_{max} ~408-412 nm

^bReports whether ligand was present during expression (E) and/or purification (P)

^cValue was not determined based on sample loss prior to this stage of purification

^dTris-HCl wash buffer containing 50 mM Tris-HCl, pH 7.4, 0.3 M NaCl, 100 mM glycine, and 20% glycerol; Tris-HCl elution buffer containing 50 mM Tris-HCl, pH 7.4, 0.3 M NaCl, 100 mM glycine, 80 mM histidine, and 20% glycerol

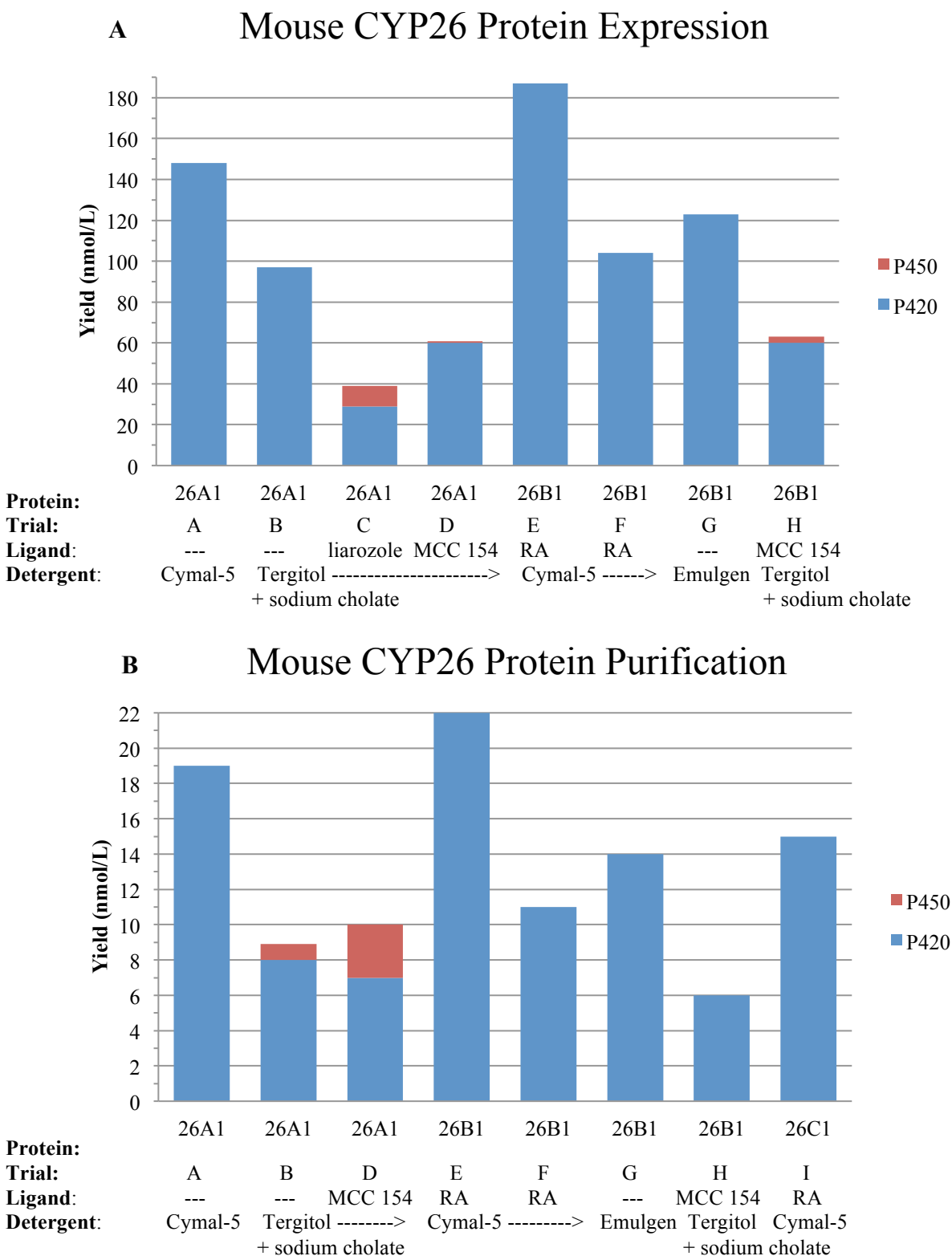


Figure 4.5. Mouse cytochrome P450 26 protein expression (A) and purification (B). Protein yields reported as nanomoles of protein per liter of expression media and determined by reduced carbon monoxide difference following expression and NiNTA chromatography. Data not shown from expression trial I and purification trial C because reduced carbon monoxide difference spectrum were not collected.

what is typically observed for the expression of CYP2A enzymes (approximately 35-40 grams) under identical expression conditions. Both qualities suggest that the expression of human CYP26A1 was lacking in comparison to the normal, healthy expression of P450 protein.

A number of variables were therefore addressed to promote a higher level of expression, including coexpression with the chaperone plasmid pGro7 (Takara Bio Inc., Mountain View, CA) (Table 4-3, Rows B-G), a reduced expression period of two days versus three, and addition of the natural substrate retinoic acid (Table 4-3, Rows D-G) or an inhibitor of the ‘MCC’ series (Table 4-3, Row H). The pGro7 plasmid encodes genes for the groES-groEL protein folding chaperone team, which is designed to facilitate the protein folding process over the course of expression. A reduction in the expression period by a day was intended to reduce cell accumulation along the wall of the flask during expression, which may be an indicator of cell death. Finally, the introduction of a ligand such as the natural substrate or an inhibitor may promote higher levels of protein expression by facilitating the stabilization of the protein as it is generated. The only expression that suggested moderate improvement, based on protein yield using reduced carbon monoxide difference spectral determination prior to NiNTA chromatography and slightly darker coloration of the cell pellet, was the result of the addition of the inhibitor MCC 187 (Table 4-3, Row H). Whether the improvement was due to the use of an optimized detergent system, the presence of an optimized stabilizing ligand in the protein expression and protein extraction steps, or a combination of the three cannot be established, but overall, the use of the pGro7 chaperone plasmid tended to suggest either negative or no effect on the amount of CYP26 enzyme expressed. This is based on the fact that the major difference between expressions in TOPP3 cells (Table 4-3, Rows A,H) and TOPP3 pGro7 cells (Table 4-3, Rows B-G) was that the former tended to yield more protein following extraction, with no

significant difference in cell pellet mass or coloration between the two. As a result, expressions of the five additional CYP26 proteins exclusively utilized the TOPP3 *E. coli* cell line without the pGro7 chaperone plasmid.

With the limited progress demonstrated by optimization to the expression of human CYP26A1, the remaining five CYP26 proteins in human and mouse were similarly pursued in hopes of greater success. Of the five remaining CYP26 proteins, mouse CYP26A1 (Table 4-4, Row A) and mouse CYP26B1 (Table 4-4, Row E) demonstrated the greatest prospect for expression and purification based on total nanomoles of protein determined to be present prior to the first chromatographic step (pre-NiNTA) as measured by the reduced carbon monoxide difference spectrum. The typical cell pellet following a three-day expression of mouse CYP26A1 or CYP26B1 was similar to that of human CYP26A1, with a slightly darker top layer, deeper brown coloration throughout, and an average cell mass of 30 grams per 2.25 L of expression culture, with a couple expressions of mouse CYP26B1 exceeding 35 grams.

Subsequent efforts to optimize the generation of the five remaining CYP26 proteins, including mouse CYP26A1 and CYP26B1, were focused on facilitating protein stabilization. To accomplish this, a variety of tight-binding ligands, including both substrate and inhibitors, were introduced into the cell culture media during expression and/or to the purification buffer during membrane extraction. The additional presence of liarozole during the extraction of mouse CYP26A1 from the *E. coli* membrane resulted in a dramatic decrease in protein recovery from 218 nmol P420 (Table 4-4, Row B) to 87 nmol (Table 4-4, Row C), though a small proportion of P450 was recovered at this stage for the first time. Substitution of liarozole by the more potent inhibitor MCC 154 during both expression and membrane extraction resulted in a slight improvement in overall yield compared to the use of liarozole with a total of 138 nmol recovered

following membrane extraction (Table 4-4, Row D), though only 2 nmol was attributed to P450 protein with a maximum wavelength of absorbance at 450 nm in the reduced carbon monoxide difference spectrum. The substrate RA was used from the very first expression of mouse CYP26B1 to facilitate protein stabilization, which generally resulted in yields of 234-420 nmol (Table 4-4, Rows E-F) following membrane extraction. Substitution of RA with the potent inhibitor MCC 154 during expression and membrane extraction resulted in a decrease in overall yield to 142 nmol (Table 4-4, Row H), with the appearance of a very small population of P450. Altogether, quantitative measures of total protein recovered following membrane extraction and qualitative measures of cell pellet mass and coloration suggested that the introduction of tight binding ligands failed to make any significant degree of improvement on the expression of either mouse CYP26A1 or CYP26B1.

Human CYP26B1, human CYP26C1, and mouse CYP26C1 were only expressed a single time each and were not pursued for further optimization. Unlike the dark coloration exhibited by the mouse CYP26A1 and CYP26B1 *E. coli* cell pellets, the human CYP26B1 cell pellet harvested after three days of expression was much lighter brown in color with a rosy tint (Figure 4.6) and a similarly red-brown top layer that was very thin. Both qualities are in direct opposition with the deep brown coloration and dark, thick top layer attributed to TOPP3 cells expressing other P450 enzymes in appreciable yields, although the cell mass was very comparable to any of the other five CYP26 proteins investigated at 33 grams. The human CYP26C1 pellet was not quite as poor as human CYP26B1, and exhibited a normal brown tone, a very thin, dark top layer, and a cell mass just below average at 28 grams. Qualitatively, visual inspection of the mouse CYP26C1 *E. coli* cell pellet suggested that this protein was expressed in high levels based

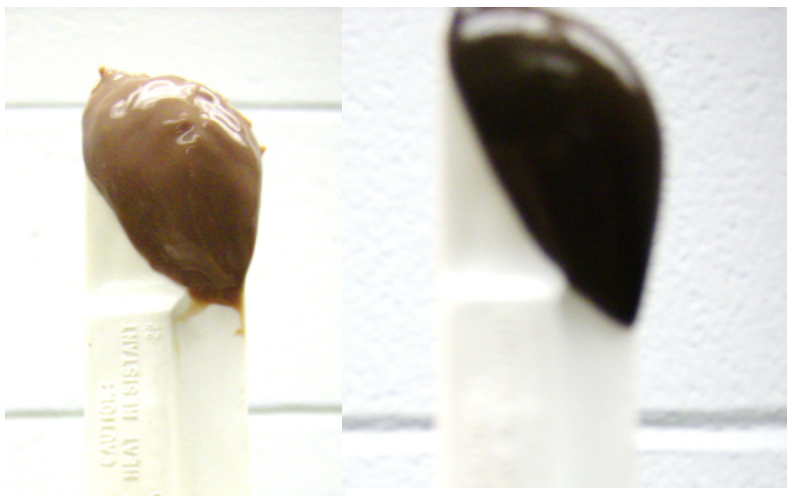


Figure 4.6. Representative cell pellet samples of CYP26-expressing TOPP3 *E. coli* cells. The human CYP26B1 cell pellet (left) harvested after three days of expression is light brown in color with a rosy tint. This quality of coloration is quite different than the dark brown coloration exhibited by mouse CYP26A1 (right) and mouse CYP26B1 (not shown). The darker brown cell pellet is more consistent with the higher levels of cytochrome P450 expression such as observed with human CYP2A expressing cells.

on the deep brown color and dark top layer exhibiting the same thickness seen with mouse CYP26A1 and mouse CYP26B1.

Purification of CYP26 proteins

A total of eight attempts were made to optimize the purification of human CYP26A1 to generate enough pure protein for characterization studies. The initial two purifications of human CYP26A1 utilized the detergent Cymal-5, as this detergent has proven effective in solubilizing multiple truncated mammalian P450 enzymes studied in the lab, including CYP2A6 and CYP2A13. The first purification with Cymal-5 failed in the sense that no protein was successfully recovered from the elution fractions of the NiNTA column (Table 4-4, Row A). This was because the protein washed off the column with the use of the 8 mM histidine buffer, which serves to remove impurities that have only a weak affinity for the NiNTA column. To prevent this loss, the use of two column-volumes of 8 mM histidine was replaced with four column-volumes of loading buffer. The elimination of the 8 mM histidine buffer proved to be effective in that subsequently little P450 protein appeared to be lost at the wash step of the NiNTA column (Table 4-4, Row B). Unfortunately, a total of only 11 nmol of P420 were recovered in the elution fractions. As a result, subsequent purifications used an optimized

detergent system of sodium cholate and Tergitol (1% each) (Table 4-4, Rows C-H), a combination which had been reported in the literature to work effectively for the purification of CYP26 protein expressed in insect cells. The combination of these two detergents appeared to be beneficial based on the detection of a small amount of P450 protein following extraction and ultracentrifugation, where only P420 had been present in purifications utilizing Cymal-5. Unfortunately, this same degree of improvement was not evident in the quality or yield of protein following NiNTA column chromatography. Where 11 nmol P420 was recovered following NiNTA chromatography with Cymal-5 (Table 4-3, Row B), 15 nmol of P420 was recovered at the same stage with the combination of sodium cholate and Tergitol (Table 4-3, Row C). Further optimization to the purification of human CYP26A1 involved the inclusion of substrate (Table 4-3, Rows D-G) or inhibitor (Table 4-3, Row H) to stabilize the protein over the course of purification as well as an increased concentration of NaCl from 0.1 M to 0.2 M (Table 4-3, Rows E-G) to decrease cloudiness of the protein solution upon elution. The latter was perceived to be the result of protein precipitation, which has been successfully controlled in the purification of other truncated mammalian P450 enzymes by increasing the ionic strength of the buffer. When an increase in the salt content of the elution buffer failed to completely prevent protein precipitation, measures were taken to further dilute the protein with buffer as it eluted off the column (Table 4-3, Row G). The combination of these approaches failed to significantly increase the yield of human CYP26A1 protein following NiNTA chromatography, so the purification of five additional CYP26 proteins were therefore pursued.

Following multiple failed attempts to optimize the purification of human CYP26A1, each of the five remaining CYP26 proteins were purified once using the standard purification protocol described in Chapter 2: Methods. The results of these five initial purifications were used to

determine which protein(s) represented the most potential for success in purification using a comparison of the total yield of protein recovered following NiNTA column chromatography (post-NiNTA) and the color of the protein solution over the course of protein extraction and purification. A dark red color serves as a visual indication of a high content of heme-containing protein in solution, with lighter red indicating lesser concentrations and a lack of red altogether indicating the presence of little or no heme-containing protein. With as much as 40-50 nmol of protein recovered from the NiNTA column, mouse CYP26A1 and mouse CYP26B1 were selected for further purification optimization over the lesser yielding proteins mouse CYP26C1, human CYP26B1, and human CYP26C1.

A total of four attempts were made to optimize the purification of mouse CYP26B1. The first purification of mouse CYP26B1 resulted in a loss of half of the P450 protein at the wash step with 8 mM histidine buffer, and a recovery of only 50 nmol protein upon elution (Table 4-4, Row E). Because elimination of the wash buffer altogether results in a significant reduction in the final purity of the protein, a wash buffer containing 100 mM glycine rather than histidine was utilized in the second purification of mouse CYP26B1. Glycine has a single nitrogen donor atom and can poorly compete for Ni^{2+} binding, and thus should serve as a less stringent option for removing impurities. The reality is that more P450 protein was lost at the wash step with the glycine wash than with the histidine wash, with the 24 nmol of protein recovered following NiNTA chromatography originating from the wash fractions (Table 4-4, Row F). Subsequent purifications replaced the application of two column-volumes of wash buffer with four column-volumes of loading buffer (Table 4-3, Rows G-H). This reduced the loss of P450 during the wash step, but overall had little effect on the final yield of protein following NiNTA chromatography. As with human CYP26A1, alternative detergents and tight-binding ligands were investigated in

hopes of providing improved protein stabilization and higher yield. The combined use of Cymal-5 and RA for the purification of mouse CYP26B1 allowed for the recovery of 24-50 nmol P420 (Table 4-4, Rows E-F), whereas the combination of the optimized detergent system sodium cholate and Tergitol and the potent inhibitor MCC 154 allowed for the recovery of only 13 nmol P420 (Table 4-4, Row H). The use of Emulgen-913 in the absence of stabilizing ligand allowed for the recovery of 32 nmol P420 following NiNTA chromatography (Table 4-4, Row G), which is less than the 50 nmol of P420 recovered from the first purification of mouse CYP26B1 with Cymal-5 in the presence of RA (Table 4-4, Row E) but greater than the 13 nmol recovered from the purification of mouse CYP26B1 using sodium cholate and Tergitol in the presence of MCC 154 (Table 4-4, Row H). Altogether, the use of alternative detergents and tight-binding ligands failed to promote a significant improvement in the yield of mouse CYP26B1 following NiNTA chromatography.

With the results of the initial purification of mouse CYP26A1 (Table 4-4, Row A) indicating similar promise as mouse CYP26B1 (Table 4-4, Row E), optimization to the purification of mouse CYP26A1 was pursued over the course of three additional purifications. Unlike human CYP26A1, the fractions did not exhibit any cloudiness upon elution from the NiNTA column that would suggest precipitation, so no attempts were made to alter the concentration of NaCl in the elution buffer or to otherwise alter the protein upon elution. As a result, the only modifications made to the purification process were the choice of detergent and stabilizing ligand, since the 8 mM histidine buffer was eliminated from the very first purification (Table 4-4, Row A). Once again, the combination of sodium cholate and Tergitol appeared to make a small improvement by promoting the appearance of a small amount of P450 protein upon

NiNTA elution (Table 4-4, Rows B, D), whereas only P420 had been present previously. However, the addition of stabilizing ligands failed to similarly promote the proportion of P450 over P420 or to increase the quantity of protein recovered in the NiNTA elution fractions. The use of the inhibitor MCC 154 in combination with the detergents sodium cholate and Tergitol resulted in the recovery of 16 nmol P420 and 7 nmol P450 (Table 4-4, Row D) compared to the 17 nmol P420 and 2 nmol P450 recovered following NiNTA chromatography in the absence of stabilizing ligand using the same combination of detergents (Table 4-4, Row B). A final attempt was made to perform a scale-up of the purification in the absence of ligand by starting with a 60 gram cell pellet, but the amount of protein recovered following NiNTA chromatography (Table 4-4, Row B) was less than or equal to the purification smaller mouse CYP26A1-expressed *E. coli* cell pellets (Table 4-4, Rows A, D).

Characterization of Human and Mouse CYP26A1 by Western blot and Reduced Carbon Monoxide Difference

Reduced carbon monoxide difference (CO-difference) spectra served as the primary means of monitoring the presence and quality of CYP26 protein over the course of each purification that was performed. As a whole, the CO-difference spectra indicated that the CYP26 proteins were poor in quality due to the predominance of a peak at 420 nm rather than at 450 nm, which was often either absent or much less pronounced. Representative CO-difference spectra for human CYP26A1 and mouse CYP26A1 are shown in Figure 4.7. The CO-difference spectra of both CYP26 proteins illustrate the presence of a larger proportion of P420 compared to P450 prior to (post-ult) and following NiNTA chromatography (NiNTA elution).

Western blot analysis was used as a secondary method for the detection of CYP26 protein over the course of purification. Protein was sampled prior to NiNTA chromatography (post-ult),

as well as at the loading, wash, and elution stages of NiNTA chromatography. Initially, an anti-His antibody was utilized for the detection of CYP26 protein by means of the 4X-histidine tag engineered into each of the six modified CYP26 proteins. Unfortunately, no band at ~53 kDa band (expected molecular weight) was detected within CYP26-containing samples using the anti-His antibody, so a more specific polyclonal antibody of human CYP26A1 was purchased. Though this new antibody was unable to detect CYP26B1 or CYP26C1, it allowed for the

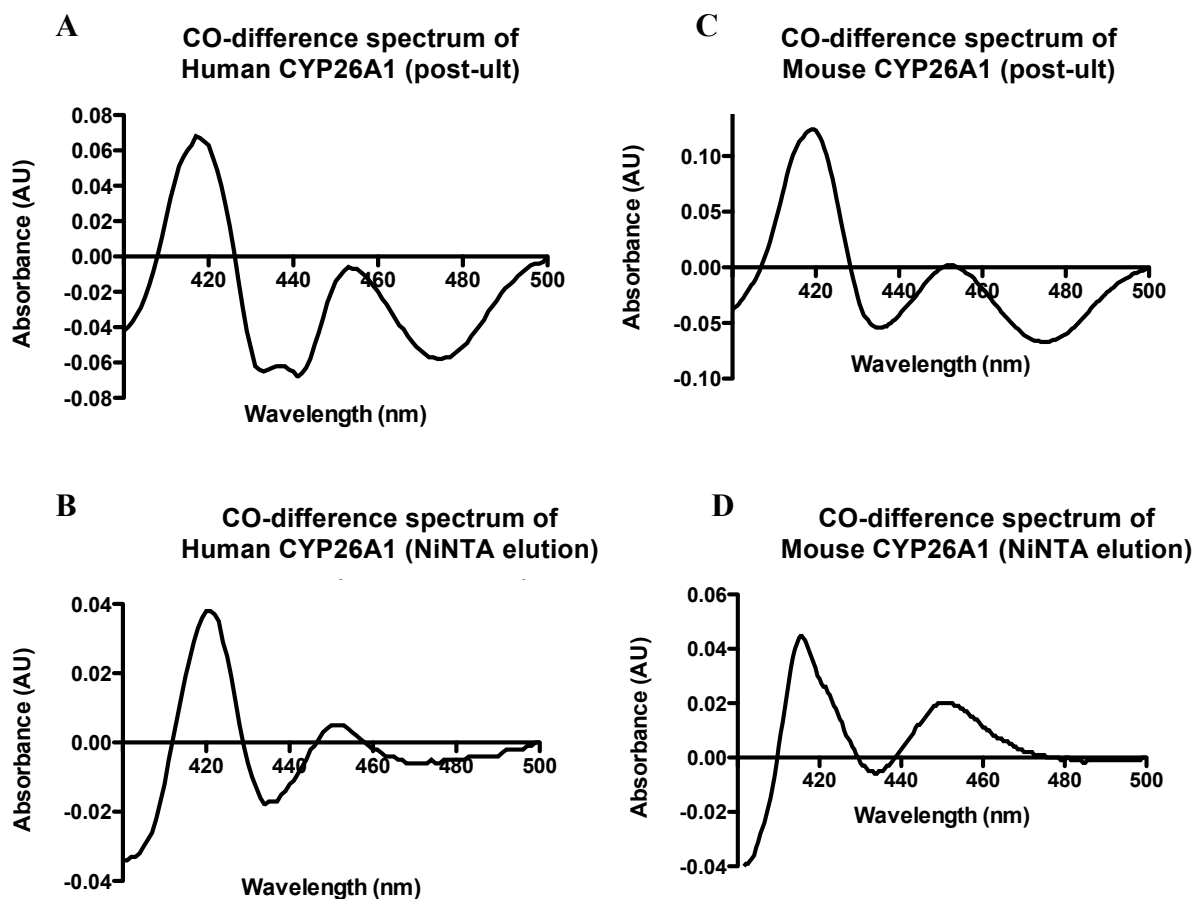


Fig 4.7. Reduced carbon monoxide difference spectra of CYP26A1. Reduced carbon monoxide difference (CO-difference) spectra were used to quantify the amount of active (P450) and inactive (P420) protein in preparations of human CYP26A1 (A,B) and mouse CYP26A1 (C,D) prior to (post-ult) and following NiNTA chromatography (NiNTA elution). The reduced carbon monoxide difference spectra of human CYP26A1 and mouse CYP26A1 indicate the presence of a larger proportion of P420 compared to P450 in all samples analyzed, as well as a significant loss of protein following NiNTA chromatography.

successful detection of both human and mouse CYP26A1 with a band near 50 kDa in NiNTA elution fractions, and a faint band at the same molecular weight from protein sampled prior to NiNTA chromatography (Figure 4.8).

Functional Characterization of Mouse CYP26A1 using Retinoic Acid Metabolism

The CYP26 protein generated over the course of expression and purification studies was further characterized by its ability to metabolize the substrate retinoic acid (RA) over the course of three separate trials. Mouse CYP26A1 was selected for these studies over the other five CYP26 proteins based on the fact that 1) CYP26A1 is reported to be the most dedicated to

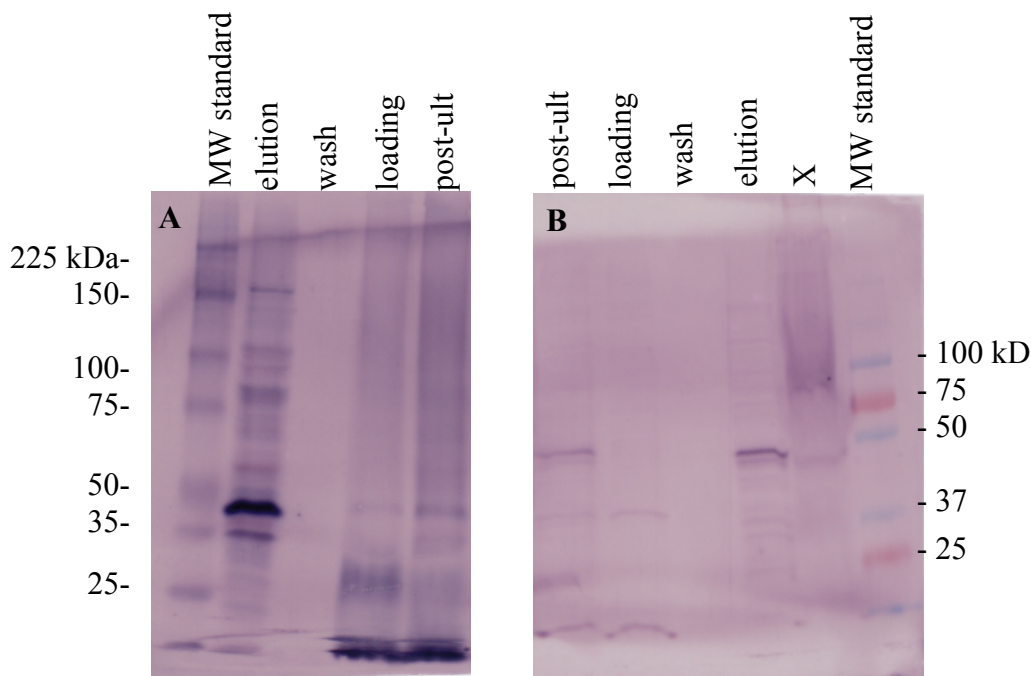


Fig 4.8. Detection of CYP26A1 by Western blot. Human CYP26A1 (A) and mouse CYP26A1 (B) protein sampled following ultracentrifugation (post-ult) and at the loading, wash, and elution stages of NiNTA chromatography were each analyzed using Western blot analysis with human CYP26A1 polyclonal antibody (AbCam). Protein bands near ~50 kDa were detected in both human and mouse protein samples collected following ultracentrifugation (post-ult) and following NiNTA chromatography (elution). The absence of a protein band near ~50 kDa in the NiNTA wash samples suggests that CYP26 protein (both human and mouse) was not lost during this stage of NiNTA chromatography, although a faint band present in the human CYP26A1 loading sample suggests that some CYP26 protein was lost during the loading stage.

retinoic acid metabolism within the CYP26 family and 2) mouse CYP26A1 could be generated in greater quantities with a larger proportion of P450:P420 compared to the human form. Two alternative preparations of mouse CYP26A1 were selected these assays. One was a microsomal preparation of *E. coli* cells expressing mouse CYP26A1. The second was mouse CYP26A1 purified using NiNTA chromatography. Prior to retinoic acid metabolism, the total content of P420 and P450 within each of the protein preparations was determined by the reduced carbon monoxide difference spectrum. While the microsomal preparation consisted entirely of P420 protein at a concentration of 20.0 μM , the NiNTA-purified protein consisted of a small amount of P450 at a concentration of 0.8 μM in addition to a larger population of P420 at a concentration of 3.3 μM .

The combined results of all three trials failed to indicate any metabolic activity for mouse CYP26A1 in the presence of the substrate RA (Figure 4.9). Comparison of the microsomal and purified mouse CYP26A1 reaction samples to a standard containing 1 μM RA in the first of three trials (Figure 4.9 A) appeared to indicate no consumption of RA within the purified protein sample reactions, although a small degree of variation between the standard and the microsomal protein preparation encouraged further investigation. As a result, a second trial was performed to further assay the function of microsomal mouse CYP26A1 with the following modifications: 1) an increased substrate concentration of 10 μM RA, 2) additional negative control reactions (no reaction, no NADPH, no P450 reductase), and 3) parallel assays to investigate the prospective utility of CYP2E1 as a positive control. The results of this second trial (Figure 4.9 B) further provided evidence of the inability of mouse CYP26A1 protein to metabolize RA, but the suggestion of a very slight reduction in RA peak area in the CYP2E1 reaction samples gave

A Retinoic Acid Metabolism: Trial 1

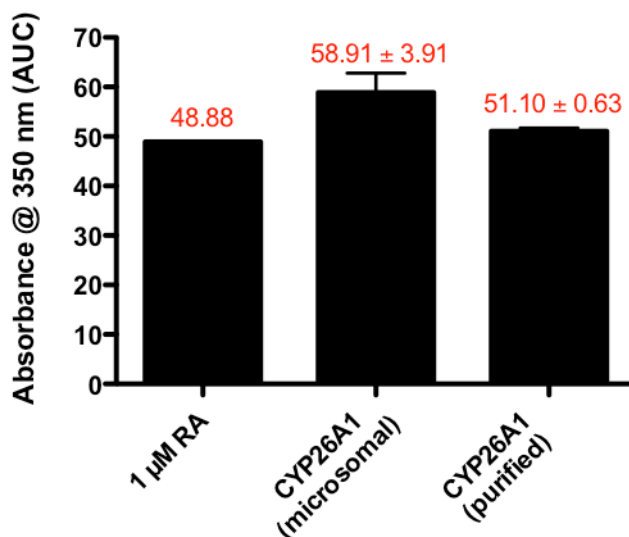
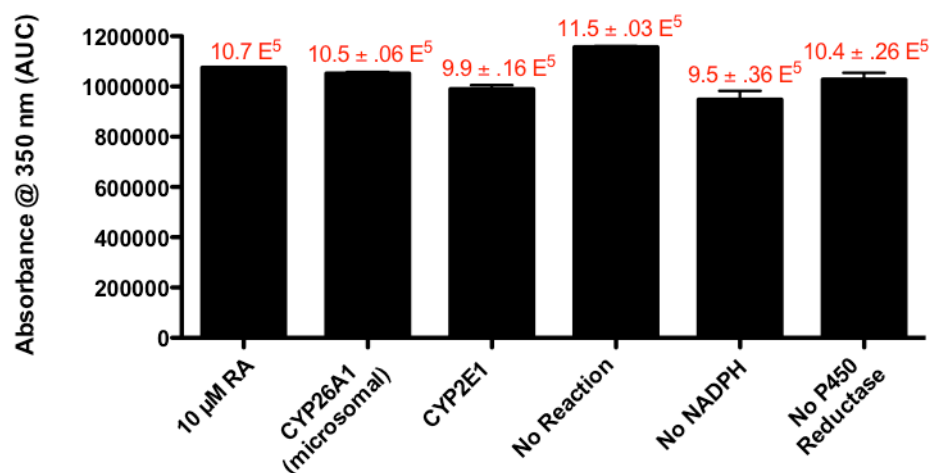
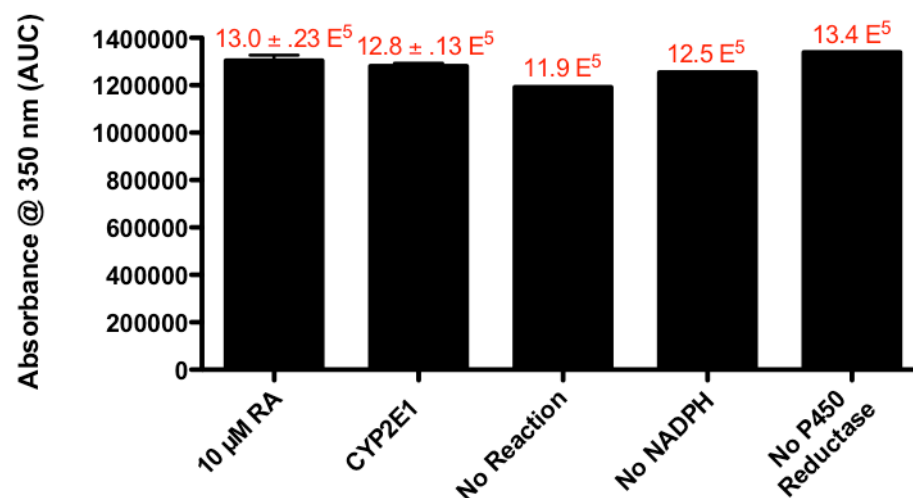


Figure 4.9 Characterization of recombinant CYP26 protein by RA metabolism. The metabolic function of mouse CYP26A1 and human CYP2E1 were evaluated based on the ability to metabolize the substrate RA over the course of three separate trials (A, B, and C). In sample reactions containing concentrations of 1 μ M RA (A) or 10 μ M RA (B, C), metabolic activity was assessed based on comparison of the RA peak area to an RA standard and various control reactions. A lack of reduction in the RA peak area signified an inability of either CYP26A1 or CYP2E1 to metabolize the substrate RA.

B Retinoic Acid Metabolism: Trial 2



C Retinoic Acid Metabolism: Trial 3



reason to further investigate CYP2E1-mediated RA catabolism in a third and final trial. The results of the third trial (Figure 4.9 C) served as final verification of CYP2E1's inability to metabolize RA based on the lack of a significant reduction in the RA peak area upon comparison to all relevant controls.

Discussion

The development of truly selective CYP26 inhibitors and improved RAMBAs would be greatly facilitated by more detailed structural and functional characterization of the CYP26 family of enzymes. Very little is known about the structures, metabolic pathways, or kinetics of the CYP26 enzymes aside from the fact that they serve a dominant role in the catabolism of RA through *at*RA hydroxylation. The present study involved the development of a new method for the expression and purification of CYP26 proteins with yield and purity that exceeded published methods of CYP26 protein production, which involve either expression in transfected mammalian cells or baculovirus infected insect cells.^{6,7,10,20,22,28,29} This study represents the first account of recombinant CYP26 protein expression in *E. coli* resulting in any amount of active P450 protein, as evaluated by the reduced carbon monoxide difference spectrum. The only other published attempt to express CYP26A1 in *E. coli* was a reported failure based on the fact that only P420 was detected by the reduced carbon monoxide difference spectrum.³⁰

These studies specifically addressed the initial prerequisite of providing the capacity for generating large quantities of CYP26 enzyme by employing *E. coli* as an expression host. The additional challenges that come with studying a membrane-bound protein were subsequently addressed by modifying the CYP26 proteins for enhanced expression and ease of purification. Specifically, common molecular biology techniques were used to remove the N-terminal

transmembrane sequence, incorporate a short hydrophilic sequence, and add four histidine residues to the C-terminus of each of the six CYP26 proteins used in these studies.

The real challenge within the project arose during optimization studies designed to enhance the yield and quality of CYP26 during expression and purification. A number of variables were assessed to specifically address both of these qualities, including use of the chaperone plasmid pGro7 and the most effective detergents and stabilizing ligands based on available reports. The detergents employed include Cymal-5, a detergent successfully employed for the purification of the CYP2A family of proteins,^{24,25} and the combination of sodium cholate and Tergitol, which has been published as an effective detergent system for the purification of full-length CYP26 expressed in insect cells.^{6,7,31} The ligands used to promote protein stabilization include the native substrate retinoic acid, the clinically-developed RAMBA liarozole, and two compounds from a recently published series of low nanomolar inhibitors referred to as ‘MCC’ inhibitors.¹⁹ Unfortunately, a combination of even the best available detergents and stabilizing ligands demonstrated limited effectiveness in generating P450 in higher quality or enhanced yield. The most optimized purifications of the CYP26 proteins exhibiting the best expression did not exceed yields of 50 nmol of total protein following a single chromatographic step, with the majority of that protein indicating a lack of activity according to assessment by the reduced carbon monoxide difference spectrum. This lack of activity appeared to be confirmed when two different preparations of CYP26A1 failed to metabolize the substrate retinoic acid.

Despite the limited success in the studies summarized here, these results serve as a critical foundation for future work for the optimization of CYP26 expression and purification. The range of possibilities that could lead to the successful generation of this family of proteins

has by no means been exhausted. For the sake of time, the CYP26 proteins were expressed within these studies in a single *E. coli* cell line (with or without the use of a plasmid chaperone), and optimization was focused on using the best stabilizing ligands and detergents available. Many other available *E. coli* cell lines remain to be tested, as well as a great variety of detergents. Another possibility may be that the CYP26 proteins require alternative modifications to the amino acid sequence. Since all previous studies have been conducted with full-length CYP26 protein, it is possible that the modifications to the structure employed in these studies may have disrupted the native stability of CYP26 to a point that could not be rescued with any combination of detergents and stabilizing ligands. Finally, new technology in the expression and purification of recombinant P450 proteins may offer additional insights into the successful generation of particularly challenging proteins, such as the CYP26 proteins.

Conclusion

Although the CYP26 enzymes are known to be important mediators of RA catabolism in the body, the ability to generate detailed structural and functional data on this family of enzymes has been hindered by the inability to generate sufficient amounts of recombinant enzyme necessary for these studies. To address this problem, expression and purification studies were pursued for all three members of the CYP26 family (CYP26A1, CYP26B1, CYP26C1) from both mouse and human with the immediate goal of generating CYP26 protein with enhanced yield and purity. The results of these studies serve as the first and only known record of the recombinant expression of CYP26A1 and CYP26B1 in *E. coli* leading to any amount of active P450 protein by the reduced carbon monoxide difference spectrum. Of the six CYP26 enzymes expressed, mouse CYP26A1 and mouse CYP26B1 demonstrated the highest expression levels based on 1) total nanomoles of protein determined using reduced carbon monoxide difference

spectral determination prior to the first chromatographic step and 2) the quality of the TOPP3 *E. coli* cell pellet harvested after three days of CYP26 protein expression. As a result, these two proteins, in addition to the original target of interest human CYP26A1, were selected for additional studies with the purpose of increasing the yield and quality of protein generated from the initial expressions and purifications. A number of variables were addressed over the course of these optimization studies. During expression of CYP26, protein stability was addressed through the use of the protein folding chaperone pGro7 and various stabilizing ligands including the natural substrate retinoic acid, the clinically-developed retinoic acid metabolism blocking agent liarozole, and two inhibitors of a recently published 3-(1*H*-imidazol- and triazol-1-yl) -2,2-dimethyl-3-[4-(naphthalen-2-ylamino)phenyl]propyl series of derivatives designated as ‘MCC’ inhibitors.¹⁹ During purification of CYP26, the wash buffer was modified to reduce P450 loss prior to elution, stabilizing ligands continued to be employed, and several detergents were sampled. Of the changes that were made, the use of the detergents sodium cholate and tergitol and the incorporation of the ‘MCC’ inhibitors appeared to have the greatest benefit to the expression and purification of CYP26 protein. By incorporating both of these modifications, CYP26 protein could be generated in yields of 300-400 nmol per 2.25 L expression with the ability to recover 5-50 nmol following NiNTA chromatography. However, reduced carbon monoxide difference assays conducted prior to and following NiNTA chromatography indicated that the quality of CYP26 protein was poor based on the predominance of an absorbance peak at 420 nm compared to absorbance at 450 nm. When functional assays of RA metabolism were conducted with mouse CYP26A1 protein, no significant difference in the substrate RA was observed compared to control reactions. As a result, further optimization will be required to

reach the original goal set forth to generate pure recombinant CYP26 enzymes for basic kinetic and structural determination studies.

References

1. Sun, S.-Y. and Lotan, R. (2002) Retinoids and their receptors in cancer development and chemoprevention. *Crit Rev Oncol Hematol* **41**, 41-55.
2. Tang, X.-H. and Gudas, L.J. (2011) Retinoids, retinoic acid receptors, and cancer. *Annu. Rev. Pathol.: Mech. Dis.* **6**, 345-364.
3. Njar, V.C.O., Gediya, L., Purushottamachar, P., Chopra, P., Vasaitis, T.S., Khandelwal, A., Mehta, J., Huynh, C., Belosay, A. and Patel, J. (2006) Retinoic acid metabolism blocking agents (RAMBAs) for treatment of cancer and dermatological diseases. *Bioorg. Med. Chem.* **14**, 4323-4340.
4. Thatcher, J.E. and Isoherranen, N. (2009) The role of CYP26 enzymes in retinoic acid clearance. *Expert Opin. Drug Metab. Toxicol.* **5**, 875-886.
5. Chithalen, J.V., Luu, L., Petkovich, M. and Jones, G. (2002) HPLC-MS/MS analysis of the products generated from all-trans-retinoic acid using recombinant human CYP26A. *J. Lipid Res.* **43**, 1133-1142.
6. Lutz, J.D., Dixit, V., Yeung, C.K., Dickmann, L.J., Zelter, A., Thatcher, J.E., Nelson, W.L. and Isoherranen, N. (2009) Expression and functional characterization of cytochrome P 450 26A1, a retinoic acid hydroxylase. *Biochem. Pharmacol.* **77**, 258-268.
7. Topletz, A.R., Thatcher, J.E., Zelter, A., Lutz, J.D., Tay, S., Nelson, W.L. and Isoherranen, N. (2012) Comparison of the function and expression of CYP26A1 and CYP26B1, the two retinoic acid hydroxylases. *Biochem. Pharmacol.* **83**, 149-163.
8. White, J.A., Ramshaw, H., Taimi, M., Stangle, W., Zhang, A., Everingham, S., Creighton, S., Tam, S.-P., Jones, G. and Petkovich, M. (2000) Identification of the human cytochrome P450, P450RAI-2, which is predominantly expressed in the adult cerebellum and is responsible for all-trans-retinoic acid metabolism. *Proc. Natl. Acad. Sci. U. S. A.* **97**, 6403-6408.
9. Luu, L., Ramshaw, H., Tahayato, A., Stuart, A., Jones, G., White, J. and Petkovich, M. (2001) Regulation of retinoic acid metabolism. *Adv. Enzyme Regul.* **41**, 159-175.
10. Taimi, M., Helvig, C., Wisniewski, J., Ramshaw, H., White, J., Amad, M.a., Korczak, B. and Petkovich, M. (2004) A novel human cytochrome P450, CYP26C1, involved in metabolism of 9-cis and all-trans isomers of retinoic acid. *J. Biol. Chem.* **279**, 77-85.
11. Warrell, R.P., Jr., Frankel, S.R., Miller, W.H., Jr., Scheinberg, D.A., Itri, L.M., Hittelman, W.N., Vyas, R., Andreeff, M., Tafuri, A., Jakubowski, A. and et, a. (1991) Differentiation therapy of acute promyelocytic leukemia with tretinoin (all-trans-retinoic acid). *N Engl J Med* **324**, 1385-93.
12. Gallagher, R.E. (2002) Retinoic acid resistance in acute promyelocytic leukemia. *Leukemia* **16**, 1940-1958.
13. Ross, A.C. and Zolfaghari, R. (2011) Cytochrome P450s in the regulation of cellular retinoic acid metabolism. *Annu. Rev. Nutr.* **31**, 65-87.
14. Muindi, J.R., Frankel, S.R., Huselton, C., DeGrazia, F., Garland, W.A., Young, C.W. and Warrell, R.P., Jr. (1992) Clinical pharmacology of oral all-trans retinoic acid in patients with acute promyelocytic leukemia. *Cancer Res* **52**, 2138-42.

15. Muindi, J., Frankel, S.R., Miller, W.H., Jr., Jakubowski, A., Scheinberg, D.A., Young, C.W., Dmitrovsky, E. and Warrell, R.P., Jr. (1992) Continuous treatment with all-trans retinoic acid causes a progressive reduction in plasma drug concentrations: implications for relapse and retinoid "resistance" in patients with acute promyelocytic leukemia. *Blood* **79**, 299-303.
16. Njar, V.C.O. (2002) Cytochrome P450 retinoic acid 4-hydroxylase inhibitors: potential agents for cancer therapy. *Mini-Rev. Med. Chem.* **2**, 261-269.
17. Miller, W.H., Jr. (1998) The emerging role of retinoids and retinoic acid metabolism blocking agents in the treatment of cancer. *Cancer (N. Y.)* **83**, 1471-1482.
18. McCaffery, P. and Simons, C. (2007) Prospective teratology of retinoic acid metabolic blocking agents (RAMBAs) and loss of CYP26 activity. *Curr. Pharm. Des.* **13**, 3020-3037.
19. Gomaa, M.S., Bridgens, C.E., Veal, G.J., Redfern, C.P.F., Brancale, A., Armstrong, J.L. and Simons, C. (2011) Synthesis and biological evaluation of 3-(1H-imidazol- and triazol-1-yl)-2,2-dimethyl-3-[4-(naphthalen-2-ylamino)phenyl]propyl derivatives as small molecule inhibitors of retinoic acid 4-hydroxylase (CYP26). *J. Med. Chem.* **54**, 6803-6811.
20. Helvig, C., Taimi, M., Cameron, D., Jones, G. and Petkovich, M. (2011) Functional properties and substrate characterization of human CYP26A1, CYP26B1, and CYP26C1 expressed by recombinant baculovirus in insect cells. *J. Pharmacol. Toxicol. Methods* **64**, 258-263.
21. White, J.A., Beckett-Jones, B., Guo, Y.-D., Dilworth, F.J., Bonasoro, J., Jones, G. and Petkovich, M. (1997) cDNA cloning of human retinoic acid-metabolizing enzyme (hP450RAI) identifies a novel family of cytochromes P450 (CYP26). *J. Biol. Chem.* **272**, 18538-18541.
22. White, J.A., Guo, Y.D., Baetz, K., Beckett-Jones, B., Bonasoro, J., Hsu, K.E., Dilworth, F.J., Jones, G. and Petkovich, M. (1996) Identification of the retinoic acid-inducible all-trans-retinoic acid 4-hydroxylase. *J Biol Chem* **271**, 29922-7.
23. Wester, M.R., Stout, C.D. and Johnson, E.F. (2002) Purification and crystallization of N-terminally truncated forms of microsomal cytochrome P450 2C5. *Methods Enzymol.* **357**, 73-79.
24. DeVore, N.M., Smith, B.D., Urban, M.J. and Scott, E.E. (2008) Key residues controlling phenacetin metabolism by human cytochrome P450 2A enzymes. *Drug Metab. Dispos.* **36**, 2582-2590.
25. Smith, B.D., Sanders, J.L., Porubsky, P.R., Lushington, G.H., Stout, C.D. and Scott, E.E. (2007) Structure of the human lung cytochrome P 450 2A13. *J. Biol. Chem.* **282**, 17306-17313.
26. Wu, Z.-L., Qiao, J., Zhang, Z.-G., Guengerich, F.P., Liu, Y. and Pei, X.-Q. (2009) Enhanced bacterial expression of several mammalian cytochrome P450s by codon optimization and chaperone coexpression. *Biotechnol. Lett.* **31**, 1589-1593.
27. Liu, C., Russell, R.M., Seitz, H.K. and Wang, X.-D. (2001) Ethanol enhances retinoic acid metabolism into polar metabolites in rat liver via induction of cytochrome P4502E1. *Gastroenterology* **120**, 179-189.
28. Pennimpede, T., Cameron, D.A., MacLean, G.A., Li, H., Abu-Abed, S. and Petkovich, M. (2010) The role of CYP26 enzymes in defining appropriate retinoic acid exposure during embryogenesis. *Birth Defects Res., Part A* **88**, 883-894.

29. Sonneveld, E., Van, D.B.C.E., Van, D.L.B.-J.M., Schulkes, R.-K.A.M., Petkovich, M., Van, D.B.B. and Van, D.S.P.T. (1998) Human retinoic acid (RA) 4-hydroxylase (CYP26) is highly specific for all-trans-RA and can be induced through RA receptors in human breast and colon carcinoma cells. *Cell Growth Differ.* **9**, 629-637.
30. Lee, S.-J., Perera, L., Coulter, S.J., Mohrenweiser, H.W., Jetten, A. and Goldstein, J.A. (2007) The discovery of new coding alleles of human CYP26A1 that are potentially defective in the metabolism of all-trans retinoic acid and their assessment in a recombinant cDNA expression system. *Pharmacogenet. Genomics* **17**, 169-180.
31. White, J.A., Petkovich, M.P., Jones, G. and Ramshaw, H. (2009) Antisense inhibition of P450RAI-2 (cytochrome P 450 26B1)-induced retinoic acid (RA) hydroxylation for treating diseases including keratosis and cancer. 99pp., Cont.-in-part of Appl. No. PCT/CA2000/0001493. (Cytochroma Inc., Can.).

Chapter 5

Conclusions

The goal of this thesis research was to contribute to an understanding of how substrates and inhibitors interact with individual P450 enzymes so that it may be applied to the prediction of chemical toxicology and the development of enhanced chemotherapeutic agents. Two different families of P450 enzymes have been examined to better understand the biochemical properties that serve as the foundation for methods of selectively targeting P450 enzymes. The first is the xenobiotic metabolizing CYP2A family, which is involved in the activation of several procarcinogens, including the tobacco-related nitrosamine 4-(methylnitrosamino)-1-(3-pyridyl)-1-butanone (NNK). The second is the CYP26 family, which is involved in the metabolism of retinoic acid (RA), the endogenous derivative of vitamin A.

The human CYP2A family consists of the functional enzymes CYP2A6 and CYP2A13 which share an amino acid sequence identity of 94%.¹ While CYP2A6 is mainly expressed in the liver and CYP2A13 is primarily expressed in the respiratory tract,² both enzymes have many small, cyclic substrates in common, including nicotine,³ *para*-nitrophenol,⁴ coumarin,² and the nicotine-derived compound cotinine.³ In addition, CYP2A13 preferentially metabolizes or has the sole ability to activate a number of procarcinogenic compounds, including aflatoxin B₁,⁵ 4-aminobiphenyl,⁶ and the tobacco-related nitrosamine 4-(methylnitrosamino)-1-(3-pyridyl)-1-butanone (NNK).^{2,7} Each of these compounds requires activation to generate reactive intermediates that ultimately result in carcinogenicity. To evaluate the involvement of CYP2A6 versus CYP2A13 in the metabolism and activation of potentially harmful chemical agents *in vivo*, selective inhibitors are needed. Several compounds were reported in the literature to selectively inhibit CYP2A6 before CYP2A13 enzyme activity was recognized. These include:

phenethyl isothiocyanate (PEITC),⁸ 4-dimethylaminobenzaldehyde (DMABA),⁹ 8-methoxypsoralen (8-MOP),¹⁰ tranilcypromine,¹¹ tryptamine,¹¹ pilocarpine, (*S*)-nicotine,¹² (*R*)-(+)-menthofuran,¹³ and β -nicotyrine¹². The goal of this project was to determine which of these inhibitors are actually able to discriminate between CYP2A6 and CYP2A13. The ability of these inhibitors to discriminate between CYP2A6 and CYP2A13 activity was evaluated using parallel assays for the inhibition of *para*-nitrophenol (*p*NP) 2-hydroxylation using recombinant, purified CYP2A protein. The results of these studies suggests that only (*R*)-(+)-menthofuran and tranilcypromine demonstrate even a 10-fold preference for CYP2A6 inhibition over CYP2A13, and that only 8-MOP has a >5-fold selectivity for CYP2A13 over CYP2A6. Tryptamine and DMABA were determined to be only moderately (5- to 10-fold) selective for CYP2A6 inhibition, while the remaining compounds (*S*)-nicotine, PEITC, β -nicotyrine, and pilocarpine demonstrated relatively little preference for either CYP2A6 or CYP2A13. The results of these studies serve as the first explicit determination of the selectivity of these compounds for enzymes within the CYP2A family and can be used as a guide for the selection of CYP2A-selective inhibitors in studies that seek to accurately distinguish between CYP2A6 and CYP2A13 in the metabolism or activation of xenobiotic compounds.

Possible future directions for this project may include the use of docking studies to evaluate the binding interactions that serve as an underlying basis for the moderate, observed CYP2A selectivity. Docking studies conducted with the published crystal structures of CYP2A6 and CYP2A13 with all nine inhibitors might provide insight into the interactions governing the binding of the most selective CYP2A6 inhibitors tranilcypromine and (*R*)-menthofuran as opposed to relatively non-selective inhibitors such as (*S*)-nicotine and β -nicotyrine. Such information could be useful in the rational development of more selective CYP2A inhibitors by

taking maximal advantage of the proposed binding interactions that appear to confer the greatest selectivity between CYP2A6 and CYP2A13. Another possible means of evaluating the biochemical interactions that allow these inhibitors to discriminate between CYP2A6 and CYP2A13 activity is the use of functional assays conducted with CYP2A6 mutants. Four amino acids located within the CYP2A active site have been identified by the Scott lab to play key roles in the differing the abilities of CYP2A6 versus CYP2A13 enzymes to metabolize the substrate phenacetin.¹⁴ The inhibition assays employed in the completed studies of wild-type CYP2A enzymes can be extended to include CYP2A6 mutants containing one or more of these residue changes to evaluate the importance of these individual active site residues to the selectivity of the inhibitors characterized thus far.

The CYP26 family of enzymes are important mediators of the *in vivo* catabolism of the endogenous derivative of vitamin A, retinoic acid (RA), and serve as therapeutic targets for the prevention of RA resistance. Geometric isomers of RA such as *all-trans*-RA (*atRA*) and 13-*cis*-RA have been found useful in cancer therapy and the treatment of dermatological conditions, but resistance to RA-based therapies is often experienced in patients undergoing prolonged treatment as a result of increased plasma clearance. The development of selective and potent CYP26 inhibitors has been restricted due to the limited structural and functional data available for this family of enzymes. Present limitations in CYP26 research are due, in large part, to that fact that the majority of CYP26 research published to date has relied on assays performed with transfected cells, microsomal fractions prepared from tissue samples, or microsomal fractions prepared from cultured cells.¹⁵⁻¹⁹ These studies provide only limited structural and functional data based on the scarce quantities and low purity of these types of enzyme preparations. As a result, the immediate goal of this second project was to produce pure, recombinant, functional

CYP26 enzyme in yields that exceeded those attainable by methods currently available in the literature. The production of purified CYP26 enzymes was based on the combination of proven methods for the expression and purification of other truncated, mammalian P450 enzymes and the use of detergents and stabilizing ligands specific for the CYP26 enzymes. The combination of these approaches led to the expression of mouse CYP26A1 and CYP26B1 proteins in yields of 200-400 nmol per 2.25 L of *E. coli* expression media and the ability to recover 20-50 nmol following a single chromatographic step using immobilized metal affinity chromatography. However, reduced carbon monoxide difference spectra collected prior to and following column chromatography indicated that the majority of this protein was inactive based on the predominance of an absorbance peak at 420 nm, though a small amount of P450 was also detected. Additionally, neither purified nor microsomal preparations of mouse CYP26A1 showed any indication of metabolic activity in the presence of the natural substrate RA. Regardless, the results of these studies serve as the first and only known record to date of recombinant expression of human or mouse CYP26 enzymes in *E. coli* resulting in any amount of active P450 protein as evaluated by the reduced carbon monoxide difference spectrum. Still, further optimization will be required to reach the original goal set forth of generating pure, recombinant, functional CYP26 enzymes for basic kinetic and structural determination studies.

Within the last two years, more than one research group has published data on binding and metabolism of known CYP26 substrates and inhibitors using proteins expressed recombinantly in baculovirus infected insect cells.^{17,20,21} Though expression in insect cells has thus been demonstrated to be sufficient to conduct functional characterization studies, structural determination by X-ray crystallography requires a more robust expression system. As a result, future work in this project would involve optimizing the method of CYP26 expression in *E. coli*

that has been described so far. Since the CYP26 enzymes expressed using this host were inactive, future efforts should focus on promoting the functional integrity of the CYP26 enzymes upon expression. One potential approach to accomplishing this would be to explore alternate modifications to the N-terminal sequence. Though the truncation used in these studies was based on the successful truncation of other mammalian P450 proteins, it is possible that the integrity of the CYP26 tertiary structure is more sensitive to the removal of this region. Based on hydropathy plot analysis, a lesser truncation involving the removal of the first 24 amino acid residues (compared to 42) would still be sufficient in removing the N-terminal transmembrane helix while keeping more of the wild-type protein intact. In addition to a smaller N-terminal truncation, different *E. coli* cell lines and plasmids could be employed. Both of these components can have a significant effect on the success or failure of the recombinant expression of other mammalian P450 enzymes in *E. coli*.

The research projects described within this thesis represent critical stepping stones in the process of understanding how substrates and inhibitors interact with individual P450 enzymes. A thorough kinetic evaluation for the ability of known CYP2A inhibitors to discriminate between CYP2A6 and CYP2A13 is directly applicable to predicting and/or evaluating the chemical toxicology of xenobiotic compounds that serve as CYP2A substrates, including procarcinogens that become activated upon CYP2A-mediated metabolism. An enhanced method for generating large amounts of pure, recombinant CYP26 enzyme would enable basic structural and kinetic studies to facilitate the development of enhanced retinoic acid metabolism blocking agents for the treatment of cancer. Altogether, the studies of these two very different families of P450 enzymes serve to facilitate the selective targeting of P450 enzymes. Selective inhibition of the CYP2A enzymes provides a means of protection against harmful chemical species, while

selective inhibition of the CYP26 enzymes is important for the development of enhanced chemotherapeutic agents.

References

1. Smith, B.D., Sanders, J.L., Porubsky, P.R., Lushington, G.H., Stout, C.D. and Scott, E.E. (2007) Structure of the human lung cytochrome P 450 2A13. *J. Biol. Chem.* **282**, 17306-17313.
2. Su, T., Bao, Z., Zhang, Q.-Y., Smith, T.J., Hong, J.-Y. and Ding, X. (2000) Human cytochrome P450 CYP2A13: predominant expression in the respiratory tract and its high efficiency metabolic activation of a tobacco-specific carcinogen, 4-(methylnitrosamino)-1-(3-pyridyl)-1-butanone. *Cancer Research* **60**, 5074-5079.
3. Bao, Z., He, X.-Y., Ding, X., Prabhu, S. and Hong, J.-Y. (2005) Metabolism of nicotine and cotinine by human cytochrome P450 2A13. *Drug Metab. Dispos.* **33**, 258-261.
4. Fukami, T., Katoh, M., Yamazaki, H., Yokoi, T. and Nakajima, M. (2008) Human cytochrome P450 2A13 efficiently metabolizes chemicals in air pollutants: naphthalene, styrene, and toluene. *Chem. Res. Toxicol.* **21**, 720-725.
5. He, X.-Y., Tang, L., Wang, S.-L., Cai, Q.-S., Wang, J.-S. and Hong, J.-Y. (2006) Efficient activation of aflatoxin B1 by cytochrome P450 2A13, an enzyme predominantly expressed in human respiratory tract. *Int. J. Cancer* **118**, 2665-2671.
6. Nakajima, M., Itoh, M., Sakai, H., Fukami, T., Katoh, M., Yamazaki, H., Kadlubar, F.F., Imaoka, S., Funae, Y. and Yokoi, T. (2006) CYP2A13 expressed in human bladder metabolically activates 4-aminobiphenyl. *Int. J. Cancer* **119**, 2520-2526.
7. Patten, C.J., Smith, T.J., Murphy, S.E., Wang, M.-H., Lee, J., Tynes, R.E., Koch, P. and Yang, C.S. (1996) Kinetic analysis of the activation of 4-(methylnitrosamino)-1-(3-pyridyl)-1-butanone by heterologously expressed human P450 enzymes and the effect of P450-specific chemical inhibitors on this activation in human liver microsomes. *Arch. Biochem. Biophys.* **333**, 127-138.
8. Nakajima, M., Yoshida, R., Shimada, N., Yamazaki, H. and Yokoi, T. (2001) Inhibition and inactivation of human cytochrome P450 isoforms by phenethyl isothiocyanate. *Drug Metab. Dispos.* **29**, 1110-1113.
9. Rahnasto, M., Wittekindt, C., Juvonen, R.O., Turpeinen, M., Petsalo, A., Pelkonen, O., Poso, A., Stahl, G., Hoeltje, H.D. and Raunio, H. (2008) Identification of inhibitors of the nicotine metabolising CYP2A6 enzyme - an in silico approach. *Pharmacogenomics J.* **8**, 328-338.
10. Koenigs, L.L., Peter, R.M., Thompson, S.J., Rettie, A.E. and Trager, W.F. (1997) Mechanism-based inactivation of human liver cytochrome P450 2A6 by 8-methoxypsoralen. *Drug Metab Dispos* **25**, 1407-15.
11. Zhang, W., Kilcarslan, T., Tyndale, R.F. and Sellers, E.M. (2001) Evaluation of methoxsalen, tranlycypromine, and tryptamine as specific and selective CYP2A6 inhibitors in vitro. *Drug Metab. Dispos.* **29**, 897-902.
12. Denton, T.T., Zhang, X. and Cashman, J.R. (2004) Nicotine-related alkaloids and metabolites as inhibitors of human cytochrome P-450 2A6. *Biochem. Pharmacol.* **67**, 751-756.

13. Khojasteh-Bakht, S.C., Koenigs, L.L., Peter, R.M., Trager, W.F. and Nelson, S.D. (1998) (R)-(+)-menthofuran is a potent, mechanism-based inactivator of human liver cytochrome P450 2A6. *Drug Metab. Dispos.* **26**, 701-704.
14. DeVore, N.M., Smith, B.D., Urban, M.J. and Scott, E.E. (2008) Key residues controlling phenacetin metabolism by human cytochrome P450 2A enzymes. *Drug Metab. Dispos.* **36**, 2582-2590.
15. Chithalen, J.V., Luu, L., Petkovich, M. and Jones, G. (2002) HPLC-MS/MS analysis of the products generated from all-trans-retinoic acid using recombinant human CYP26A. *J. Lipid Res.* **43**, 1133-1142.
16. Gomaa, M.S., Bridgens, C.E., Veal, G.J., Redfern, C.P.F., Brancale, A., Armstrong, J.L. and Simons, C. (2011) Synthesis and biological evaluation of 3-(1H-imidazol- and triazol-1-yl)-2,2-dimethyl-3-[4-(naphthalen-2-ylamino)phenyl]propyl derivatives as small molecule inhibitors of retinoic acid 4-hydroxylase (CYP26). *J. Med. Chem.* **54**, 6803-6811.
17. Helvig, C., Taimi, M., Cameron, D., Jones, G. and Petkovich, M. (2011) Functional properties and substrate characterization of human CYP26A1, CYP26B1, and CYP26C1 expressed by recombinant baculovirus in insect cells. *J. Pharmacol. Toxicol. Methods* **64**, 258-263.
18. White, J.A., Beckett-Jones, B., Guo, Y.-D., Dilworth, F.J., Bonasoro, J., Jones, G. and Petkovich, M. (1997) cDNA cloning of human retinoic acid-metabolizing enzyme (hP450RAI) identifies a novel family of cytochromes P450 (CYP26). *J. Biol. Chem.* **272**, 18538-18541.
19. White, J.A., Guo, Y.D., Baetz, K., Beckett-Jones, B., Bonasoro, J., Hsu, K.E., Dilworth, F.J., Jones, G. and Petkovich, M. (1996) Identification of the retinoic acid-inducible all-trans-retinoic acid 4-hydroxylase. *J Biol Chem* **271**, 29922-7.
20. Topletz, A.R., Thatcher, J.E., Zelter, A., Lutz, J.D., Tay, S., Nelson, W.L. and Isoherranen, N. (2012) Comparison of the function and expression of CYP26A1 and CYP26B1, the two retinoic acid hydroxylases. *Biochem. Pharmacol.* **83**, 149-163.
21. Lutz, J.D., Dixit, V., Yeung, C.K., Dickmann, L.J., Zelter, A., Thatcher, J.E., Nelson, W.L. and Isoherranen, N. (2009) Expression and functional characterization of cytochrome P 450 26A1, a retinoic acid hydroxylase. *Biochem. Pharmacol.* **77**, 258-268.